ELECTROLESS DEPOSITED PALLADIUM MEMBRANES AND NANOWIRES

By

Zhongliang Shi

Department of Mining and Materials Engineering,
McGill University, Montreal, Canada

June 2007

A Thesis Submitted to the Faculty of Graduate and Postdoctoral Studies, McGill University in Partial Fulfillment of the Requirements for the Degree of Doctor of Philosophy

Your file Votre référence
ISBN: 978-0-494-38645-3
Our file Notre référence
ISBN: 978-0-494-38645-3

ABSTRACT

Hydrogen is considered to be the fuel of the future as it is clean and abundant. Together with the rapidly developing fuel cell technology, it can sustain an environmentally sound and efficient energy supply system. Developing the technologies of palladium-based membrane for hydrogen separation and palladium nanostructured materials for hydrogen sensing and hydrogenation catalysts makes the "hydrogen economy" possible. This is because these technologies will allow for commercially viable production of comparatively cheap and high-quality hydrogen, and safety of its application. Based on the market requirements and interest in the development of a hydrogen economy, the purposes of this thesis are to develop thin palladium membrane for hydrogen separation and to explore an economic method for the synthesis of palladium nanowires in potential engineering applications. The original contributions of this thesis are outlined below:

The investigation of deposition progress of a palladium membrane on porous stainless steel substrate illustrates that palladium deposits will form a network structure on pore areas of the substrate surface in the initial stages. A bridge model is presented to describe the formation of a membrane. This model is confirmed from the cross-section of the deposited membranes. Based on the bridge model and the experimental measurements of palladium membranes deposited on the pore area of the substrates, the thickness of a palladium membrane deposited on 0.2 μm grade porous stainless steel substrate can be effectively controlled around 1.5~2 μm, and the thickness of a palladium membrane deposited on 2 μm grade porous Inconel substrate can be effectively controlled around 7.5~8 μm. Comparing the thickness and quality of palladium membranes deposited on the same substrates with the data in the literature, the thicknesses of the membranes prepared in this program are lower. The obtained result will be beneficial in the design and manufacture of suitable membranes using the electroless deposition process.

In the initial deposition stages, palladium nanoparticles cannot be deposited at the surface of the SiO_2 inclusions that appear at the substrate surface. With the extension of deposition time, however, palladium nanoparticles gradually cover the SiO_2 inclusions layer by layer due to the advance deposited palladium nanoparticles on the steel substrate surrounding them. The effect of the SiO_2 inclusions on palladium deposits cannot be neglected when an ultra-thin membrane having the thickness similar to the size of inclusions is to be built.

The chemical reaction between phosphorus (or phosphate) and palladium at high temperature can take place. This reaction causes surface damage of the membranes. If palladium membranes are built on the porous substrates that contain phosphorus or phosphate used in the inorganic binders, they cannot be used over 550°C. This result also implies that palladium membranes cannot be employed on the work environment of phosphorus or phosphates.

Palladium nanowires are well arranged by nanoparticles at the rough stainless steel surface. The formation procedures consist of 3 stages. In the initial stage, palladium nanoparticles are aligned in one direction, then the nanowire is assembled continuously

using follow-up palladium deposits, and finally the nanowire is built smoothly and homogeneously. It is also found that palladium nanoparticles generated from the autocatalytic reaction are not wetting with the steel substrate and they are not solid and easily deformed due to the interfacial tension when they connect to each other.

Various palladium nanowire arrays possessing the morphologies of single wires, parallel and curved wires, intersections and network structures are illustrated. The results demonstrate that palladium nanowires can be built in a self-assembled manner by palladium nanoparticles in the initial deposition stages. Such self-assembled nanowires may attract engineering applications because electroless deposition process and preparation of a substrate are simple and inexpensive.

The diameter of palladium nanowires can be effectively controlled by the concentration of $PdCl_2$ in the plating solution and deposition time. The size of palladium nanoparticles generated from the autocatalytic reaction is directly dependent on the concentration of $PdCl_2$ in the plating solution. The higher the concentration of $PdCl_2$ in the plating solution is, the smaller the deposited palladium nanoparticles are. The experimental results provide a controllable method for the fabrication of palladium nanowire arrays with potential engineering applications.

RÉSUMÉ

L'hydrogène est considéré comme étant le combustible de l'avenir parce qu'il est propre et abondamment disponible. En plus, avec le développement rapide de la technologie de la pile à combustible, l'hydrogène est le mieux indiqué pour alimenter ce système qui est une source d'énergie électrique très efficace et qui ne nuit pas à l'environnement. Le développement des membranes de palladium pour la séparation de l'hydrogène et des matériaux nano structurés à base de fils de palladium ainsi que les catalyseurs pour produire l'hydrogène rendent possibles l'ère de l'économie de l'hydrogène. En effet un tel développement permet de disposer de systèmes capables de produire de l'hydrogène de haute pureté à bon marché et du contrôlé sécuritaire des dispositifs utilisant l'hydrogène. Afin de répondre au besoin potentiel du marché lié à l'économie de l'hydrogène, les buts de cette thèse sont de : i) Développer une mince couche de membrane de palladium pour la séparation de l'hydrogène; ii) Développer la synthèse de nano fils de palladium à l'aide d'une méthode très économique pour des applications industrielles de détection de l'hydrogène. Les contributions originales de cette thèse sont indiquées dans ce qui suit:

1) Le développement de la déposition d'une membrane de palladium sur le substrat d'acier inoxydable poreux montre que les couches de palladium formeront une structure de réseau sur les parties poreuses initiales à la surface du substrat. Un modèle de pont a été proposé pour décrire la croissance de la membrane. Ce modèle a été confirmé par une analyse de la coupe transversale des membranes déposées. En se basant sur ce modèle et sur les paramètres expérimentaux des membranes déposées sur les parties poreuses des substrats, il a été montré que l'épaisseur de la membrane déposée sur un substrat de d'acier inoxydable de 0.2 microns peut être contrôlée efficacement à une valeur comprise entre 1.5 et 2 microns. Alors que cette épaisseur peut être bien contrôlé à une valeur comprise entre 7.5 et 8 microns lorsque le substrat utilisé est de l'Inconel ayant une épaisseur de 2 microns. La comparaison des résultats obtenus dans ce travail et ceux de la littérature sur des épaisseurs et al qualité des membranes déposées sur les mêmes substrats montre que l'épaisseur des membranes préparées dan ce travail est nettement plus faible. Ainsi la méthode utilisée ici est nettement plus avantageuse que celles indiquées dans la littérature car elle permet en plus de mieux contrôler l'épaisseur des membranes.

2) Pour des temps de déposition court (temps d'initiation des dépôts), les nano particules de palladium ne peuvent pas être déposées sur des inclusions de SiO_2 qui sont à la surface des substrats. Par contre pour des temps élevés de déposition, les nano particules de palladium couvriront graduellement les inclusions de SiO_2 qui sont disposées en couches en raison de la déposition important des nano particules de palladium et de la nature du substrat qui les entoure. L'effet des inclusions de SiO_2 sur les dépôts de palladium ne peut pas être négligé quand une membrane extrêmement mince ayant l'épaisseur similaire à la taille des inclusions est élaborée.

3) Si les couches sont élaborées sur des substrats poreux qui contiennent le phosphore ou le phosphate utilisé dans les liants inorganique, les membranes de

palladium ne peuvent pas être utilisées au-dessus de 550°C. En effet une réaction chimique entre le phosphore (ou le phosphate) et le palladium peut avoir lieu à haute température. Cette réaction causera des dommages sur la surface de la membrane. Ce résultat indique aussi que, dans certaines conditions d'utilisations, les membranes de palladium ne peuvent pas être employées dans un environnement en présence de phosphore ou de phosphates.

4) Des nano fil de palladium nano structurés ont été obtenus par dépôt électroless de nano particules de palladium à la surface rugueuse d'acier inoxydable. Leur croissance s'effectue en trois étapes pour les temps élevés de déposition : i) dans la première étape, le nano fil est formé par croissance successive des nano particules de palladium sont alignées dans une direction; ii) dans la deuxième étapes, le nano fil est formé par croissance successive des nano particules dans cette direction et; iii) finalement le nano fil est facilement élaboré de façon homogène. Il a aussi été montré que les nano particules de palladium ont été produites par réaction auto catalytique au cours de la quelle est aussi trouvé que les nanoparticules de palladium ont produit la réaction autolytique au cours de la quelle l'électrolyte ne mouille pas le substrat d'acier. Elles ne sont pas solides et sont facilement déformées en raison de la tension interraciale quand elles se connectent.

5) Diverses rangées de nano fil de palladium ayant des morphologies similaires à un fil ou à des fils parallèles et courbés, avec des structures qui s'interpénètrent ont été mises en évidence. Les résultats observés démontrent que le nano fil est constitué d'un assemblage individuel de nano particules formées durant les étapes initiales de la déposition. La méthode electroless qui est simple et peu onéreuse s'avère donc étant un outil puissant d'élaboration de nano fil de palladium pour des applications en génie. Le diamètre du nano fil peut efficacement être contrôlée en jouant sur la concentration de $PdCl_2$ de la solution de placage et du temps de déposition. Il a été montré que la taille de la nano particule de palladium déposé diminue lorsque la concentration en $PdCl_2$ augmente.

Acknowledgements

First and foremost, I would like to express my deep and sincere gratitude to my supervisor, Professor Jerzy A Szpunar for giving me the opportunity to be his Ph.D. student. Hydrogen economy and nanotechnology are fascinating research fields, I gained great insights and understanding of these subjects under his kind guidance. His broad knowledge and scholarly attitude set an example for me, not limited to the past 4 years but for the rest of my life. He offered generous help not only to my research but also to my daily life.

Secondly, I would like to thank the financial support — Industry Graduate Scholarship from the Natural Science and Engineering Research Council of Canada (NSERC) and AH2T Inc. Montreal. Based on the requirement of this scholarship, I must work at AH2T Inc. one day a week. I am deeply grateful to my company supervisors, Dr. Shanqiang Wu and Dr. Mustapha Roshd for their detailed and constructive comments and important support throughout this work. I also thank other colleagues at AH2T Inc., Dr. Jinghai Xie and Dr. Naizhen Cao for the happy time when I work there. I want to thank Dr. Claude Lalande (Manager of Fellowships and Awards, Graduate and Postdoctoral Studies Office, McGill University) and his colleagues, Ms. Jocelyne Regnier (External Fellowships Officer) and Ms. Maggie Do Couto (Administrator Coordinator — Fellowships and Awards) for assistant of my Scholarship.

Especially, I warmly thank Mr. Slavek Poplawski for his assistant with my experiments at our Texture lab, and his valuable advice and friendly help. I would like to thank my former and current colleagues for all the happy time and their valuable help when I needed. They are Dr. Hualong Li, Dr. Hanbai Lin, Dr. Jae-Young Cho, Dr. Jianlong Lin, Dr. Shixue (Andy) Wen, Dr. Raze Bateni, Dr. Guang Song, Dr. Wen Qin, Dr. Shahrooz Nafisi, Mr. Cheol Nam, Mr. Alain Kassangana, Mr. Alex Blander, Mr. Marwan Azzi, Mr. James Lim, Mr. Shahab Faghihi, Mr. Tedric Soh, Mr. Vladimir Basabe, Mr. Minhui Huang, Mr. Duanjie Li, Mr. Paul Abumov, Mr. Chang Heon, Mr. Sriraman Rajagopalan, Ms. Emilie Hsu and Mrs Yuehua Tan. I also thank Ms Barbara Hanley, Administrative and Student Affairs Coordinator of our department for her kindest help.

Additionally, I wish to extend my warmest thanks to all those who have helped me with my work. They are: Prof. Sasha Omanovic at Department of Chemical Engineering who allowed me to use his lab, Prof. Andrew Kirk and Dr. Aju S. Jugessur, and Prof. Ishiang Shih at Electrical Engineering Department who supported some E-beam pattern samples and measured physical properties of deposited nanowire arrays, and Mr. Vito Logiudice Manager of Nanotools Micromachining Fabrication Lab. at Physics Department who helped me use equipment there.

Finally, I owe my loving thanks to my wife Xingxiu Deng and our daughter Daisy Xuan Shi. Without their encouragement and understanding, it would have been impossible for me to finish this work. My special gratitude is due to my parents for their constant love, understanding, encouragement, support, and patience during my study at McGill University.

FORWARD

This thesis contains nine chapters. Seven chapters (from chapter 2 to chapter 8) are already published, accepted or submitted for publication as peer-reviewed papers in Physical, Chemical and Materials Journals. It should be clearly stated that due to the manuscript-based format, i.e., whole chapters to be copies of papers. Some minor duplication has inevitably occurred.

This thesis, entitled "Electroless deposited palladium membranes and nanowires', contains two parts. One is on palladium membranes. The other is on palladium nanowires. In the part of palladium membranes, the formation of palladium membrane on porous steel substrate was observed and a bridge model was presented to describe the procedures of a membrane formation, then, hydrogen selectivity and permeability of palladium membranes prepared in this thesis were compared with the data from the literature (**Chapter 2**). As well-known, the prospect for palladium membrane application is to reduce the membrane thickness in order to maximize hydrogen permeability and reduce its cost. Based on the obtained results in Chapter 2, the ultra-thin palladium membranes were built for hydrogen permeation tests after the porous substrates were modified. The obtained results are beneficial for designing and fabricating desired thickness of palladium membrane by an electroless deposition process (**Chapter 3**). Tens of membranes were built on two porous substrates for hydrogen separation and permeation tests at elevated temperatures. Their microstructure transformation during hydrogen permeation tests at high temperatures was characterized and it is found that the chemical reaction between palladium and phosphorus can take place and it causes surface damage of the membranes. (**Chapter 4**) After that, three types of palladium nanostructures are demonstrated in **Chapter 5**. Then, I focused on palladium nanowires. Various palladium nanowire arrays in a self-assembled manner are reported. The experimental results demonstrate palladium nanowires can be built by assembly of nanoparticles generated in the initial deposition stages without any external field except an autocatalytic reaction. (**Chapter 6**) If palladium nanowires can be produced in a controllable manner, it will be important for designing the required palladium nanowire arrays in potential engineering applications. Based on the obtained results, the diameter of palladium nanowires can be controlled by the electroless deposition process, detail information is shown in **Chapter 7**. Effects of SiO_2 inclusions on the formation of palladium membranes and nanowires are illustrated in **Chapter 8**.

Contributions of Authors

All papers have been submitted for publication with the supervisor, Dr. Jerzy A Szpunar, as a co-author. Dr. Shanqiang Wu is also included as a co-author, in recognition of his advice on the initial setup of electroless deposition and hydrogen separation experiments. Nevertheless, all of the work has been done by the author of this thesis, with the exception of the normal supervision and advice given by the supervisor and co-authors.

TABLE OF CONTENTS

LIST OF FIGURES

LIST OF TABLES

CHAPTER 1

INTRODUCTION, LITERATURE REVIEW AND RESEARCH PURPOSE

1.1 Introduction

Hydrogen as the perfect fuel is one of the most important future energy sources. It is quite different from the fuels that we use today. So far, hydrogen is usually generated from fossil fuels, natural gas or oil using the method of "steam reforming". [1] During this process, different by-products are also formed and cause air pollution. Therefore, to generate hydrogen from renewable energy sources and obtain high quility hydrogen attracts great attention because it is an important approach to solve the problems of energy shortage and environmental pollution. [1] "It also provides great economic and environmental benefits to our society." [1]

With the global interest in the development of hydrogen as an ecologically clean fuel and the rapidly developing fuel cell technology, it is expected that in the foreseeable future hydrogen consumption will increase drastically. There are large research efforts in USA, Canada and other countries to develop economically viable methods of an effective hydrogen separation or purification. As we know, hydrogen we used today is mainly generated by the "steam reforming" method. In order to separate hydrogen from the reformed steams that contain hydrogen and to obtain high quality hydrogen, membrane separation is regarded nowadays as a preferred method for hydrogen production.

In the meantime, "hydrogen sensor technology is a critical component for safety and other practical concerns in hydrogen as a fuel for fuel cells and the proposed hydrogen economy. For example, hydrogen sensors will detect leaks from hydrogen-powered cars and fueling stations long before the gas becomes an explosive hazard." [2] They play an important role in the application of fuel cells. "With respect to fuel cells and energy production, two types of hydrogen sensors are required: one for detection of impurities in the fuel, which could impact the fuel cell process, and the other for detecting hydrogen leaks, which are a safety concern. Research and development of hydrogen sensors is ongoing and advancing rapidly."[2]

Developing the technologies of palladium-based hydrogen separation membrane and palladium nanostructured materials for hydrogen sensing and hydrogenation catalysts makes the "hydrogen economy" possible because these technologies will offer commercial viability for the production of comparatively cheap and high-quality hydrogen, and safety of its application. [3] Based on the market requirements and great interest for the development of hydrogen economy, this thesis focuses on two parts. One is to develop thin palladium membrane for hydrogen separation. The other is to explore an economic method to synthesize palladium nanowires for potential engineering application.

1.1.1 Palladium membranes

There are two basic types of membranes that can be used for gas separation. One is a porous membrane in which the gases are literally separated on the basis of their

molecular weight or size by small pores through the membrane. [3] The other is a nonporous membrane or a dense membrane. It does not contain holes or pores in the conventional sense. It relies on the principle that gases dissolve in (atomization) and diffuse through the solid membrane. [3]

This part contains 3 sections:

1. Hydrogen separation mechanisms of the membranes
   (1) There are two mechanisms of porous membrane used for hydrogen separation. One is Knudsen diffusion mechanism. The other is molecular sieving mechanism. So far, the investigation of porous membranes that can provide significantly higher hydrogen selectivity for industrial gas separation is still underway.
   (2) Dense membrane used for hydrogen separation relies on solution diffusion mechanism. The design and fabrication of a thin and defect-free dense membrane attracts great attention in industrial applications because the thickness of the membrane will determine the flux of hydrogen.
2. Background of palladium membranes research and applications (literature review)
   (1) To summarize research and development of palladium membranes.
   (2) To introduce two industrial application examples of palladium membranes for hydrogen extraction.
3. Purposes on research and development of palladium membranes

1.1.2 Palladium nanowires

"As hydrogen has the potential for burning and explosion, sensors are needed to detect hydrogen leaks. The challenge is to develop a sensor that can sense the leak within the target timeframe at the desired detection level, assess the hazard, trigger an alarm or activate a protective device, and be priced reasonably."[4] This sensor may also be used for many potential sources of the hydrogen detection (electrolyzers, reformers, biomass, tanks, and other storage possibilities). So far, the emerging fuel cell market has not yet fully defined its needs. So the development of hydrogen sensors will be based on the different applications of fuel cells.

Hydrogen sensors vary from other gaseous sensors in which they must detect over the general level of ambient hydrogen levels and hydrogen leaks under various work environment conditions. [2] So they must be high sensitivity and have rapid response. Hydrogen sensors made of palladium nanowires, for sure, can realize these requirements.

This part contains 3 sections:

1. Mechanisms of hydrogen sensing built by palladium nanowire

There are two mechanisms of hydrogen sensor made of palladium nanowires. One is that there are nanoscopic gaps or break junctions in these nanowires that can close and reopen when hydrogen is absorbed and adsorbed in these nanowires. This characterization is used to detect the variation of electric resistance in palladium nanowires. The other is that nanowires will swell when hydrogen dissolves in palladium nanowires to form palladium hydride. This expanding will also cause the change of electrical resistance, which can be used to detect the amount of hydrogen.

2. Background of the fabrication of palladium nanowires (literature review)
   (1) To summarize different processes for the fabrication of palladium nanowires.

(2) To simply introduce electroless process for the deposition of palladium nanowires. .

3. Objectives of this program for research of palladium nanowires

1.2 Background on palladium membrane for hydrogen separation

1.2.1 Mechanisms of a membrane for hydrogen separation

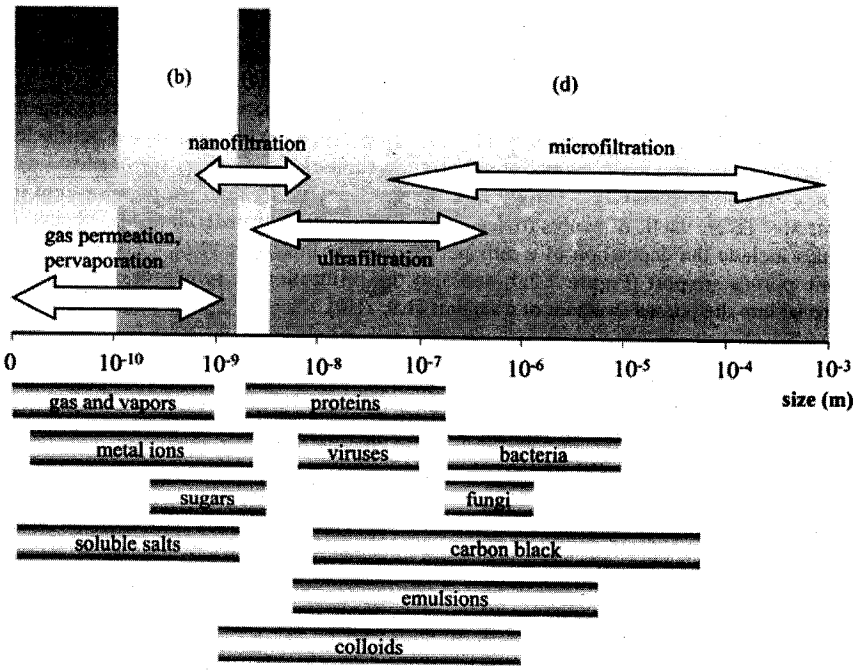

Figure 1-1 Different types of membranes and separation species (a) dense and ultramicroporous, (b) microporous, (c) mesoporous, (d) macroporous [5]

Figure 1-1 shows that the membranes can be classified into four types according to their applications, such as (a) dense and ultramicroporous, (b) microporous, (c) mesoporous, (d) macroporous. Only (a) dense or ultramicroporous membranes can be used for hydrogen separation because hydrogen kinetic diameter is very small, as shown in Table 1-1. However, the hydrogen separation mechanisms are different between the dense and the ultramicroporous membranes.

Table 1-1 Kinetic diameters of gas molecules [6]

Molecule	He	H_2	NO	CO_2	Ar	O_2	N_2	CO	CH_4	C_2H_4	Xe	C_3H_8
Kinetic Diameter (Å)	2.6	2.89	3.17	3.3	3.4	3.46	3.64	3.76	3.8	3.9	3.96	4.3

There are two different mechanisms of an ultramicroporous membrane for hydrogen separation and they are depicted below:

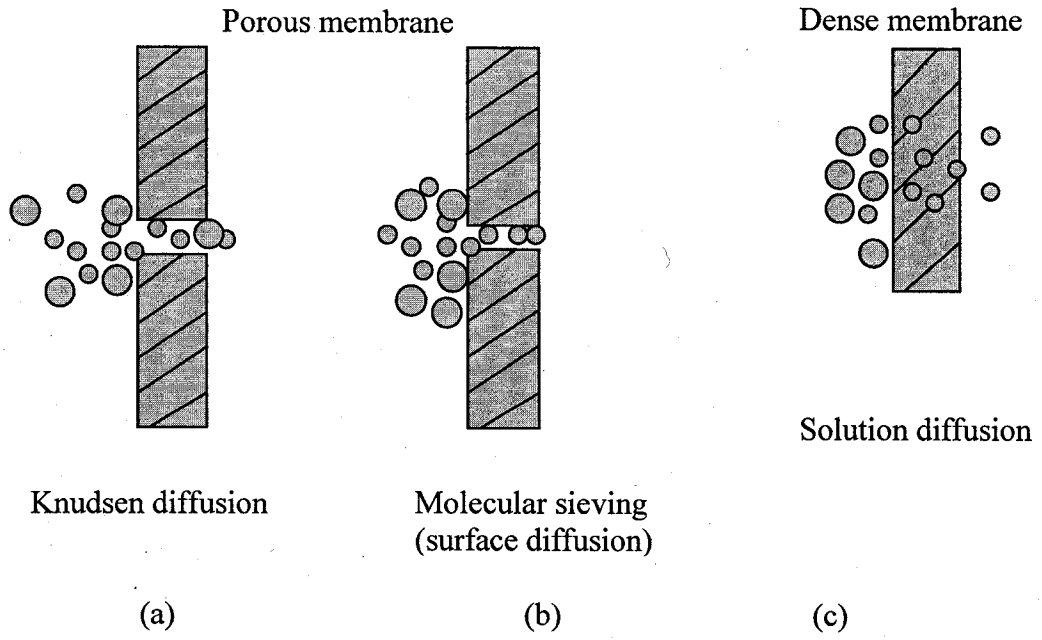

Figure 1-2 Schematic representations of main mechanisms of membrane-based hydrogen separations (a) Knudsen separation mechanism, (b) ultramicroporous molecular sieving separation mechanism, (c) solution-diffusion separation mechanism [6, 7]

One is Knudsen diffusion mechanism, as shown in Figure 1-2 (a). The ultramicroporous membrane for hydrogen separation depends on the size of microscopic pores in the membrane and interactions between the membrane material and these molecules to be separated. When the pore size decreases to the point where the majority of collisions are between the gases and the pore walls, the smaller molecules will pass through the membrane faster than the bigger ones. This process does not provide high hydrogen selectivity. [6, 7]

The other is molecular sieving mechanism, as shown in Figure 1-2 (b). When the diameter of these pores in the ultramicroporous membrane approaches the diameter of larger molecules in a mixture, only the smaller molecules will pass through. This process provides a lower pressure, purified stream of the smaller molecules. This mechanism occurs in inorganic membranes with pores in nanosize diameter. Typical materials that exhibit molecular sieving behaviour are sol-gel derived silica [8-14], alumina films [15-18], zeolites [19-21] and nanocarbon [22-24]. As the difference of kinetic diameters between hydrogen gas and any other gases in the gas mixture is too small, as shown in Table 1-1, it is actually difficult to separate hydrogen from the mixture with higher selectivity. This kind of membrane is being investigated by many scientists.

Hydrogen separation mechanism using a dense metal membrane is termed as solution diffusion process. The detail description is as following:

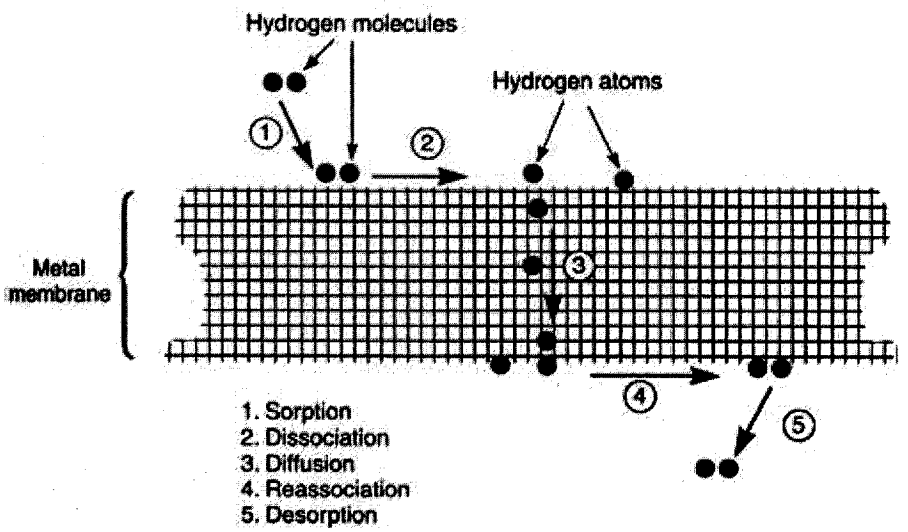

Figure 1-3 Mechanism of permeation of hydrogen through metal membranes [25]

In some cases, hydrogen in a gas mixture interacts more strongly with the membrane material than other components. It will absorb or preferentially cover the surface of the membrane. Selective transport occurs by diffusion of the atoms from the molecules adhering to the surface, as shown in Figure 1-2 (c). The detail description of hydrogen through a dense metal membrane (such as palladium membrane) is illustrated in Figure 1-3.

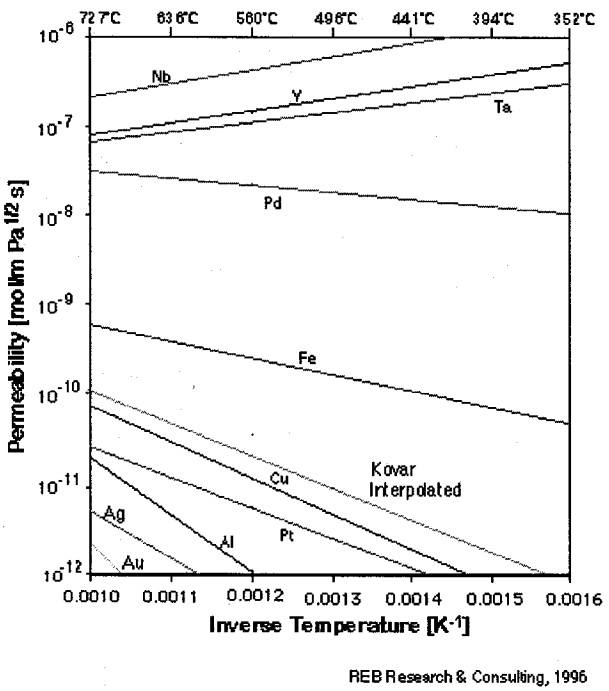

Figure 1-4 Permeability of hydrogen in aluminum, copper, iron, gold, kovar, niobium, palladium, platinum, silver, tantalum, titanium, and vanadium [26]

"When hydrogen molecules from the feed gas are absorbed on the metal membrane surface, where they dissociate into hydrogen atoms, each individual hydrogen atom or ion diffuses through the lattice. After that, hydrogen atoms or ions emerging at the permeated side of the membrane reassociate to form hydrogen molecules, then transport away from the surface to the bulk gas, completing the permeation process. At high temperature, the dissociative adsorption of hydrogen molecules on the membrane surface (inlet side at high pressure) and recombinative desorption of hydrogen molecules from the surface of the membrane (outlet side at low pressure) are fast. The pressure gradient between two sides can be considered as constant. Therefore, the flux of hydrogen through the membrane is determined by hydrogen atoms or ions diffusion through the distance of the membrane (the thickness of the membrane)."[25] The control of palladium membrane thickness is very important to the flux of hydrogen permeation and the reduction of its expense as well.

Figure 1-4 shows the permeability of hydrogen in different metals. It is well known that palladium has good hydrogen permeability. Especially, it can be easily dissociated from the hydrogen molecules into atoms and reassociated from hydrogen atoms to the molecules at its surface. Some other metals such as Zr, V and Nb, also have good hydrogen permeability but they are easily oxidized. Their permeability decreases fast after oxidation.

With the development of advanced instruments and technologies, the microstructural characterization of hydrogen in palladium is gradually understood. For example, Sykes et al [27] used scanning tunneling microscope (STM) to illustrate the behaviour of hydrogen atoms when absorbed by the metal palladium. "Hydrogen atoms are able to occupy stable sites in the subsurface palladium layer. But their presence seems to affect the electronic structure of the surface layer, as if hydrogen atoms are pushing palladium atoms apart to make space. This structural change is so great that it will prevent further hydrogen atoms adsorbing onto the surface layer, offering a potential way to control the surface properties of palladium."[27] Their findings demonstrate the special performance of palladium that can be used for "the development of more efficient hydrogen storage materials and better catalysts". [27] The investigation of "the role of subsurface palladium atoms in hydrogen absorption" also indicates that "the ability of palladium to absorb up to 900 times its own volume of hydrogen at room temperature" is beneficial to "developing it as a catalyst for hydrogenation reactions or as a hydrogen storage material". [27] Lewis et al [28] calculated hydrogen diffusion coefficient of hydrogen in palladium and palladium-based alloy membranes. Sachs, et al [29] analyzed the solubility of hydrogen in single-sized palladium clusters and found that hydrogen has a higher solubility in the α-phase region, compared to bulk palladium. Mitsui et al [30] also used STM to observe the transient formation of active sites for the dissociative adsorption of hydrogen molecules on a palladium (111) surface. They found that two-vacancy sites seem inactive and that aggregates of three or more hydrogen vacancies are required for efficient hydrogen dissociation. Overall, understanding of the behavior of hydrogen in palladium is quite important for the application of palladium.

In summary, based on the different mechanisms between ultromicroporous and dense membranes, hydrogen separation from a mixture of gases can be realized in two approaches: (1) to modify the pore size at the critical separation layer of the membrane to be smaller and smaller in order to perform the separation using Knudsen diffusion and molecular sieving separation mechanisms (an ultramicroporous membrane); (2) to

employ palladium or palladium-alloy membranes (a dense membrane) to realize the solution diffusion separation.

Since it is difficult to make the membrane that possesses nanosize pores to provide a good selectivity for high quality hydrogen separation, the dense membrane made of palladium or its alloys attracts great attention for high purity hydrogen extraction. Sometimes, in order to extract high purity hydrogen and to improve its flux as well as to reduce the cost, palladium is only deposited as an ultra-thin membrane after the surface of the substrate is modified to be a nano-porous structure. So the fundamental studies of palladium deposition, such as the size of palladium deposits related to the electroless process and the effect of the contaminants at the substrate surface, are significant for the design and fabrication of an ultra-thin membrane.

1.2.2 Background of palladium membranes for hydrogen extraction

There are many reports and efforts on palladium membranes [31-42] for hydrogen extraction, including: (1) membrane fabrication process; (2) reduction of its cost through decreasing its thickness or alloying; (3) improvement of its hydrogen embrittlement via alloying due to an α-β phase transition during high temperature cycles; (4) development of an ultra-thin membrane in micro-device application. [43-45]

Table 1-2 Relative overall ranking of the evaluation [50]

Membrane manufacturing techniques	Ranking
Electroless plating (included electrochemical deposition)	1
Pore plugging-interface reaction	0.77
Pore plugging-micro emulsion technique	0.72
Magnetron sputtering	0.63
Laser deposition	0.52
Chemical vapour deposition	0.46

There are various methods on the preparation of palladium and its alloys membrane, foil or tube for hydrogen extraction. Palladium foil and tube can be manufactured using deformation, rolling or casting processes. But they are thick. The thin palladium foil and tube are usually placed on a porous support for hydrogen extraction. Thin palladium membrane can be built on a porous substrate by many different deposition

methods, which can be classified as: physical [46], chemical [47-49] or physicochemical [46] methods according to the membrane formation characterization. In these methods, electroless plating, electrochemical deposition, sputtering and chemical vapour deposition (CVD) are often used. Especially, electroless plating of palladium membrane is the most important method for its industrial applications. The relative overall ranking of the evaluation by comparison among these processes quoted from the report [50], as listed in Table 1-2, which is based on the performance, stability, production cost, ease of production, raw materials cost, impact on environment, possible improvements on short term.

Palladium membrane is usually deposited on porous substrate. Porous and microporous metals or ceramics are usually selected as substrates for high temperature applications.

Membranes made of palladium or its alloys have extremely high hydrogen selectivity relative to other gases, since they operate by a catalytic dissociation of hydrogen and recombination on the downstream face. They are able to operate at elevated temperatures and pressures, but they are expensive. Most work has focused on attempts to produce much less costly versions of so-called 'metal membranes'. One approach is to reduce the thickness of Pd alloy membrane. The other is to replace pure Pd membrane with Pd alloys such as Pd-Ag [51, 52], Pd-Cu [54] and Pd-Fe [55].

As mentioned before, palladium membrane is an ideal material used for hydrogen separation, because it is able to "dissociate molecular hydrogen into atoms and ions at its surface". [53] However, some problems should be avoided during its application. "For example, palladium has an α-β phase transition at temperatures below 300 ^{o}C". [53] This phase transformation will cause expansion and contraction "with varying hydrogen concentration" that will cause "embrittlement and crack of the metal". [53] This detriment can be overcome and improved by alloying with silver or copper. [53, 54]

In order to demonstrate its industrial applications, two examples of palladium or palladium alloy membranes are quoted below.

One is Wah Chang [56] that manufactures Pd-Cu Membrane Modules for separating and purifying hydrogen from mixed gas streams. They are available in sizes ranging from laboratory bench scale to industrial commercial hydrogen production units and hydrogen flux from streams to PPB (concentrations by mass, parts per billion) level. [56] The Membrane Modules are used to protect fuel cells from contaminants and provide purity, dryness, and the ability to extract hydrogen from reformated gases. [56]

The other is NGK [57] that makes thin palladium alloy membranes on ceramic porous substrates for hydrogen separation. This membrane can purify hydrogen from a mixture of gases containing hydrogen gas, which is received attention as fuel for polymer electrolyte fuel cells. The microstructure of porous substrate and palladium alloy membrane is illustrated in Figure 1-5. A silica-alumina composite membrane for hydrogen separation was prepared within α-alumina support by the multi-step pore modification. "In order to enhance hydrogen selectivity, palladium particles were impregnated in the final step utilizing Pd-acetate as a Pd precursor. Although both silica and Pd induced the surface diffusion, Pd was more effective for selective hydrogen adsorption than silica. This multi-step method produced a composite membrane with moderate hydrogen selectivity and satisfactory hydrogen permeance at high temperature and at high trans-membrane pressure."[57]

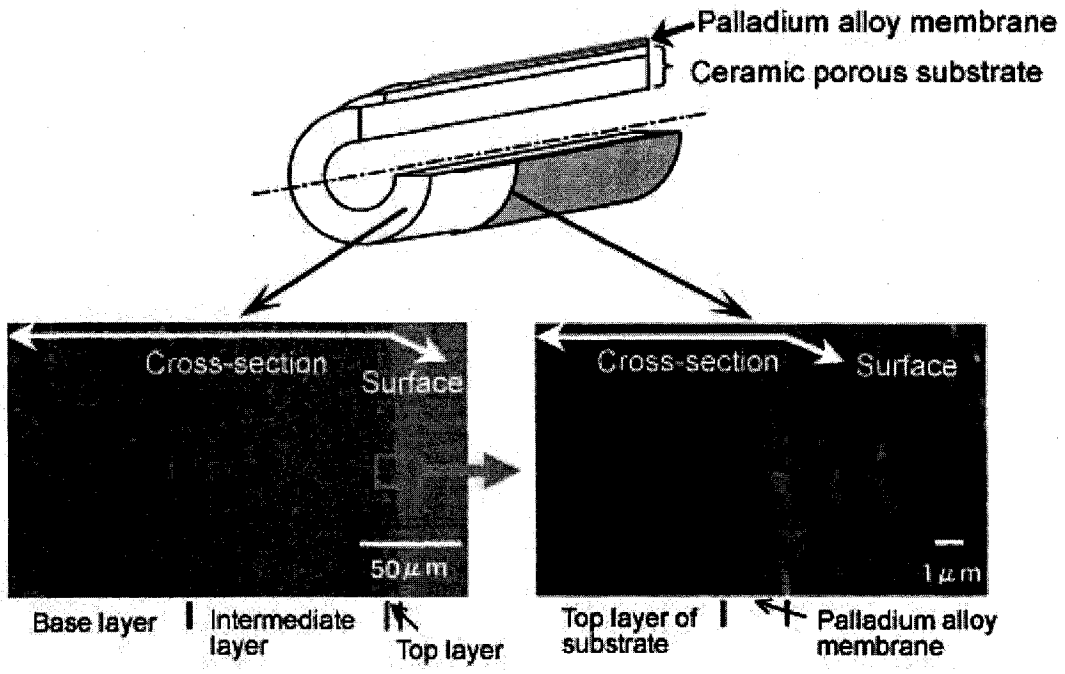

Figure 1-5 Palladium alloy membrane on the ceramic porous substrate [57]

Among these "enabling" membrane technologies for hydrogen separation from a mixture of gases at high temperature, the membrane made of palladium or its alloys is promising for high purity hydrogen extraction from the mixed gas streams in a cost-effective manner. So far, it is very challenging and difficult to fabricate a thin but defect-free dense palladium membrane for hydrogen extraction. The approach for making a thin dense palladium membrane is still being explored. The objective of this program will focus on the development of palladium membrane that is thin enough to reduce its expense and increase hydrogen flux while remaining thick enough to retain adhesion, attrition resistance and mechanical integrity during high temperature cycles. The detail purpose in this program is described below.

1.2.3 Purpose of palladium membrane research

There are numerous reports [31-42] on the development of palladium or its alloys membranes for hydrogen extraction. However, some important fundamental problems are still not given clear answers, such as: how is palladium membrane deposited on porous substrate? How does the surface situation of the substrate affect the palladium deposits and what do the surface defects and microstructure transformations of the membrane occur after hydrogen permeation at high temperatures? These questions are to be answered in this thesis.

In this thesis, 0.2 μm grade porous stainless steel and 2 μm grade porous Inconel filters, purchased from Mott Metallurgical Corporation, are used as substrates. The porous stainless steel substrate can be used up to the temperature of 480°C. Porous Inconel substrate can be used up to the temperature of 820°C. Why are these porous metal filters selected as the substrates over porous ceramics? One reason is that they have good

mechanical strength at high temperature with highly permeable, relatively low selectivity and the research results can be repeated easily on the other porous metal substrates (such as Hastealloy [58]) that can be used at higher temperature. Microporous ceramic substrate does not have good mechanical strength and can be broken easily when integrated with other parts. The other reason is that the coefficient of thermal expansion of ceramic substrate does not match that of palladium membrane, which causes cracks at the membrane when used at high temperatures.

Palladium and its alloys are well-known to be used for hydrogen extraction. Alloying such as the addition of Ag, Cu and Fe usually overcomes the hydrogen brittleness of the membrane and relatively reduces its cost. However, the main challenge is how a thin and pin-pole free membrane can be built. The thinner the membrane is fabricated, the higher hydrogen flux will be obtained. If thin palladium membrane is made, the membrane containing other alloying elements will be easily prepared in a similar approach. So this research will focus on the formation of thin palladium membrane on porous metal substrate and the control of its microstructure by the deposition process. The objectives of the present work on palladium membranes are outlined below.

(1) To investigate how a palladium membrane is built on porous stainless steel substrate by electroless deposition in order to find an approach to realize thin palladium membranes in a controllable manner on porous substrate using this deposition process.
(2) To evaluate the flux of hydrogen through the membranes which are prepared with different thickness, to measure the relationship between hydrogen flux and permeation temperature as well as partial pressure of hydrogen in a mixture of gases, and to compare the results with tha data from literature.
(3) To analyze the surface defects and microstructure transformation of the palladium membrane after hydrogen permeation at high temperature in order to reveal how the membrane itself will vary during hydrogen permeation at high temperature.

1.3 Background on palladium nanowires for hydrogen sensing

1.3.1 Mechanism of palladium nanowires for hydrogen sensing

There are two mechanisms of hydrogen sensor made of palladium nanowires. One is that there are many nanoscopic gaps or break junctions appearance at palladium nanowires and they easily close in the presence of hydrogen gas and reopen in its absence because hydrogen is reversibly occupied by palladium grains in each wire, and palladium lattice expands and contracts by several percent. [59] Atomic Force Microscopy (AFM) images of a single break junction functioning in this manner are illustrated in Figure 1-6. [59, 60] The change in resistance for sensors and switches was related to hydrogen concentration over a range from 1vol% to 10vol%. The nanowire-based hydrogen sensor responds faster than standard hydrogen sensors because hydrogen atoms only diffuse a much shorter distance in a small wire in this unique mechanism, as shown in Figure 1-7

Figure 1-7 illustrates that the mechanism of hydrogen sensor made of palladium nanowires. "These gaps open before the hydrogen-swollen palladium grains in each wire return to their equilibrium dimensions in the absence of hydrogen (mode I). Subsequently,

it is the closing of these gaps or break junctions in the presence of hydrogen (mode II), which account for the decreased electric resistance of the sensor. Many of all wires in the arrays exhibit this switching behavior between mode I and mode II devices, respectively. Arrays of mesoscopic palladium wires, prepared by electrodeposition, form the basis for hydrogen sensors and hydrogen-actuated switches that can exhibit a response time as fast as 20 ms."[59, 60] The devices were constructed by electrodepositing palladium mesowires on a highly oriented pyrolytic graphite (HOPG) surface after these mesowires were transferred to a cyanoacrylate film supported on a glass slide. The nanojunction characteristics of palladium nanowires in a hydrogen environment are also verified by experimental investigations. [62, 63]

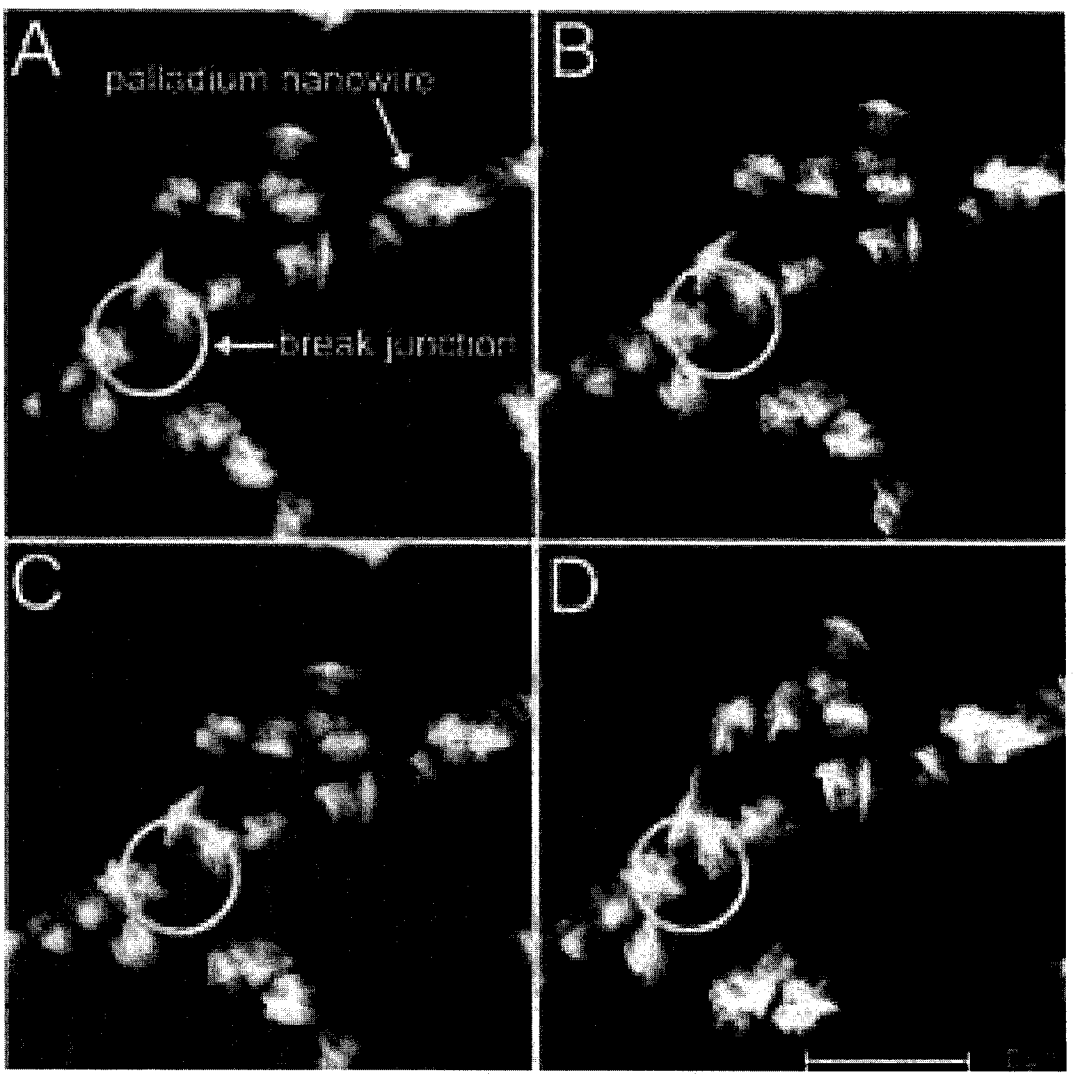

Figure 1-6 Atomic force microscope images of a palladium mesowire on graphite surface. These images were acquired either in air or in a stream of hydrogen gas as indicated. A hydrogen-actuated break junction is highlighted (circle) [59, 60]

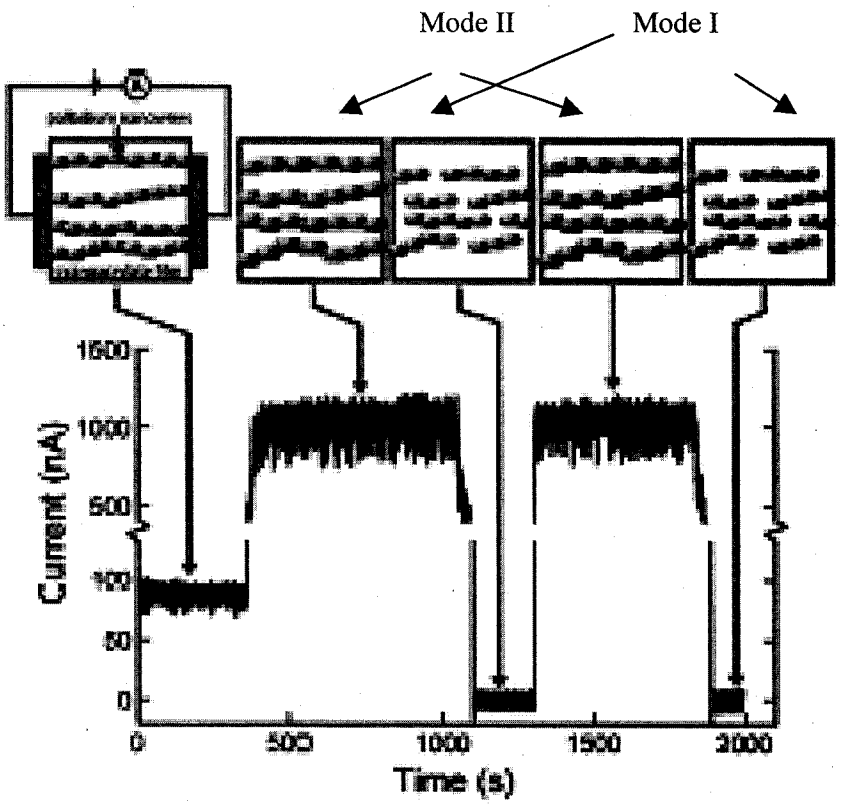

Figure 1-7 Measurement of current change when hydrogen absorbs and adsorbs in the nanowires. In this case, an irreversible transition from mode I to mode II operation was observed. The mechanism proposed from the switch from mode I to mode II [59-61]

The other is called as the standard or conventional hydrogen sensing mechanism. When palladium nanowires are solid, hydrogen is detected when it adsorbs to these solid nanowires, boosting the nanowires' electrical resistance due to the formation of palladium hydride. The formation of palladium hydride will cause the metal lattice to expand by 3.5%. [64] As a result, the process of expanding in palladium nanowires sensor will cause the change of its electric resistance that can be used to detect the concentration of hydrogen. In such systems, the absorption of hydrogen is accompanied by a measurable increase in electrical resistance. [64] Based on this phenomenon, palladium nanocluster devices technology can also be applied to a wide range of other chemical sensing applications. [64]

When palladium is exposed to a gas mixture that contains hydrogen gas, hydrogen molecules will dissociate into hydrogen atoms that diffuse into the palladium lattice and react with palladium to form palladium hydride (PdH_x). The electrical resistance of PdH_x is higher than that of pure palladium. [65]

Here, Yu, et al. [65] use sensitivity and response time to compare the hydrogen sensing performance of different samples. The sensitivity S is defined as the percentage of resistance change by the formula (1-1).

$$S = \frac{R_S - R_0}{R_0} \times 100\% \qquad (1\text{-}1)$$

Where R_0 is the resistance of the sensor in the presence of argon only and R_s is the resistance after exposure to a fixed percentage of hydrogen. The percentage of resistance change ($\Delta R / R_0$) takes into account the dimensions of the sample and allows comparison between different samples. [65]

Hydrogen sensor made of palladium nanowires will be affordable. As we know, a hydrogen sensor is only used very small amount of palladium, the cost should also be inexpensive although palladium is an expensive precious metal. [59] However, hydrogen sensor made of palladium nanowires is still being developed for the huge market, because several key problems including whether the sensors can be made to withstand poisonous contaminants in the air and whether the sensors will stand up to long-term operation should also be considerate and solved in practical use.

Hydrogen is an explosive gas currently wide used in many industries. [66] It may become the fuel of the future, replacing fossil fuels. Hydrogen sensors built by palladium nanowires will have many advantageous properties for hydrogen detection, such as, low cost, fast response time, high sensitivity, and low power consumption. [66]

The investigation of hydrogen sensors built using palladium nanowires is attracting great interest due to its huge market with rapidly developing fuel cells technology. They can be used for leak detection and process control in chemical and petroleum industries because of the special interaction between palladium and hydrogen. [66] So, there is already a huge market for the applications of hydrogen sensors. [66] These sensors could also be applied to the following areas quoted from reference [66]:

- Monitoring concentrations of hydrogen in Fuel Cells
- Leak detection during hydrogen transportation and storage
- Failure detection of impending electrical power transformer
- Monitoring industrial process gas
- Detecting hydrogen concentrations inside lead acid storage batteries
- Hydrogen leakage sensing during the chemical process and in some petrochemical applications

1.3.2 Synthetic approaches to palladium nanowires

Palladium is an ideal material for hydrogen sensing because it selectively absorbs hydrogen gas. Hydrogen sensor built by palladium nanowires promises wide application in the near future with increasing hydrogen consumption. The first practical nanoscale hydrogen sensor made of palladium nanowires at Penner's group is high sensitivity for the small amount hydrogen detection in a rapid response and requires low power. [59, 60] With the widespread use of hydrogen as a fuel, together with rapidly developing fuel cell technology, the fabrication of palladium nanowires using economic methods has attracted great interest. Some investigations on fabricating palladium nanowires have already been carried out [58-92]. Palladium nanowires built in different processes are outlined below.

Penner's group [59-61] developed the palladium meso- or nanowires on highly oriented pyrolytic graphite (HOPG) surfaces. After palladium nanowires are electrochemically grown on the steps of graphite surface. They are then embedded and transferred onto an adhesive polymer film. The film is then peeled off the graphite, flipped over, and placed on a glass slide that is easy to build a nanoscale hydrogen sensor, as shown in Figure 1-8. The application of silver contacts to the ends of 10 to 100 mesowires, arrayed electrically in parallel, produced sensors and switches that exhibited a high conductivity state in the presence of hydrogen, and a low conductivity state in the absence of hydrogen, as shown in Figure 1-8 (a, b). As hydrogen sensor using palladium nanowires can be manufactured very small, it can be easily carried and used for hydrogen leak detection in various work environments. The device can detect H_2 concentration in air from 1 to 10%. For sure, it can be used to detect hydrogen leak before it is up to the explosive limit in air. As we know if the concentration of hydrogen in air is over 4%, the mixture gas is easily explosive. Atashbar et al [67] and Xiao et al [68] use the same method to obtain step-edges decorated Pd or Pd-Ni alloy nanowires by electrodeposition.

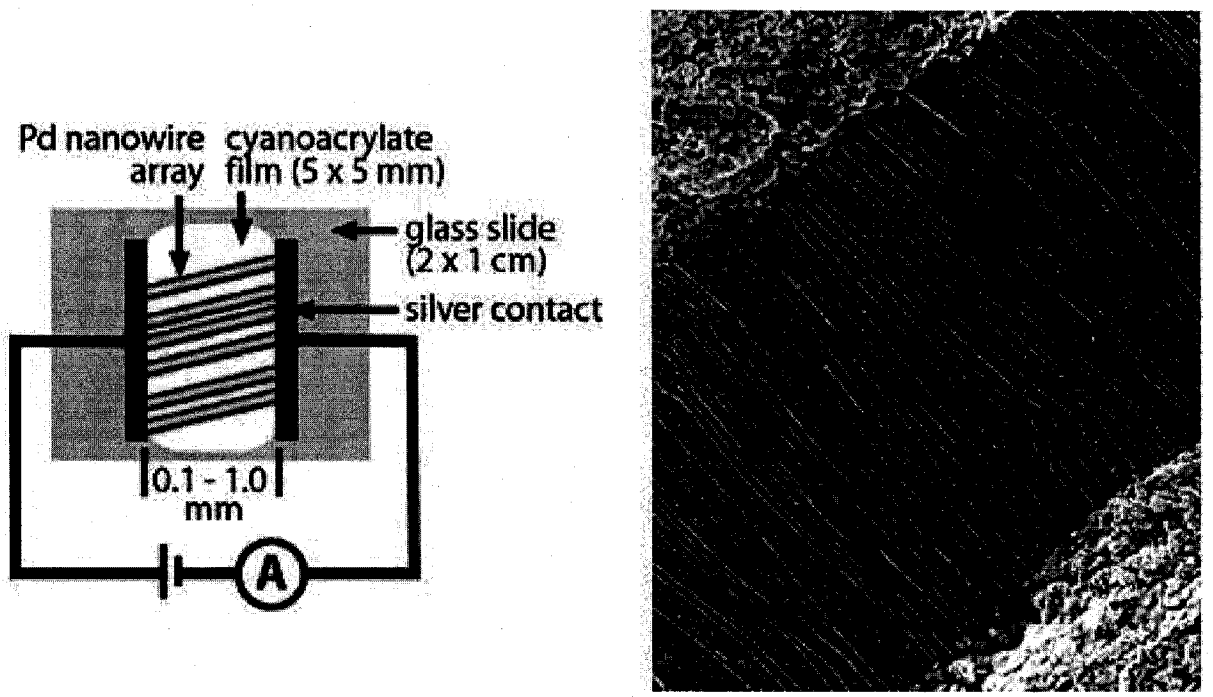

(a) (b)

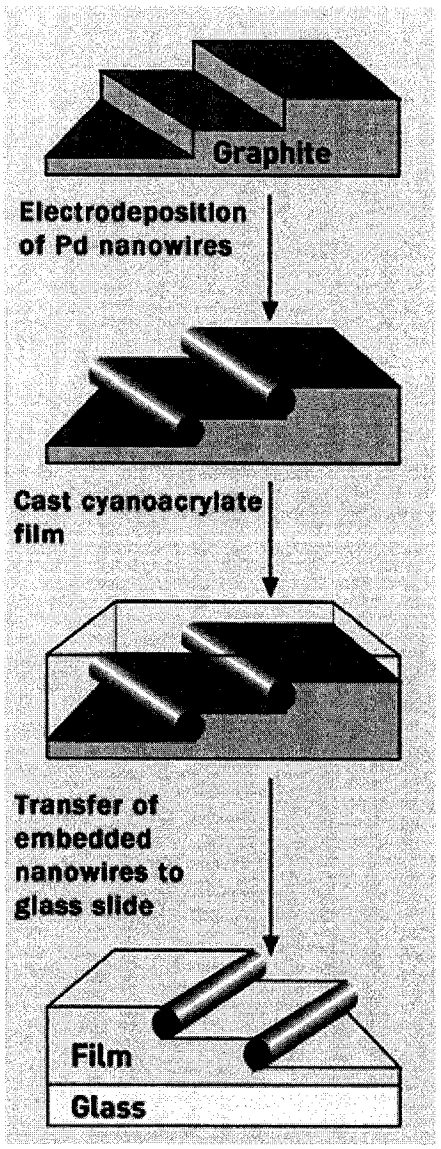

(c)

Figure 1-8 (a) Schematic diagram of a palladium mesowire array (PMA) hydrogen sensor or switch; (b) SEM image of a PMA-based hydrogen sensor; and (c) Palladium nanowires are electrochemically grown on the steps of a graphite surface and then embedded in an adhesive film. The film is then peeled off the graphite, flipped over, and placed on a glass slide. [59-61]

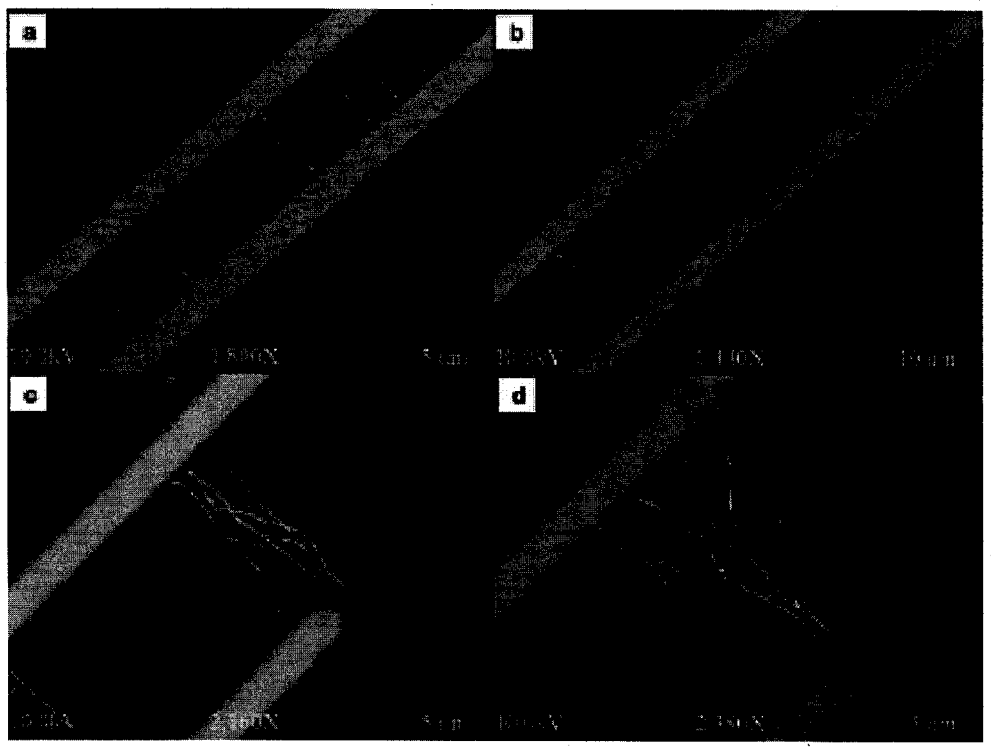

Figure 1-9 SEM images of Pd nanowires assembled between electrodes under an applied AC signal of 10 Vrms and 300 kHz. The nanowires have an approximate diameter of 100 nm. Experiments involved palladium acetate dissolved in 10 mM HEPES buffer, pH 6.5, diluted 8 from saturation. Gap spacing between electrodes: (a) 10 μm, (b) 15 μm, (c) 20 μm, (d) 25 μm. [69]

Cheng et al [69] has found that "conducting nanowires are self-assembled between microelectrodes from palladium acetate solution on applying an alternating electric field of relatively high intensity and frequency". One can see the palladium wires were formed spontaneously "along the direction of the electric field" and they have "high uniformity and conductivity" as shown in Figure 1-9. [69] Figure 1-9 illustrates that the nanowires having an approximate diameter of 100 nm formed under an AC signal of 10 V and 300 KHz. Wires are arrayed perpendicular to the electrodes and parallel to the direction of the electric field. The density of nanowires varied with electrode gap size and hence peaks electric field strength. Palladium nanowires are self-assembled along the entire length of the 10 μm- and 15 μm-wide electrodes as illustrated in Figures 1-9(a) and 1-9(b). By contrast, when the gap size is enlarged to 20 μm or 25 μm, only a few nanowires formed in Figures 1-9(c) and 1-9(d). [69] "This finding demonstrates the favorable electrical properties of obtained nanowires which have potential use for assembly of nanoscale electronic structures and systems such as nanoscale fuses, device interconnection, chemical sensors and assembly of functional molecular devices."[69]

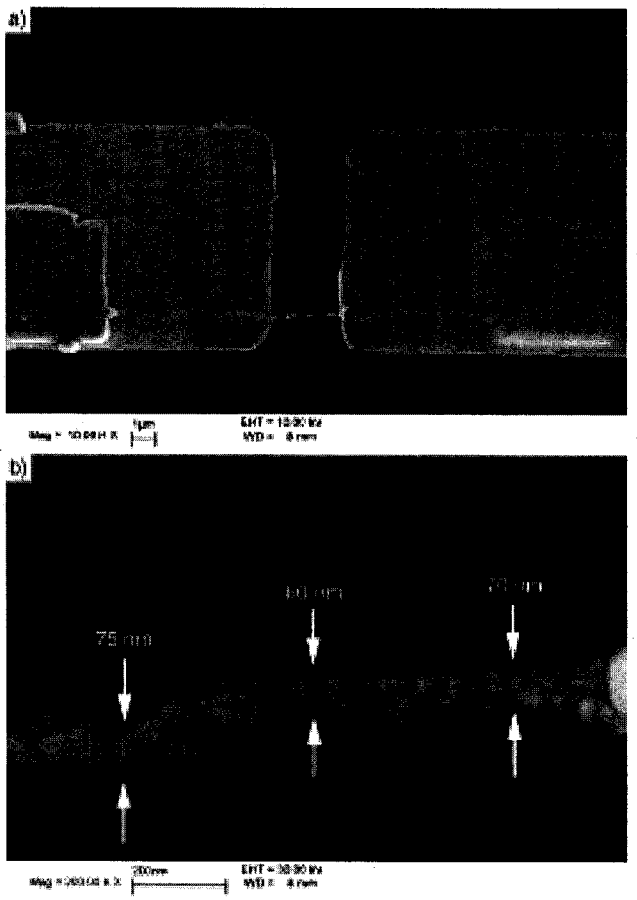

Figure 1-10 SEM images of a single Pd nanowire grown between gold electrodes using an e-beam patterned electrolyte channel and electrodeposition (a) with a diameter of between 70 and 85 nm (b) [70-73]

In order to obtain highly ordered palladium nanowire arrays for the application in microelectromechanical and nanoelectromechanical systems (MEMS/NEMS), patterns are built using photolithography or electron beam lithography. For example, Yun et al [70-73] electrochemically deposited palladium nanowires for individually addressable sensor array, as shown in Figure 1-10. One can see that "a single Pd nanowire is fabricated by electrodeposition in electrolyte channels patterned with electron-beam lithography". [72] "This fabrication technique can produce nanowires with controlled dimensions, positions, alignments and chemical compositions, and potentially enables the use of a wide range of materials for creating arrays of single nanowire sensors. Additionally, the growth of nanowires using this technique would allow for easy integration with existing silicon technology."[72] Huang et al [74] deposited Au-Pd alloying nanowire using electron-beam lithography pattern on a silicon substrate for hydrogen sensing. This nanomechanical system provides a new method for studying the formation of interstitial hydrogen in metals at very low pressures. [74]

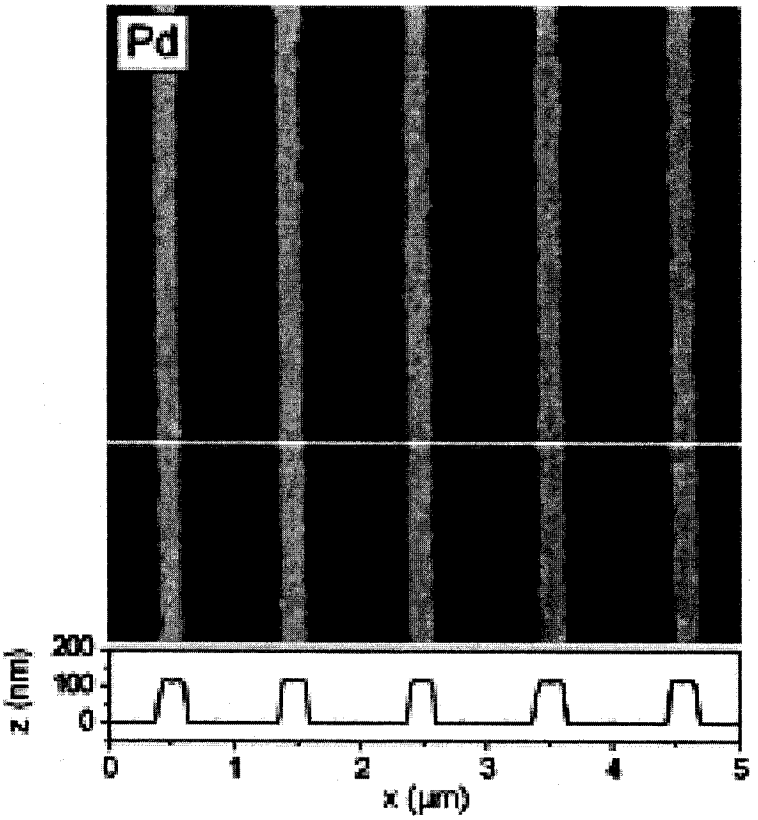

Figure 1-11 Pd nanowires deposited on the lithographic pattern of oxidized Si substrates using eicosanethiol as the ink or electroless deposition process [75]

Microcontact printing is a soft-lithographic technique for the fabrication of micropatterns. [75-77] Figure 1-11 illustrates that Pd nanowires are deposited on oxidized Si substrates produced by the "print & etch" approach using eicosanethiol (ECT) as the ink. The printed self-assembly monolayers perfectly protect the underlying metals and preserve their initial thickness (at least 100 nm) during the etch process. The width of the wires varies due to surface diffusion of ECT molecules during printing and the duration of the etch process. The horizontal lines indicate the location of the cross-section profiles shown in the insets of Figure 1-11. [75-77]

Additionally, palladium nanowires can also be built on different templates such as anodized alumina [78-80], mesoporous silica [81], carbon nanotube fibers [82-86] and DNA [87, 88]. When palladium is deposited in porous substrate, palladium anowires or nanorods built on templates have been observed in the mesopore morphology from a coiled cylindrical to a spherical cage-like geometry, as shown in Figure 1-12. One can see that the mesostructures produced by confined syntheses are useful as templates for fabricating highly ordered mesostructured nanowires and nanowire arrays. When the diameter of the templates is small (nanochannel diameter), highly ordered palladium nanowires will be built in the line of cages. [89] When the size of templates is enlarged, palladium nanotubes will be fabricated on the wall of cages. [89-93] Even though some of the experimentally observed structures have axial symmetry, Wu et al. [89] also carried out calculations in cylindrical (*r,z*) coordinates (bottom row). "The smaller dimensionality

of the axially symmetric problem allowed us to study a wider range of the parameter space. In tight confinement, hexagonal packing of the cylindrical micelles running parallel to the pore axis would impose high stress on the system. This stress can be relieved by arranging the system into a set of concentric shells. In each shell the cylinders bend and tilt with respect to the pore axis, thus forming helices or doughnuts." [89]

So far, there are many different templates used for the fabrication of metal nanowire arrays. Anodized alumina oxides (AAO) and mesoporous silica templates are ideal templates for the synthesis of palladium nanowires because they possess many desirable characteristics including tunable pore dimensions, good mechanical strength and thermal stability. [78-80] For example, Kim et al [78] successfully prepared highly ordered palladium nanowire arrays on AAO template. Lee [81] used chemical vapor infiltration process to obtain size-controlled palladium nanowires on mesoporous silica template.

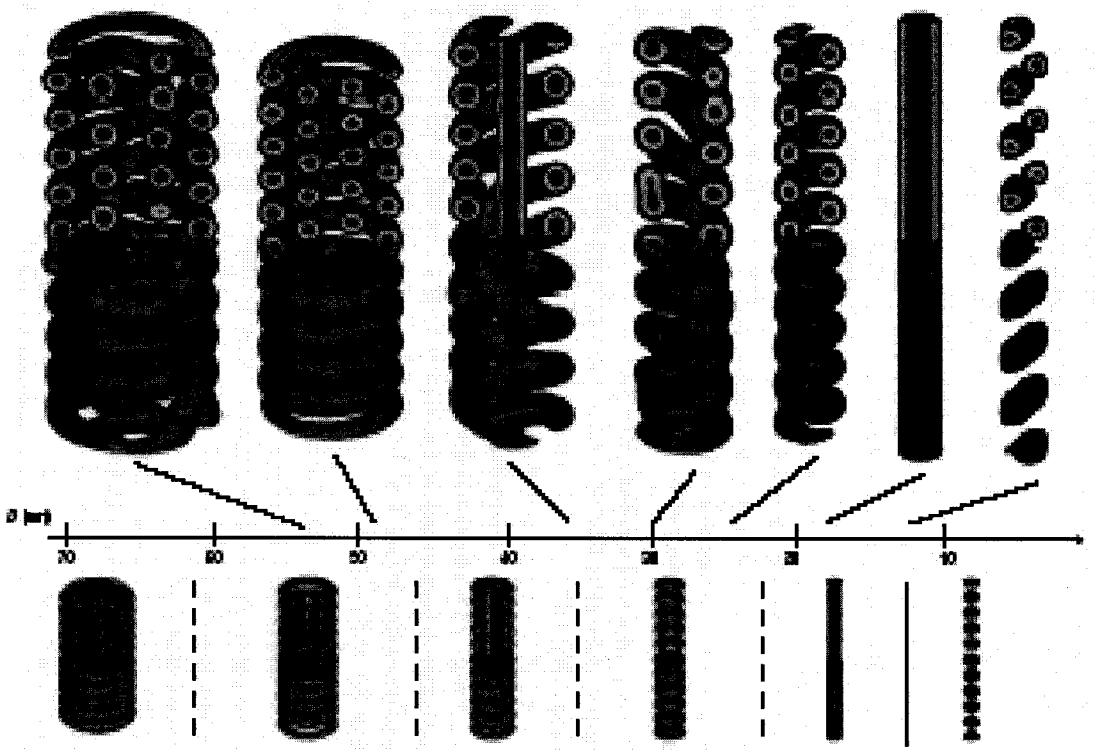

Figure 1-12 Simulated structures of the confined self-assembly in cylindrical confinement with varying cylinder diameter (D), calculated using self-consistent field theory [89]

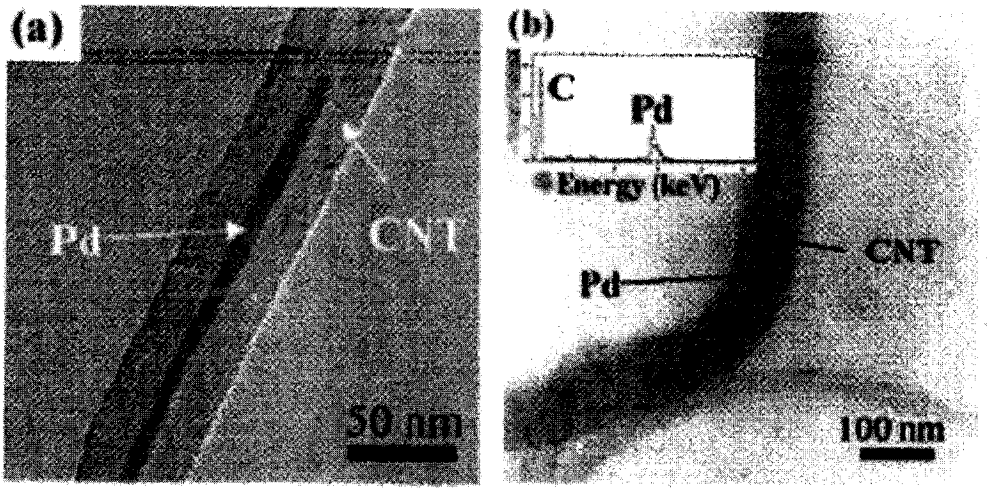

Figure 1-13 Pd nanowire formed on carbon nanotube template [83]

Metallic nanowires or nanorods can also be grown with supercritical fluid (SCF) method or chemical vapor deposition technique utilizing multiwalled carbon nanotubes (CNT) as templates. [83] These metallic nanowires can take the form of the inner cavity of the CNT. As a result, the nanowires followed the morphologies of CNT can be straight or curved. [82] Metal/CNT nanowire composite has been considered for catalysts, sensors, semiconductor devices, contrast agents in magnetic resonance imaging, new reinforced metal-nanofiber materials, and in xerography. [83]

Examples of palladium nanowires grown with the SCF methods are illustrated in Figure 1-13. [83] The transmission electron microscopy (TEM) images show the formation of palladium nanowires in CNT and they are 7 – 9 nm in diameter and more than 200 nm in length. The diameter of palladium nanowire corresponds to the inner diameter of the CNT and varies due to fluctuations in the CNT diameter. It confirms that the nanowire was made purely of palladium based on energy dispersive X-ray spectrum (EDS) conducted on a single nanowire. In addition, thin single-walled carbon nanotubes, made by a simple filtration process, subsequently coated with palladium by sputtering deposition, are shown to be promising detectors of hydrogen under very low power and short exposure time. [84]

Deng et al [87] and Nishinaka et al [88] reported a simple method for the fabrication of ordered palladium nanowires on DNA protein templates. "Molecular combing was used to stretch and align linear λ-DNA molecules into parallel or crossed patterns. Subsequent metallization of DNA through electroless palladium deposition yielded 1D parallel or 2D crossed metallic nanowire arrays. This method has potential use in building interconnects between nanosized building blocks toward nanodevice construction."[87]

Sun et al [93] describes a general approach that generates nanoscale hollow structures of metals by reacting solutions of appropriate salt solutions with solid templates of a more reactive metal. Typical examples include Au^{3+}, Pt^{2+}, and Pd^{2+} salts and nanoparticles or nanowires of silver. "The morphology, void space, and wall thickness of these hollow structures are all determined by the solid templates, which are completely converted into soluble species during the replacement reaction." [93] "Both electron

microscopy and diffraction studies indicate that single crystalline hollow structures of metals can also be obtained when the templates are single crystals. These metallic hollow structures, having well-controlled sizes and shapes, are expected to find use in a number of applications that involve nanoscale encapsulation, drug delivery, plasmon photonics, and calorimetric sensing." [93]

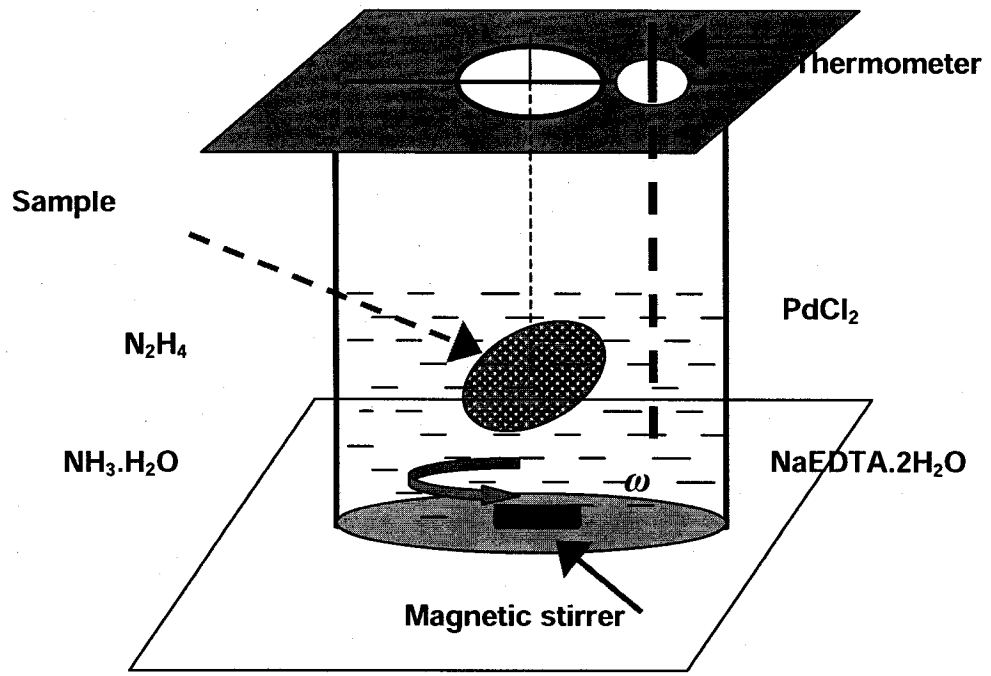

Figure 1-14 Schematic of electroless deposition of palladium

Even though there are numerous reports of the formation of palladium nanowires that are probably used for hydrogen sensing, the exploration of novel and economic approach to build palladium nanowires in a controllable manner is very important for their engineering applications. In this thesis, we present a simple and economic process of electroless plating to build palladium nanowires on porous stainless steel substrate. Electroless plating is a process that requires neither electrodes nor any external sources of electricity to deposit a metal. [94] The deposition is an autocatalytic process that is controlled by the chemical reduction of metallic ions in an aqueous solution containing a reducer. Autocatalytic plating is defined as "deposition of a metallic coating by controlled chemical reduction that is catalyzed by the metal or alloy being deposited". [94] The deposition of palladium can be described by the chemical reaction equation (1-2). The experimental operation is illustrated in Figure 1-14.

$$2Pd\,[NH_3]_4^{2+} + N_2H_4 + 4OH^{-1} \rightarrow 2Pd^{o} + N_2 + 4H_2O + 8\,NH_3 \qquad (1\text{-}2)$$

Based on the autocatalytic reaction equation, palladium generated from the plating solution is directly dependent on the concentration of Pd^{2+}, pH data (the addition of NH_3

or OH^{-1}), the addition of reducer (N_2H_4) and experimental temperature. So the deposition of palladium nanowires can be controlled based on the reaction equation (1-2).

1.3.3 Purpose of palladium nanowires research

With the widespread use of hydrogen as a fuel, hydrogen sensors are required based on safety concern. Palladium is a typical material for this type of applications because palladium adsorbs hydrogen easily. However, the fabrication of palladium nanowires is challenging and various techniques for producing controllable and economic palladium nanowires are being explored.

Purpose of this thesis will demonstrate a simple and inexpensive electroless deposition technique for creating palladium nanowires on rough stainless steel surface. Palladium nanowires are well organized by nanoparticles that are generated from the autocatalytic reaction in the initial stage of the deposition and without any external field. This discovery is promising for the desired palladium nanowire arrays built in a simple and inexpensive method for potential engineering applications.

The objectives of palladium nanowires research are outlined below.

(1) To investigate how and why palladium nanowire is built on porous stainless steel substrate by electroless deposition process in order to understand the formation mechanism and to control the dimension of palladium nanowires.

(2) To analyze the effect of surface defects on the formation of palladium nanowires in order to design required palladium nanowire arrays for engineering application.

1.4 References

1. http://www.pca.state.mn.us/oea/p2/hydrogen.cfm
2. http://www.anl.gov/Media_Center/News/2005/news050525.html
3. Membrane separations technology principles and applications, edited by Richard D. Noble and S. Alexander Stern, ELSEVIER, Amsterdam, 1995, p. 593.
4. The hydrogen economy: the creation of the worldwide energy web and the redistribution of power on earth, Jeremy Rifkin, Pengium Group (USA) Inc. 2003
5. Jose G. Sanchez Marcano, Theodore T. Tsotsis. Catalytic membranes and membrane reactors, Wiley-VCH Verlag GmbH, Weinheim, 2002, p. 4.
6. W.J. Koros and G.K. Fleming. Review, membrane-based gas separation, Journal of Membrane Science, 83, 1-80 (1993).
7. Pratibha Pandey, R.S. Chauhan. Membrane for gas separation, Progress in Polymer Science, 26, 853-893 (2001).
8. Arian Nijmerijer. Hydrogen-selectrive silica membranes for use in membrane steam reforming, Thesis, University of Twente, Enschede, 1999.
9. Young-Seok Kim, Seung-Man Yang. Preparation of continuous mesoporous silica thin film on a porous tube, Advanced Materials, 14, 1078-1081 (2002).
10. Masashi Asaeda, Shin Yamasaki. Separation of inorganic/organic gas mixtures by porous silica membranes, Separation and Purification Technology, 25, 151-159 (2001).
11. V. Richard, E. Favre, D. Tondeur, A. Nijmeijer. Experimental study of hydrogen, carbon dioxide and nitrogen permeation through a microporous silica membrane, Chemical Engineering Journal, 84, 593-598 (2001).
12. Nieck E. Benes, Herve Jobic, Valerie Reat, Henny J.M. Bouwmeester, Henk Verweij. Mobility of hydrogen in microporous silica studied with quasi-elastic neutron scattering, Separation and Purification Technology 32, 9-15 (2003).
13. Dong-Wook Lee, Bongkuk Sea, Kwan-Young Lee, and Kew-Ho Lee. Preparation and characterization of SiO_2 composite membranes for purification of hydrogen for PEMFC, Ind. Eng. Chem. Res. 41, 3594-3600 (2002).
14. R.M. de Vos and H. Verweij. High-selectivity, high-flux silica membranes for gas separation, Science, 279, 1710-1711 (1998).
15. R.S.A. de Lange, K. Keizer, A.J. Burggraaf. Analysis and theory of gas transport in microporous sol-gel derived ceramic membranes. Journal of Membrane Science, 104, 81-100 (1995).
16. Pasi Mikkola, Erkki Levanen, Jarl B. Rosenholm, Tapio Mantyla. Colloidal processing of aluminum oxide powder for membrane applications, Ceramics International, 29, 393–401 (2003).
17. P.M. Biesheuvel. Porous ceramic membranes - suspension processing, mechanical and transport properties, and application in the osmotic tensiometer, Thesis, University of Twente, Enschede, 2000.
18. A. Nijmeijer, H. Kruidhof, R. Bredesen and H. Verweij. Preparation and properties of hydrothermally stable g-alumina membranes, J. Am. Ceram. Soc. 84, 136-40 (2001).
19. A.S.T. Chiang, Keui-jung Chao. Membranes and films of zsolite and zeolite-like materials, Journal of Physics and Chemistry of Solids, 62, 1899-1910 (2001).

20. Franziska Scheffler, Ralph Herrmann, Wilhelm Schwieger, Michael Scheffler. Preparation and properties of an electrically heatable aluminium foam/zeolite composite, Microporous and Mesoporous Materials, 67, 53-59 (2004).
21. Zhongqiang Xu, Qingling Chen, Guanzhong Lu. Preparation of zeolite membranes on porous ceramic substrates with zeolite seeds, Journal of Natural Gas Chemistry, 11, 171-179 (2002).
22. Mark B. Shiflett, Henry C. Foley. On the preparation of supported nanoporous carbon membranes. Journal of Membrane Science, 179, 275–282 (2000).
23. M.B. Rao, S. Sircar. Performance and pore characterization of nanoporous carbon membranes for gas separation, Journal of Membrane Science, 110, 109-118 (1996).
24. Sarah M. Cooper, Brett A. Cruden, and M. Meyyappan. Gas transport characteristics through a carbon nanotubule, Nano Letters, 4, 377-381 (2004).
25. Richard W. Baker. Membrane technology and applications, the second edition, Wiley, p 303, 311 (2004).
26. http://www.rebresearch.com/H2perm2.htm
27. E. Charles H. Sykes, Luis C. Fernandez-Torres, Sanjini U. Nanayakkara, Brent A. Mantooth, Ryan M. Nevin and Paul S. Weiss, Observation and manipulation of subsurface hydride in Pd {111} and its effect on surface chemical, physical, and electronic properties, Proc. Natl. Acad. Sci. 102, 17907-17911 (2005).
28. F.A. Lewis, J.P. Magennis, S.G. McKee and P.J.M. Ssebuwufu. Hydrogen chemical potentials and diffusion coefficients in hydrogen diffusion membranes, Nature, 306, 673-675 (1983).
29. C. Sachs, A. Pundt, R. Kirchheim, M. Winter, M. T. Reetz, D. Fritsch. Solubility of hydrogen in single-sized palladium clusters, Physical Review B. 64, 075408 (2001).
30. T. Mitsui, M.K. Rose, E. Fomin, D.F. Ogletree and M. Salmeron. Dissociative hydrogen adsorption on palladium requires aggregates of three or more vacancies, Nature, 422, 705-707 (2003).
31. Timothy L. Ward, Tien Dao. Model of hydrogen permeation behavior in palladium membranes, Journal of Membrane Science, 153, 211-231(1999).
32. F.C. Gielens, H.D. Tong, C.J.M. van Rijn, M.A.G. Vorstman, J.T.F. Keurentjes, High-flux palladium-silver alloy membranes fabricated by microsystem technology, Desalination 147, 417-423 (2002).
33. Yanglong Guo, Guanzhong Lu, Yunsong Wang, Ren Wang, Preparation and characterization of Pd-Ag/ceramic composite membrane and application to enhancement of catalytic dehydrogenation of isobutene, Sep. Purif. Technol. 32, 271-279 (2003).
34. Kaihu Hou, Ronald Hughes. Preparation of thin and highly stable Pd/Ag composite membranes and simulative analysis of transfer resistance for hydrogen separation, Journal of Membrane Science, 214, 43-55 (2003).
35. G. Xomeritakis, Y.S. Lin, Fabrication of a thin palladium membrane supported in a porous ceramic substrate by chemical vapor deposition, Journal of Membrane Science, 120, 261-272 (1996).
36. Ting-Chia Huang, Ming-Chi Wei, Huey-Ing Chen. Preparation of hydrogen-permselective palladium-siliver alloy composite membranes by electroless co-deposition, Separation and Purification Technology, 32, 239-245 (2003).

37. Sushil Adhikari and Sandun Fernando. Hydrogen membrane separation technologies, Ind. Eng. Chem. Res. 45, 875-881 (2006).
38. Shin-Kun Ryi, Jong-Soo Park, Sung-Hyun Kim, Sung-Ho Cho, Joo-Seok Park and Dong-Won Kim. Development of a new porous metal support of metallic dense membrane for hydrogen separation, Journal of Membrane Science, 279, 439-445 (2006).
39. Balamurali Krishna R. Nair and Michael P. Harold. Hydrogen generation in a Pd membrane fuel processor: Productivity effects during methanol steam reforming, Chemical Engineering Science, 61, 6616-6636 (2006).
40. D. Yepes, L.M. Cornaglia, S. Irusta and E.A. Lombardo. Different oxides used as diffusion barriers in composite hydrogen permeable membranes, Journal of Membrane Science, 274, 92-101 (2006).
41. J. Shu, B. P. A. Grandjean, E. Ghali and S. Kaliaguine. Simultaneous deposition of Pd and Ag on porous stainless steel by electroless plating, Journal Membrane Science, 77, 181-195 (1993).
42. Seung-Eun Nam, Sang-Hak Lee, Kew-Ho Lee. Preparation of a palladium alloy composite membrane supported in a porous stainless steel by vacuum electrodeposition, Journal of Membrane Science, 153, 163-173 (1999).
43. F.C. Gielens, H.D. Tong, C.J.M. van Rijn, M.A.G. Vorstman, J.T.F. Keurentjes. Microsystem technology for high-flux hydrogen separation membranes, Journal of Membrane Science 243, 203-213 (2004).
44. C.J.M. van Rijn. Nano and micro engineered membrane technology, Membrane Science and Technology Series, 10. Elsevier 2004, p 267
45. S.V. Karnik, M.K. Hatalis, M.V. Kothare. Palladium based micro-membrane for water gas shift reaction and hydrogen gas separation, Processings of the 5th International Conference on Microreaction Technology (IMRET 5), Strasbourg, France, May 27-30, 2001.
46. John E. Mahan. Physical Vapor Deposition on Thin Films, A Wiley-Interscience Publication, John Wiley & Sons, Inc., 2000.
47. Sumio Sakka. Sol-gel science and technology: topic in fundamental research and applications, Boston, Kluwer Academic Publishers, 2003
48. M. Schlesinger, M. Paunovic. Modern Electroplating, fourth edition, Toronto, Wiley, 2000.
49. M. Pilaski, M.M. Lohrengel. Electrochemical microstructuring of ultra-thin passive films on aluminium, Electrochimica Acta, 48, 1309-1313 (2003).
50. P.P.A.C. Pex, Y.C. van Delft, L.A. Correia, H.M. van Veen, D. Jansen, J.W. Dijkstra. Palladium alloy membranes for energy efficient membrane reactors, Proc. Of the 8th International Conference on Inorganic Membranes, Cincinnati, July 18-22, p. 524-527 (2004).
51. B. Celan Akis. Preparation of Pd-Ag/PSS composite membranes for hydrogen separation, Master thesis, Worcester Polytechnic Institute, 2004.
52. Jun Shu. Development of palladium-based catalytic membrane reactors, Ph.D thesis, Laval University, 1994.
53. Pratibha Pandey, R.S. Chauhan. Membranes for gas separation, Progress in Polymer Science, 26, 853-893 (2001).
54. B. H. Howard, R. P. Killmeyer, K. S. Rothenberger, A. V. Cugini, B. D. Morreale, R. M. Enick and F. Bustamante. Hydrogen permeance of palladium–copper alloy

membranes over a wide range of temperatures and pressures, Journal of Membrane Science, 241, 207-218 (2004).
55. Kennth J. Bryden, Jackie Y. Ying. Nanostructured palladium-iron membranes for hydrogen separation and membrane hydrogenation reactions, Journal of Membrane Science 203, 29-42 (2002).
56. http://www.wahchang.com/wahchang/pages/products/hmm/HydrogenMetalMembrane.pdf.
57. http://www.ngk.co.jp/english/info/develo/topics3/
58. http://www.mottcorp.com
59. F. Favier, E.C. Walter, M.P. Zach, T. Benter, and R.M. Penner. Hydrogen sensors and switches from electrodeposited palladium mesowire arrays, Science 293, 2227-2231 (2001).
60. E.C. Walter, R.M. Penner, H. Liu, K.H. Ng, M.P. Zach, and F. Favier, Sensors from electrodeposited metal nanowires, Surface and Interface Analysis 34, 409-412 (2002).
61. Erich C. Walter, Michael P. Zach, Frederic Favier, Benjamin J. Murray, Koji Inazu, John C. Hemminger, and Reginald M. Penner, Metal nanowire arrays by electrodeposition, Chemphyschem 4, 131-138 (2003).
62. Sz. Csonka, A. Halbritter, G. Mihaly, O.I. Shklyarevskii, S. Speller, and H. van Kempen, Conductance of Pd-H nanojunctions, Physical Review Letters 93, 016802 (2004).
63. Massood Z Atashbar, Deep Banerji, Srikanth Singamaneni and Valery Bliznyuk. Deposition of parallel arrays of palladium nanowires and electrical characterization using microelectrode contacts, Nanotechnology 15, 374–378 (2004).
64. F.A. Lewis. The palladium hydrogen system, Academic Press, New York, 1967.
65. Shufang Yu, Ulrich Welp, Leonard Z. Hua, Andreas Rydh, Wai K. Kwok, and H. Hau Wang. Fabrication of palladium nanotubes and their application in hydrogen sensing, chem. mater. 17, 3445-3450 (2005).
66. http://www.nanoclusterdevices.com/index.cfm/Applications/Hydrogen_Sensors/index
67. Massood Z. Atashbar, Deep Banerji, and Srikanth Singamaneni. Room-temperature hydrogen sensor based on palladium nanowires, IEEE Sensors Journal, 5, 792-797 (2005).
68. Yaokun Xiao, Gang Yu, Juan Yuan, Jinyin Wang, Zongzhang Chen, Fabrication of Pd-Ni alloy nanowire arrays on HOPG surface by electrodeposition, Electrochimica Acta 51, 4218-4227 (2006).
69. Chuanding Cheng, Ravi Kanth Gonela, Qun Gu, and Donald T. Haynie. Self-assembly of metallic nanowires from aqueous solution, Nano Letters, 5, 175-178 (2005).
70. Mangesh A. Bangar, Kumaran Ramanathan, Minhee Yun, Choonsup Lee, Carlos Hangarter, and Nosang V. Myung, Controlled growth of a single palladium nanowire between microfabricated electrodes, Chem. Mater. 16, 4955-4959 (2004).
71. Minhee Yun, Nosang V. Myung, Richard P. Vasquez, Choonsup Lee, Erik Menke, and Reginald M. Penner, Electrochemically grown wires for individually addressable sensor arrays, Nano Letters 4, 419-422 (2004).

72. Yeonho Im, Chiinsup Lee, Richard P. Vasquez, Mangesh A. Bangar, Nosang V. Myung, Eric J. Menke, Reginald M. Penner, and Minhee Yun. Investigation of a single Pd nanowire for use as a hydrogen sensor, small 2006, 2, No.3, 356-358
73. Minhee Yun, Nosang V. Myung, Richard P. Vasquez, Jianjun Wang, and Harold Monbouquette, Nanowire growth for sensor arrays, Nanofabrication Technologies, Ed. E.A. Dobisz, SPIE Proceedings, 5220 (2003).
74. X.M.H. Huang, M. Manolidis, Seong Chan Jun, and J. Hone, Nanomechanical hydrogen sensing, Applied Physics Letters 86, 143104 (2005).
75. Matthias Geissler, Heiko Wolf, Richard Stutz, Emmanuel Delamarche, Ulrich-Walter Grummt, Bruno Michel, and Alexander Bietsch. Fabrication of metal nanowires using microconnect printing, Langmuir, 19, 6301-6311 (2003).
76. Alain Carvalho, Matthias Geissier, Heinz Schmid, Bruno Michel, and Emmanuel Delamarche, Self-assembled monolayers of eicosanethiol on palladium and their use in microcontact printing, Langmuir, 18, 2406-2412 (2002).
77. Byron D. Gates, Qiaobing Xu, Michael Stewart, Declan Ryan, C. Grant Willson, and George M. Whitesides. New approaches to nanofabrication: molding, printing, and other techniques, Chem. Rev. 105, 1171-1196 (2005).
78. Kyungtae Kim, Moonjung Kim, Sung M. Cho, Plused electrodeposition of palladium nanowire arrays using AAO template, Materials Chemistry and Physics, 96, 278-282 (2005).
79. A. Johansson, J. Lu, J. –O. Carlsson and M. Boman. Deposition of palladium nanoparticles on the pore walls of anodic alumina using sequential electroless deposition, J. Appl. Phys. 96, 5189-5194 (2004).
80. Sarah J. Hurst, Emma Kathryn Payne, Lidong Qin, and Chad A. Mirkin. Multisegmented one-dimensional nanorods prepared by hard-template synthetic methods, Angew. Chem. Int. Ed. 45, 2672-2692 (2006).
81. Kyung-Bok Lee, Sang-Min Lee, Jinwoo Cheon, Size-controlled synthesis of Pd nanowires using a esoporous silica template via chemical vapor infiltration, Adva. Mater. 13, 517-520 (2001).
82. L.H. Chan, K.H. Hong, S.H. Lai, X.W. Liu and H.C. Shih. The formation and characterization of palladium nanowires in growing carbon nanotubes using microwave plasma-enhanced chemical vapor deposition, Thin Solid Films, 423 (2003) 27-32
83. US patent 6,235,675 (Title: Methods of forming materials containing carbon and boron, methods of forming catalysts, filaments comprising boron and carbon, and catalysts), issued May, 2001
84. Jennifer Sippel-Oakley, Hung-Ta Wang, Byoung S. Kang, Zhuangchun Wu, Fan Ren, Andrew G. Rinzler, and Stephen J Pearton, Carbon nanotube films for room temperature hydrogen sensing, Nanotechnology 16, 2218-2221 (2005).
85. A. Govindaraj, B.C. Satishkumar, Manashi Nath, and C.N.R. Rao. Metal nanowires and intercalated metal layers in single-walled carbon nanotube bundles, Chem. Mater. 12, 202-205 (2000).
86. Alejandro Anson, Esperanza Lafuente, Esteban Urriolabeitia, Rafael Navarro, Ana M. Benito, Wolfgang K. Maser, and M.Teresa Martinez. Hydrogen capacity of palladium-loaded carbon materials, J. Phys. Chem. B 110, 6643-6648 (2006).
87. Zhaoxiang Deng and Chengde Mao, DNA-templated fabrication of 1D parallel and 2D crossed metallic nanowire arrays, Nano Letters 3, 1545-1548 (2003).

88. Taro Nishinaka, Atsushi Takano, Yuko Doi, Makiko Hashimoto, Akira Nakamura, Yushu Matsushita, Jiro Kumaki, and Eiji Yashima. Conductive metal nanowires templated by the nucleoprotein filaments, complex of DNA and RecA protein, J. Am. Chem. Soc. 127, 8120-8125 (2005).
89. Yiying Wu, Guosheng Cheng, Kirill Katsov, Scott W. Sides, Jianfang Wang, Jing Tang, Glenn H. Fredrickson, Martin Moskovits, and Galen D. Stucky, Composite mesostructures by nano-confinement, Nature materials 3, 816-822 (2004).
90. Tali Sehayek, Michal Lahav, Ronit Popovitz-Biro, Alexander Vaskevich, and Israel Rubinstein. Templates synthesis of nanotubes by room-temperature coalescence of metal nanoparticles, chem. Mater. 17, 3743-3748 (2005).
91. Martin Steinhart, Zhihong Jia, Andreas K. Schaper, Ralf B. Wehrspohn, Ulrich Gosele, and Joachim H. Wendorff. Palladium nanotubes with tailored wall morphologies, Adv. Mater. 15, 706-708 (2003).
92. Yugang Sun, Brian T. Mayers, and Younan Xia, Template-engaged replacement reaction: a one-step approach to the large-scale synthesis of metal, nanostructures with hollow interiors, Nano Letters, 2, 481-485 (2002).
93. Y. Xia, P. Yang, Y. Sun, Y. Wu, B. Mayers, B. Gates, Y. Yin, F. Kim, H. Yan. One-dimensional nanostructures: synthesis, characterization, and applications, Adv. Mater. 15, 353-389. (2003).
94. Edited by Glenn O. Mollory, June B. Hajdu. Electroless plating - Fundamental and Applications, William Andrew Publishing/Noyes, 1990, p 511.

CHAPTER 2 [1]

OBSERVATION OF PALLADIUM MEMBRANE FORMATION

2.1 Abstract

Membranes made of palladium and its alloys are used for the extraction of high quality hydrogen from a mixture of gases. Most of recent research is focused on the development technologies for depositing a durable ultra-thin palladium membrane on a porous substrate in order to assure a good mechanical support and maximize the flux of hydrogen permeation. The formation of palladium membrane deposited on porous stainless steel substrate by an electroless process is recorded and described in this chapter. The deposition progress of palladium around the pore area at the surface of the substrate in the initial stages is illustrated. A bridge model is presented to describe the membrane formation around the pore area of the substrate. This model, together with the micrographs showing the deposition progress on the pore areas, will lead to the control of the deposition process for a membrane fabrication as well as the design and modification of a substrate.

2.2 Introduction

The progress in adopting hydrogen as a clean fuel is directly related to the development of more efficient methods for hydrogen extraction from a hydrogen-containing gas mixture in a reactor. Membrane separation technology is regarded nowadays as a preferred method for production of high quality hydrogen. The membranes made of palladium and its alloys are familiar for the extraction of high purity hydrogen. [1-4] The interaction between palladium and hydrogen has been studied extensively in hydrogenation catalysts and chemical engineering because palladium absorbs hydrogen easily and palladium membranes have high hydrogen permeability, chemical compatibility and excellent hydrogen selectivity. [4-10] There are numerous reports of palladium membranes fabricated on the porous supports by an electroless deposition. [4, 11-16] Most efforts have been focused on the reduction of palladium membrane thickness and the improvement of hydrogen permeability, as palladium is expensive. [17-22] Palladium membrane is usually deposited on the porous substrate that can provide good mechanical support and probably reduce the thickness of the membrane. The surface of porous substrate usually comprises two different areas. One is coarse area. The other is pore area. The fabrication of a membrane and its quality is directly dependent on the progress of its deposition around the pore area. So far, there is no report of the investigation of the deposition progress at the porous substrate in the initial stages. The purpose of this research is to observe how a palladium membrane is built around the pore area with the extension of deposition time by the electroless process and to present a model to describe the deposition process.

[1] This chapter has been published as two articles in Journal of Membrane Science, 280, 705-711 (2006) and Applied Physics Letters, 87, 12913 (2005).

2.3 Experimental section

In this investigation, a 0.2 μm grade porous 316L stainless steel plate (30 cm x 38 cm) purchased from Mott Metallurgical Corporation was used as a substrate. Such metallic medium made by metal powders has been widely used as the substrates to provide mechanical strength for palladium membranes preparation. Samples were cut into size 20 mm x 20 mm and ϕ 45 mm (to deposit palladium membrane for hydrogen permeation test) and they were cleaned in an ultrasonic bath with acetone for 15 min. After cleaned, the samples were activated with 10% hydrochloric acid and rinsed with deionized water. Then, they were transferred immediately into an electroless plating bath for the deposition time of 30 s ~ 300 s for the samples (20 mm x 20 mm) and of 60 min for the samples (ϕ 45 mm). The temperature in the plating bath was kept constant at 60°C. The detailed palladium plating baths preparation using hydrazine as a reducing agent is listed in Table 2-1.

Table 2-1 Composition and experimental parameters of electroless plating bath [22]

Component	Concentration
$PdCl_2$	2 g/l
$Na_2EDTA.2H_2O$	40.1 g/l
$NH_3.H_2O$ (28%)	198 ml/l
N_2H_4 (1M)	5.6 ml/l
PH	10 ~ 10.4
Temperature (°C)	60

Microstructural characteristics and composition of the palladium deposits are observed and analyzed by a PHILIPS XL30 FE SEM (Field Emission Scanning Electron Microscopy) equipped with an EDS (Energy Dispersive Spectroscopy, GENESIS 2000 X-ray Microanalysis System). These membranes deposited on the porous steel substrates were also identified by X-ray diffraction (Rigaku Rotating Anode Diffractometer using monochromatic Cu Kα radiation). The gas-tightness of the membranes is determined by nitrogen gas at the absolute gas pressure difference of $3.5x10^5$ Pa and the temperature of 550°C. Over thirty palladium membrane samples having the thickness of 2~4 μm were prepared and carried out for hydrogen permeation tests in a permeation cell at the temperature range from 300°C to 550°C and the absolute hydrogen pressure difference from $1.4x10^5$ Pa to $3.5x10^5$ Pa, respectively. Eight of them were employed to have hydrogen selectivity examined using the mixture of gases between H_2 and N_2 or among H_2 and N_2 as well as CO in a CP-3800 gas chromatograph and the same condition as for hydrogen permeation tests. The experimental apparatus for the gas permeation tests was similar to elsewhere. [21]

2.4 Results and discussion

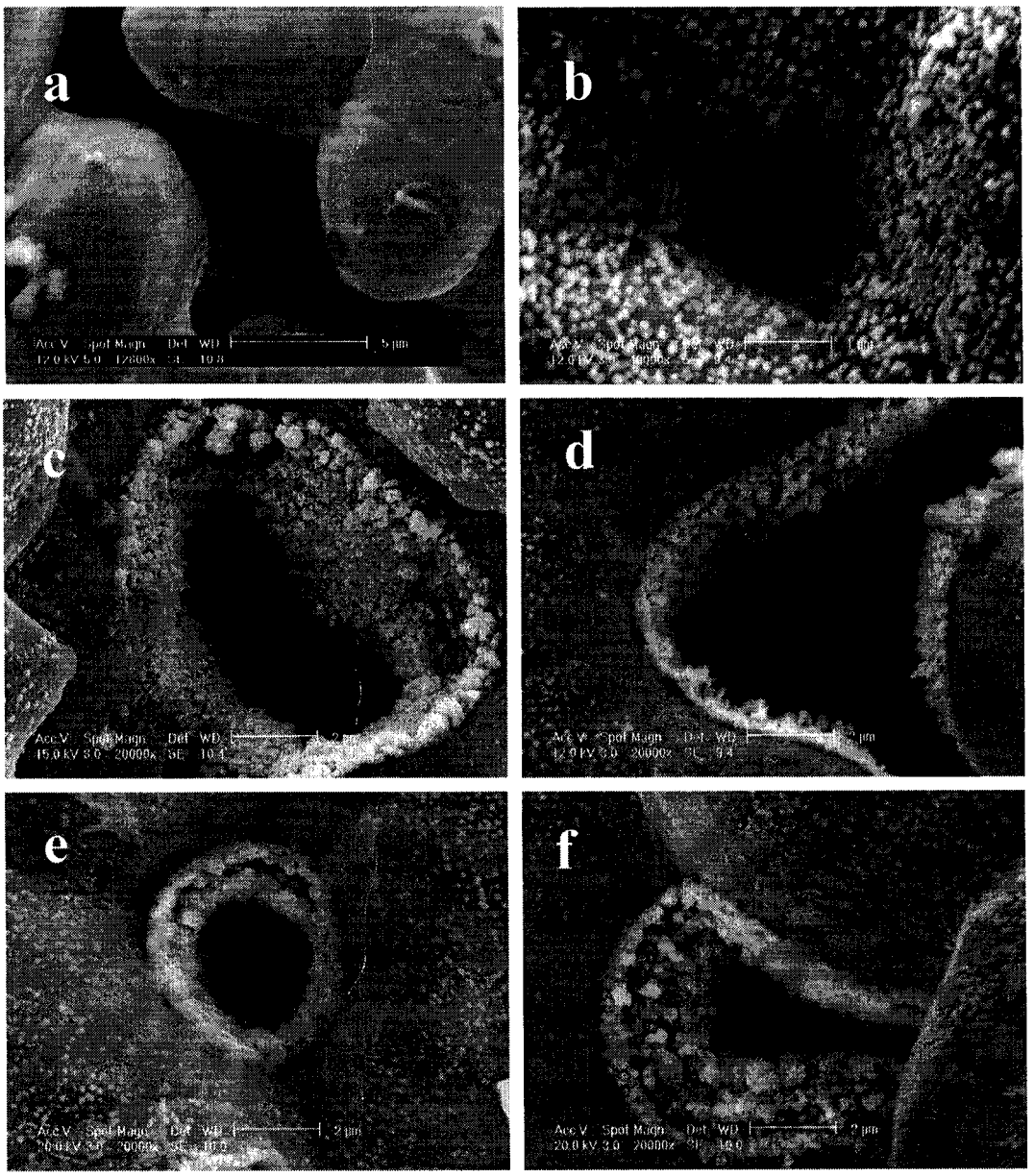

Figure 2-1 SEM micrographs showing the palladium deposits on the surface of the substrate within 120 s (The deposition time: (a) 0 s, (b) 45 s, (c, d) 90 s, (e, f) 120 s)

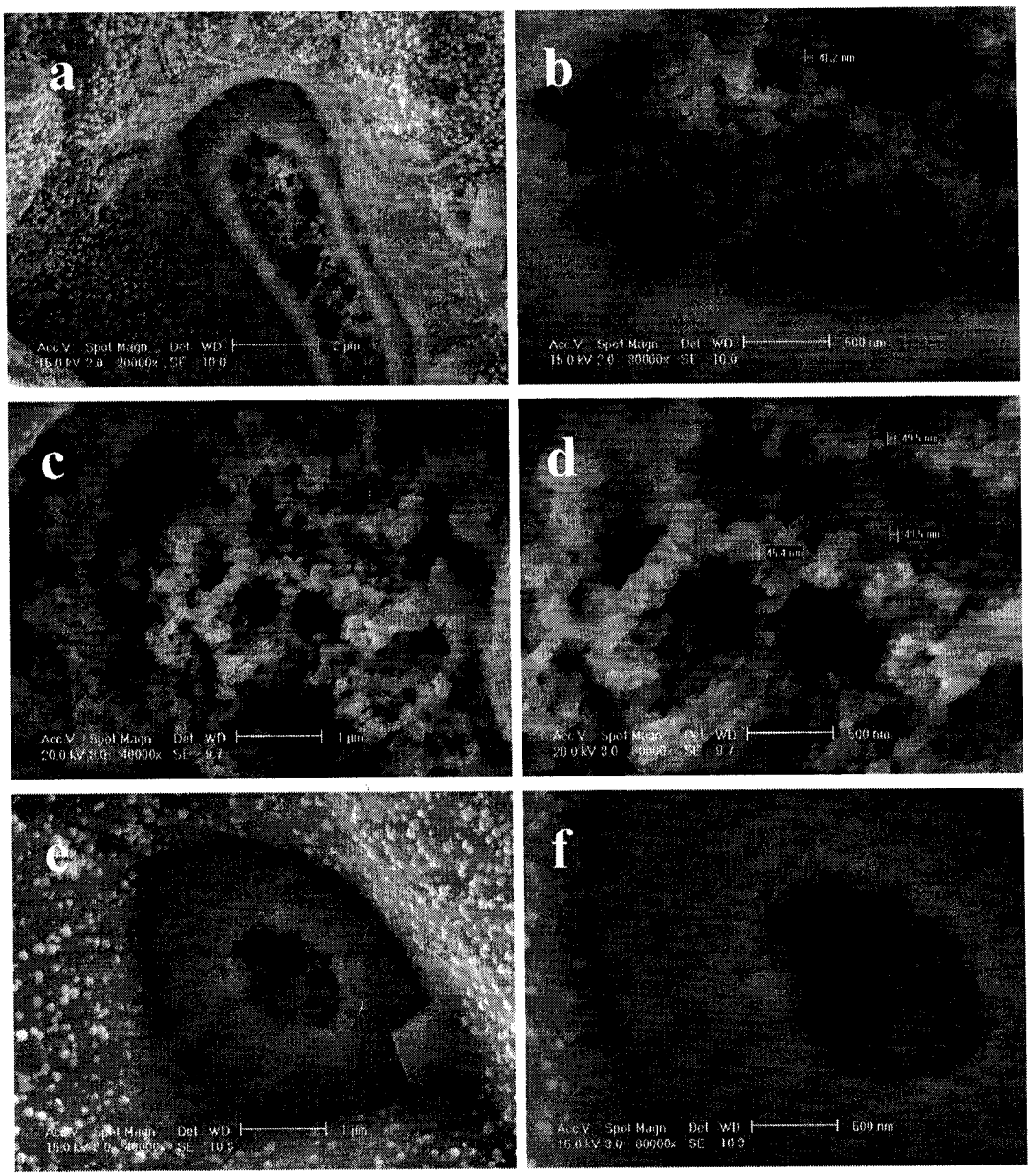

Figure 2-2 SEM micrographs showing the palladium deposits on the surface of the substrate within 300 s (The deposition time: (a-d) 150 s, (e, f) 300 s)

Electroless deposition occurs simply by immersion of samples in a plating bath and does not need rectifiers, batteries or anodes. The deposition is an autocatalytic process that is controlled by the chemical reduction of metallic ions in an aqueous

solution containing a reducer without any external electrical power. The deposition of palladium can be described by the chemical reaction equation (2-1):

$$2Pd\,[NH_3]_4^{2+} + N_2H_4 + 4OH^{-1} \rightarrow 2Pd^{o} + N_2 + 4H_2O + 8\,NH_3 \qquad (2\text{-}1)$$

Electroless deposition has been often used for depositing a uniform dense palladium membrane on any complex porous substrate. Because the surface of the porous substrate is coarse, it is difficult to control the deposition time and the thickness of a membrane. The investigation of the deposition progress of palladium deposits on the pore areas illustrates the formation of a membrane on the porous substrate and the interface between the membrane and the substrate that is related to the mechanical properties of the membrane.

The surface of the 0.2 μm grade stainless steel substrate is coarse and there are many pores in size of ranging from 0.2 to 10 μm, as shown in Figure 2-1 (a). The pores are interconnected and do not allow over 5% particles having the size of 0.2 μm to pass through from one side to the other (named as 0.2 μm grade in Mott Corp.). When palladium is deposited at the surface, the pores must be fully covered by the palladium deposits. Of course, the longer the deposition time, the thicker the deposited membrane, yet the smaller the obtained flux of hydrogen through it. Based on the observation of palladium deposits around the pore area at the initial stages, one can see how a membrane is built on the porous substrate surface.

SEM images in Figures 2-1 and 2-2 show the palladium deposits on the pore areas at the different deposition time from 0 to 300 s. It can be seen in Figure 2-1 (b) that a great number of palladium nanoparticles (diameter about 100 nm) are located around the pore after the deposition time of 45 s. With the extension of deposition time to 90 s, a layer of palladium is already suspended on the wall of the pore, as shown in Figure 2-1 (c, d). The other areas at some distance from the pore are not covered by the palladium nanoparticles. This illustrates that the palladium nanoparticles are primarily deposited on the wall of pores. After that, these deposited particles can attract the incoming ones. A palladium layer that is deposited on the wall and makes the wall solid is like a bridge piers. The interior rim of the deposited palladium layer is coarse and it is easily extended with increasing of the deposition time. The palladium layer on the rim will attract the palladium particles in any direction and broaden itself, as shown in Figure 2-1(e, f). Figure 2-2(a-d) shows that some areas on the pore have already created a network structure at the deposition time of 150 s. After detailed observation of the palladium network, we can see that the size of the palladium particles located at the bridge is small, about 30~50 nm. With increasing the deposition time to 300 s, the palladium wall becomes solid and covers almost the whole pore area in an arch-roof structure, as illustrated in Figure 2-2 (e, f).

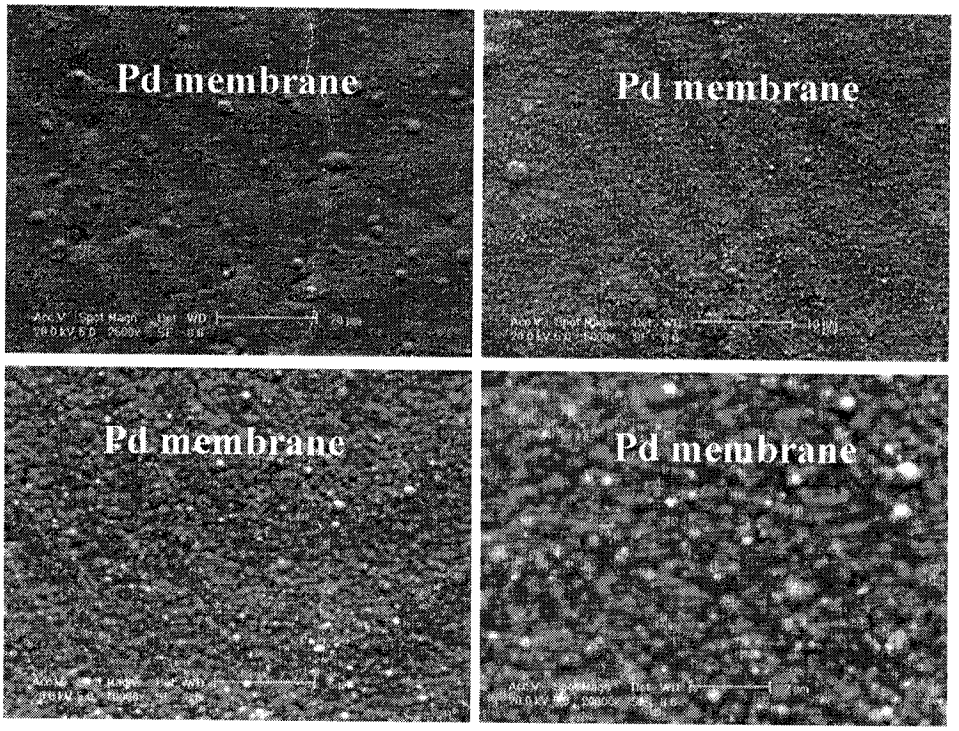

Figure 2-3 SEM micrographs showing the surface of the palladium membrane (The deposition time: 60 min)

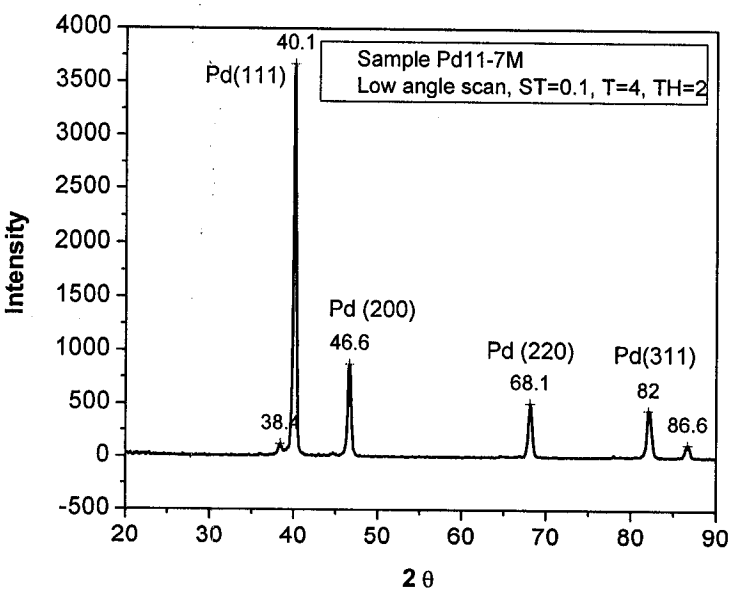

Figure 2-4 X-ray diffraction profile of the palladium membrane deposited on the porous stainless steel

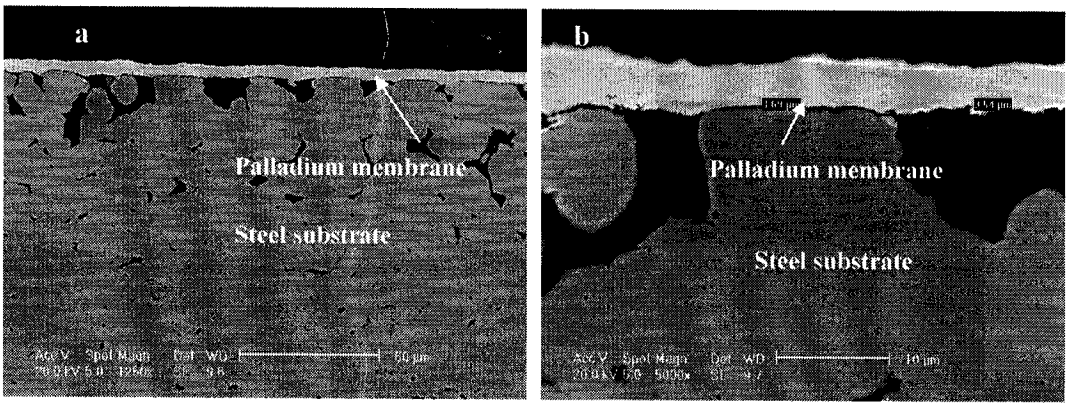

Figure 2-5 SEM micrographs showing the cross-section structures of the palladium membrane deposited on the porous stainless steel substrate

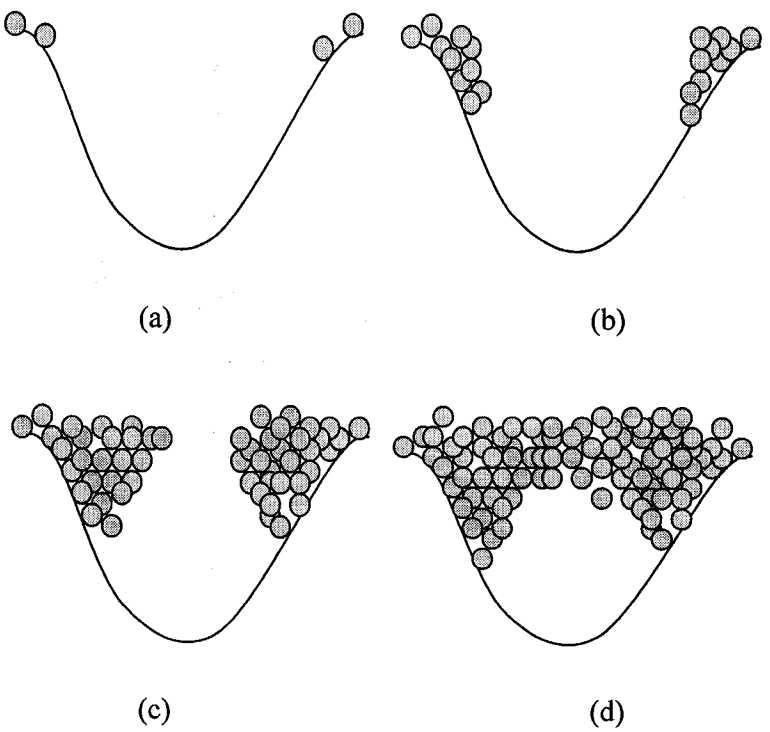

Figure 2-6 Schematic of a bridge model showing the particles covered the pore area

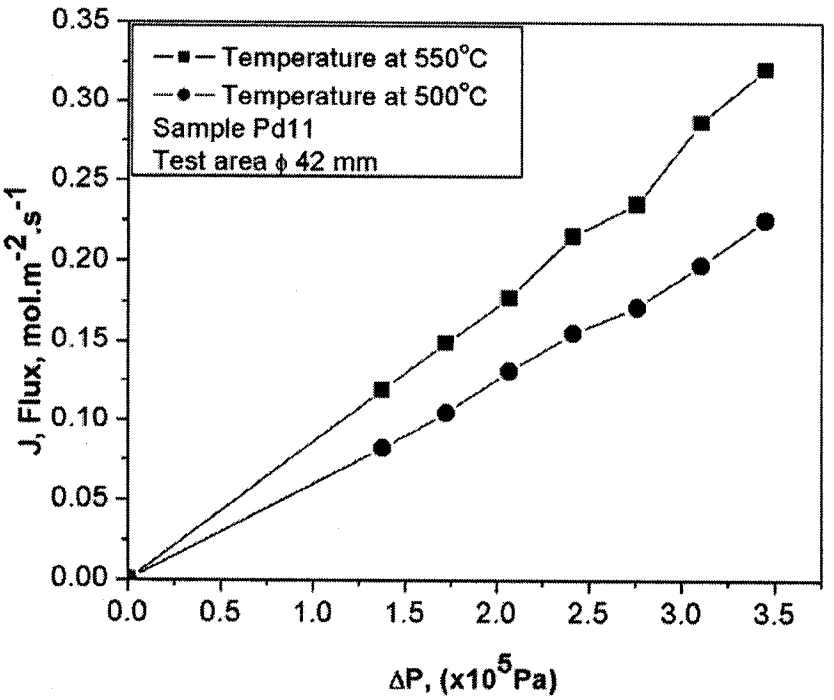

Figure 2-7 Flux of hydrogen permeating the palladium membrane as a function of absolute pressure difference at the temperatures of 500°C and 550°C

Micrographs in Figure 2-3 (a-d) illustrate the surface of palladium membrane having different magnification on the porous steel substrate after electroless deposition of 60 min. The palladium membrane is dense and uniform as well. No other phase is identified by X-ray diffraction, as shown in Figure 2-4. The cross section of the palladium membrane is stretched across the pores on the substrate, as shown in Figure 2-5 (a, b). The thickness of the palladium membrane was about 3.5 μm. The continuous palladium membrane is not tightly bonded with the porous steel substrate, which is caused by cutting or hot mounting of the sample preparation for observation. It can be seen that the palladium membrane extends like a bridge across the pores. A bridge model is presented to illustrate the mechanism of the membrane formation on the pore area, as shown in Figure 2-6 (a-d). A few palladium nanoparticles are deposited on the wall at the initial stage of deposition, as shown in Figure 2-6 (a). More palladium nanoparticles are attracted by them and deposited at the edge with extension of the deposition time in Figure 2-6 (b). Figure 2-6 (c) illustrates a great number of the palladium nanoparticles that are packed together like a bridge pier. Finally, a palladium nanoparticles bridge is being set up with increasing the deposition time in Figure 2-6 (d). After the bridges are built, the palladium is easily deposited on the bridges and made them wider to cover the whole pore area. Finally, a dense membrane is built and covers the whole substrate.

Figure 2-7 shows that the flux of hydrogen through one palladium membrane is as a function of the pressure difference of hydrogen gas at the temperatures of 500°C and 550°C. When the pressure increases, the hydrogen flux will rise. The test area (ϕ 42 mm) of this membrane was dense and no leakage was detected as it was examined by nitrogen gas at the absolute pressure difference of $3.5x10^5$ Pa. The thickness of the membrane is 3.5 μm and all the pores in the size of 0.2~10 μm are fully covered and the membrane is strong enough to withstand the pressure of $4.5x10^5$ Pa at the temperature of 550°C. This result reveals that most palladium deposits are only landed at the surface of the substrate in place of being deposited into the bottom of these pores. The deposition time and thickness of a dense membrane on the porous substrate can be reduced effectively because the bridging mechanism is present, compared with the deposition time needed when the palladium deposits fill the pores. Based on the above bridge model, together with the observation of palladium deposition progress on the 0.2 μm grade porous stainless steel substrate, the minimum thickness of the dense palladium membrane built on the 0.2 μm grade stainless steel substrate can be controlled around 1.5~2 μm.

Over 30 palladium membrane samples having thickness of 2~4 μm were prepared for hydrogen permeation tests. All samples were dense and no leakage was detected as they were examined by nitrogen gas at the absolute pressure difference of $3.5x10^5$ Pa. In the meantime, hydrogen selectivity of eight membrane samples was examined using CP-3800 gas chromatograph on the absolute pressure difference of mixture gases at $3.5x10^5$ Pa and the temperatures from 300°C to 550°C. Five of them were inspected with a gas mixture between H_2 and N_2. The composition of the mixture of gases consisted of: (1) 21%H_2 and 79%N_2, (2) 26%H_2 and 74%N_2, (3) 35%H_2 and 65%N_2, (4) 42%H_2 and 58%N_2, and (5) 49%H_2 and 51%N_2. The other three samples were checked with the mixture gases containing H_2, N_2 and CO. The composition of the mixture gases was: (1) 39%H_2, 3%CO and 58%N_2; (2) 38%H_2, 5%CO and 57%N_2. No N_2 or N_2 and CO was detected in the permeated side under the above tested pressure and temperatures. It means only hydrogen can pass through the membranes and the other gases (N_2 or N_2 and CO) are blocked. The experimental results show that the prepared palladium membranes are dense and their hydrogen selectivity is infinite. After that, hydrogen fluxes through these membranes are measured under the absolute pressure difference of hydrogen gas at $3.5x10^5$ Pa and the temperatures from 300°C to 550°C.

The measured hydrogen fluxes are compared with the data from literature [4, 11, 23-25], listed in Table 2-2. One can see the values of hydrogen flux through the membranes are very high even if the data has a wide range. The reasons resulting in the variety of the values are being investigated. The results reveal that the thickness of palladium membrane can be controlled effectively by electroless deposition process. If the pores at the substrate surface are modified to be small, the palladium membrane will be easily built around them and the membrane thickness can be well controlled.

Table 2-2 Comparison of hydrogen flux through the Pd membranes in this paper with data in literature [4]

Reference	Year	Pd (μm)	T (K)	P_{H2} (inlet) (kPa)	P_{H2} (outlet) (kPa)	n	J ($mol.m^{-2}.s^{-1}$)
*Yeung, et al [23]	1999	1.6	850	303	101	0.5	0.255
**Kusakabe, et al[24]	2001	3	773	101.3	Ar sweep	1	0.203
**Kusakabe, et al[24]	2001	3	873	101.3	Ar sweep	1	0.355
***Collins &Way [25]	1993	11.4	823	156~2445	101~140	0.6	0.285
***Collins &Way [25]	1993	11.4	873	156~2445	101~140	0.57	0.366
***Collins &Way [25]	1993	17	773	156~2445	101~140	0.59	0.214
***Collins &Way [25]	1993	17	823	156~2445	101~140	0.56	0.255
***Collins &Way [25]	1993	17	873	156~2445	101~140	0.55	0.332
NETL-Ma [4]	2003	21.3	723	95~2573	Sweep (<67)	0.5	0.0454
NETL-Ma [4]	2003	21.3	723	95~2573	Sweep (<67)	0.62	0.0322
NETL-Ma [4]	2003	22.2	723	95~2573	Sweep (<300)	0.5	0.0853
NETL-Ma [4]	2003	21.3	723	95~2573	Sweep (<300)	0.58	0.0659
****Jarosch [11]	2001	156	1023	425~603	Sweep	0.5	0.00844
****Jarosch [11]	2001	156	1123	425~603	Sweep	0.5	0.0107
****Jarosch [11]	2001	244	823	425~603	Sweep	0.5	0.0206
This program, Pd on 0.2 μmPSS	2004~5	2~4	773	239~447	101.3	0.5, 1	**0.25~0.75**
This program, Pd on 0.2 μmPSS	2004~5	2~4	823	239~447	101.3	0.5, 1	**0.30~0.90**

Notes: * The Pd membranes were deposited on a Vycor by the electroless process. [23]
** The Pd membranes were deposited on the pure Cu sheet by a novel method based on photolithograph and electrolysis. [24]
*** The Pd membranes were deposited on the porous alumina supports that the top layer with pore diameter is around 10-200nm by the electroless process. [25]
**** The Pd membranes were deposited on the porous Inconel tube substrate by the electroless process. [11]

2.5 Conclusions

The observation of palladium deposits around the pore area on the stainless steel substrate after different deposition time shows that palladium nanoparticles are deposited on the wall of the pores and makes a strong palladium "pier" attract oncoming nanosize particles. With the extension of deposition time, a network structure around a pore is built. After that, palladium is easily deposited on this network structure and forms a thin membrane that fully covers the pore area.

A bridge model is presented to describe the deposition progress of palladium nanoparticles around the pore area. This bridge model is well-illustrated by the observation of the cross-section structure of the membrane deposited on the porous stainless steel substrate. The obtained results reveal that the deposition time and the thickness of a membrane built on a porous substrate can be effectively controlled.

2.6 References

1. Y. Zhang, M. Komaki and C. Nishimura, Morphological study of supported thin Pd and Pd–25Ag membranes upon hydrogen permeation, Journal of Membrane. Science, 246, 173-180 (2005).
2. B.D. Morreale, M.V. Ciocco, R.M. Enick, B.I. Morsi, B.H. Howard, A.V. Cugini and K.S. Rothenberger, The permeability of hydrogen in bulk palladium at elevated temperatures and pressures, Journal of Membrane Science, 212, 87-97 (2003).
3. D.-W. Lee, Y.-G. Lee, S.-E. Nam, S.-K. Ihm and K.-H. Lee, Study on the variation of morphology and separation behavior of the stainless steel supported membranes at high temperature, Journal of Membrane Science, 220, 137-153 (2003).
4. K.S. Rothenberger, A. V. Cugini, B.H. Howard, R.P. Killmeyer, M.V. Ciocco, et al., High pressure hydrogen permeance of porous stainless steel coated with a thin palladium film via electroless plating, Journal of Membrane Science, 244, 55-68 (2004).
5. F.C. Gielens, H.D. Tong, C.J.M. van Rijn, M.A.G. Vorstman and J.T.F. Keurentjes, Microsystem technology for high-flux hydrogen separation membranes, Journal of Membrane Science, 243, 203-213 (2004).
6. S.-E. Nam and K.-H. Lee, Hydrogen separation by Pd alloy composite membranes: introduction of diffusion barrier, Journal of Membrane Science, 192, 177-185 (2001).
7. T.L. Ward and T. Dao, Model of hydrogen permeation behavior in palladium membranes, Journal of Membrane Science, 153, 211-231 (1999).
8. A. Li, W. Liang and R. Hughes, Fabrication of dense palladium composite membranes for hydrogen separation, Catalysis Today, 56, 45-51 (2000).
9. P. Quicker, V. Hollein and R. Dittmeyer, Catalytic dehydrogenation of hydrocarbons in palladium composite membrane reactors, Catalysis Today, 56, 21-34 (2000).
10. C.-S. Jun and K.-H. Lee, Palladium and palladium alloy composite membranes prepared by metal-organic chemical vapor deposition method (cold-wall), Journal of Membrane Science, 176, 121-130 (2000).
11. K. Jarosch and H.I. de Lasa, Permeability, selectivity and testing of hydrogen diffusion membranes suitable for use in steam reforming, Ind. Eng. Chem. Res. 40, 5391-5397 (2001).
12. Y.S. Cheng and K.L. Yeung, Effects of electroless plating chemistry on the synthsis of palladium membranes, Journal of Membrane Science, 182, 195-203 (2001).
13. A. Li, W. Liang and R. Hughes, The effect of carbon monoxide and steam on the hydrogen permeability of a Pd/stainless steel membrane, Journal of Membrane Science, 165, 135-141 (2000).
14. A. Li, W. Liang and R. Hughes, Characterisation and permeation of palladium/stainless steel composite membranes, Journal of Membrane Science, 149, 259-268 (1998).

15. H.-B. Zhao, K. Pflanz. J.-H. Gu, A. –W. Li, N. Stroh, H. Brunner and G.-X. Xiong, Preparation of palladium composite membranes by modified electroless plating procedure, Journal of Membrane Science, 142, 147-157 (1998).
16. I.P. Mardilovich, E. Engwall and Y. H. Ma, Dependence of hydrogen flux on the pore size and plating surface topology of asymmetric Pd-porous stainless steel membranes, Desalination, 144, 85-89 (2002).
17. L. Yang, Z. Zhang, X. Gao, Y. Guo, B. Wang, et al., Changes in hydrogen permeability and surface state of Pd-Ag/ceramic composite membranes after thermal treatment, Journal of Membrane Science, 252, 145-154 (2005).
18. Y. Guo, G. Lu, Y. Wang and R. Wang, Preparation and characterization of Pd-Ag/ceramic composite membrane and application to enhancement of catalytic dehydrogenation of isobutene, Separation and Purification Technology, 32, 271-279 (2003).
19. K.J. Bryden and J.Y. Ying, Nanostructured palladium-iron membranes for hydrogen separation and membrane hydrogenation reactions, Journal of Membrane Science, 203, 29-42 (2002).
20. S.-E. Nam and K.-H. Lee, A study on the palladium/nickel composite membrane by vacuum electrodeposition, Journal of Membrane Science, 170, 91-99 (2000).
21. S.-E. Nam, S.-H. Lee and K.-H. Lee, Preparation of a palladium alloy composite membrane supported in a porous stainless steel by vacuum electrodeposition, Journal of Membrane Science, 153, 163-173 (1999).
22. J. Shu, B. P. A. Grandjean, E. Ghali and S. Kaliaguine. Simultaneous deposition of Pd and Ag on porous stainless steel by electroless plating, Journal of Membrane Science, 77, 181-195 (1993).
23. K. Yeung, S. Christiansen and A. Varma. Palladium composite membrane by electroless plating technique, relationship between plating kinetics, film microstructure and membrane performance, Journal of Membrane Science, 159, 107-122 (1999).
24. K. Kusakabe, M. Takahashi, H. Maeda and S. Morooka. Preparation of thin palladium membranes by a novel method based of photolithography and electrolysis, J. Chem. Eng., Japan, 34, 703-708 (2001).
25. J.P. Collins and J.D. Way. Preparation and characterization of a composite palladium-ceramic membrane, Ind. Eng. Chem. Res. 32, 3006-3013 (1993).

CHAPTER 3 [1]

SYNTHESIS OF AN ULTRA-THIN PALLADIUM MEMBRANE FOR HYDROGEN EXTRACTION

3.1 Abstract

Based on observation of the microstructure of palladium deposited on a porous stainless steel surface using an electroless process, we find that the palladium membrane is made of nanoparticles and its thickness is directly dependent on the size of the nanoparticles. The size of palladium nanoparticles can be effectively controlled by concentration of $PdCl_2$ in the plating solution. The higher concentration of $PdCl_2$ in the plating bath will result in a smaller size of palladium particles deposited on the substrate. The smaller the size of palladium nanoparticles is generated from the solution, the thinner the dense palladium membrane is built. The result obtained from hydrogen permeation through the ultra-thin palladium membrane having a thickness of 400 nm demonstrates that the ultra-thin membrane is solid and it can be used at the temperature of 550°C and hydrogen pressure difference of 50 psi. These experimental results will allow optimizing the design of an ultra-thin palladium membrane for hydrogen extraction.

3.2 Introduction

Global interest in the development of a "hydrogen economy" and an associated demand for hydrogen as a source of clean energy has led to the development of new materials and methods for hydrogen generation, storage, separation and sensing. [1] So far, palladium and palladium alloys are regarded as the most important materials for high quality hydrogen extraction from a mixture of gases. The interaction between palladium and hydrogen has been studied extensively and palladium membranes have been widely applied for hydrogenation catalysts in chemical engineering because palladium absorbs and adsorbs hydrogen easily. Palladium membranes have high hydrogen permeability, good chemical compatibility and excellent hydrogen selectivity. [2-8] They are usually built by electroless, electrochemical and sputtering depositions. Most efforts have been focused on the reduction of the membrane thickness in order to maximize hydrogen permeability and reduce the membrane cost. [9-11] No matter what kind of process is employed to build palladium membrane, the membrane should be dense enough to allow hydrogen permeation and block the other gases. As it is well known, the mechanism of hydrogen permeation through a palladium membrane mainly involves three steps, such as dissociative adsorption, recombinative desorption at the membrane surface and diffusion

[1] This chapter was presented on the conference of European Materials Research Society (E-MRS), Symposium A – Nanostructured Composite Films: Synthesis, Characterization, Properties, and Applications, September 4-8, 2006, Warsaw, Poland and referred to publish in Reviews on Advanced Materials Science (Journal)

through the membrane. The flux of hydrogen through a membrane is generally determined by its thickness. However, the fabrication of a dense and ultra-thin palladium membrane is quite challenging and attracts new application in micro-devices. [12, 13] The purpose in this chapter is to observe how palladium is deposited on the stainless steel substrate at different concentrations of $PdCl_2$ in the plating bath, to investigate how the dense membrane is built and to explain how an ultra-thin membrane can be fabricated. These experimental results are beneficial to the design and fabrication of an ultra-thin palladium membrane for engineering applications.

3.3 Experimental section

In this program a 0.2 μm grade porous 316L stainless steel plate, purchased from Mott Metallurgical Corporation was used as a substrate to deposit a palladium membrane. The substrate is defined as 0.2 μm grade that means over 95% of the particles having the size of 0.2 μm are rejected by this substrate during filtering. Figure 3-1 (a) and 3-2 (a) show that the pore sizes at the substrate surface range from 0.2 to 10 μm. The substrate samples have the sizes of 20 mm x 20 mm and ϕ 45 mm. The square substrate samples are used to characterize the microstructure of the palladium deposits in the initial stages at different concentrations of $PdCl_2$ in the plating solution. They were cleaned in an ultrasonic bath with acetone for 15 min. Their surfaces were activated with 10% hydrochloric acid and rinsed with deionized water. After such treatments, these substrate samples were transferred immediately into the electroless plating baths that were containing different concentration of $PdCl_2$ for the deposition of palladium. The deposition time was from 30 s to 300 s at a constant temperature of 60°C. The substrate samples having a diameter of 45 mm are used to deposit palladium membranes for hydrogen permeation tests. As we have already observed the formation procedures of palladium membrane on this substrate in Chapter 2, the minimal thickness of palladium membrane built on this substrate is around 1.5 μm according to our measurement. [6] In order to obtain ultra-thin membrane (thickness, less than 1 μm) on this substrate, the pore area of this substrate was modified using nickel powders. The size of nickel powders is around 60 nm. The surface of the specimens after such treatment is relatively flat, as illustrated in Figure 3-1 (b, c). Then, the samples were heated at 650°C for 2 hrs under the protective atmosphere using flowing argon gas. The surface microstructure of modified substrate after sintered is shown in Figure 3-1(d). After this treatment, their surfaces of the specimens were activated with 10% hydrochloric acid and rinsed with deionized water. These substrate samples were then transferred into the electroless plating bath with different concentrations of $PdCl_2$ for the deposition of palladium membrane. The deposition time was 30 min at a constant temperature of 60°C. The detailed palladium plating baths preparation using hydrazine as a reducing agent is described in Table 3-1. Microstructural characteristics of palladium membranes were analyzed using a PHILIPS XL30 FEG SEM (Field Emission Scanning Electron Microscopy) equipped with an EDS (Energy Dispersive Spectroscopy, GENESIS 2000 X-ray Microanalysis System). The gas-tightness of the membranes was examined and no leakage was detected with nitrogen gas at the pressure of 50 psi from room temperature to 550°C. The hydrogen permeation tests for the deposited membranes were carried out in a permeation cell at the temperature from 25°C to 550°C and hydrogen pressure difference from 20 psi to 50 psi. The

measurement of hydrogen flux using a soap bubble meter was at the temperature from 300°C to 550°C. The experimental apparatus used for the gas permeation tests was similar to the one described elsewhere. [14]

Table 3-1 Composition of the electroless plating bath and experimental parameters

Component	Composition and experimental parameters
$PdCl_2$	1.8~2 g/l, 2.4 g/l, 3.0 g/l, 4.2 g/l
$Na_2EDTA.2H_2O$	40.1 g/l
NH_3 (28%)	198 ml/l
N_2H_4 (1M)	5.6 ml/l
PH	10 ~ 10.4
Temperature (°C)	60

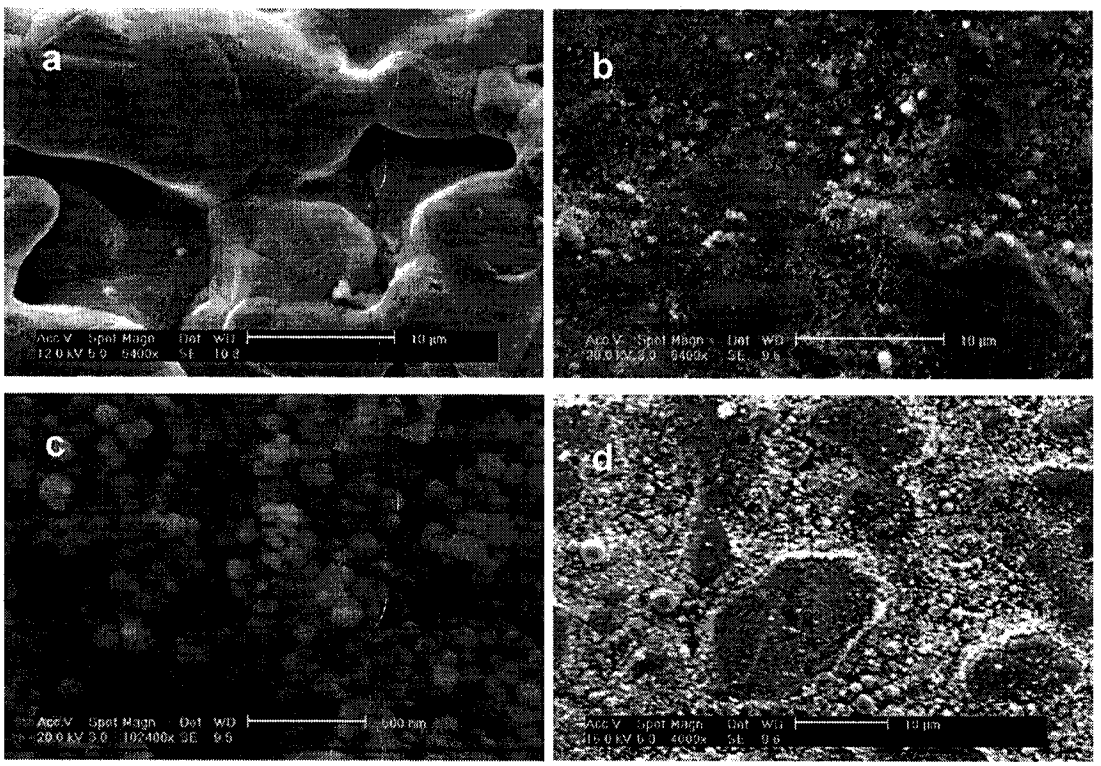

Figure 3-1 SEM micrographs showing original surface microstructure of porous stainless steel substrate (a) modified surface microstructures using nickel powders (b, c) and (d) modified surface microstructure after heat treatment at 650°C for 2 hrs

3.4 Results and Discussion

Figure 3-2 shows the surface microstructure of a porous stainless steel substrate. It can be seen that some spherical phases are observed at surface of the substrate, as shown in Figure 3-2 (b, c). These spherical particles, analyzed by EDS in Figure 3-2 (d), are SiO_2 inclusions that are most likely generated from soluble silicate used as inorganic binders during powder metallurgical process. The size of the SiO_2 inclusions ranges from 150 to 600 nm. Their existence at surface of the substrate was used to estimate the thickness of palladium deposits at the initial stages of deposition.

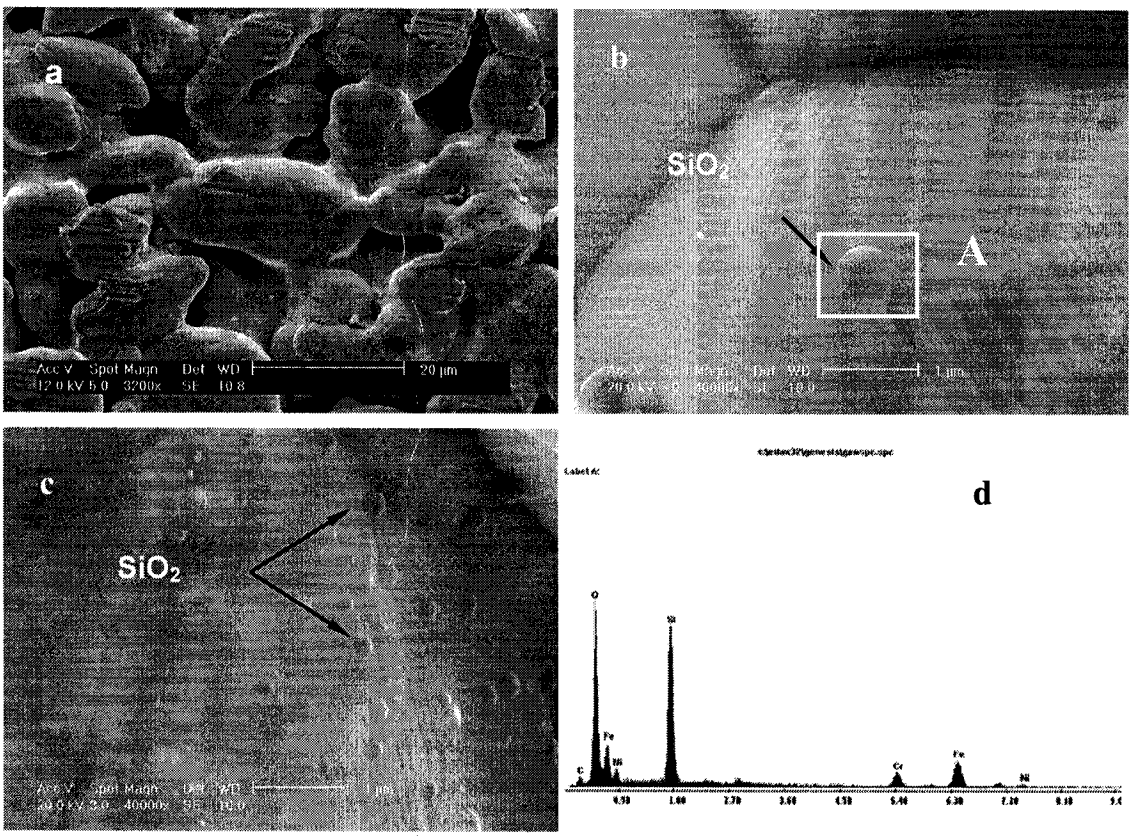

Figure 3-2 SEM micrographs (a-c) showing the surface microstructure of porous stainless steel substrate, energy-dispersive x-ray spectrum (d) from the marked area A (b) spheric shape SiO_2-riched particle at the substrate surface

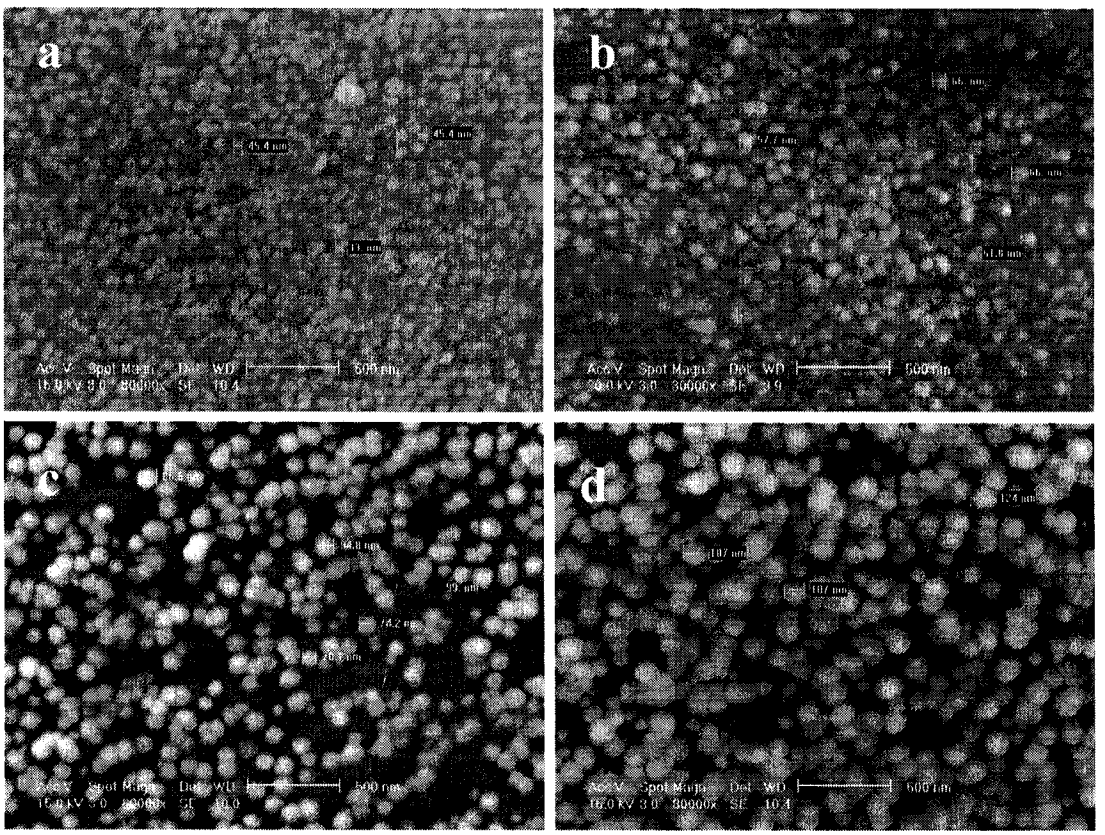

Figure 3-3 SEM micrographs showing palladium nanoparticles deposited on the surface of the stainless steel substrate at different concentration of $PdCl_2$ in the plating bath under the same time of 150 s

((a) The size: 30 ~ 50 nm, C_{PdCl2}: 4.2 g/l; (b) The size: 50 ~ 70 nm, C_{PdCl2}: 3 g/l; (c) The size: 70 ~ 100 nm, C_{PdCl2}: 2.4 g/l; (d) The size: 100 ~ 130 nm, C_{PdCl2}: 1.8~2 g/l)

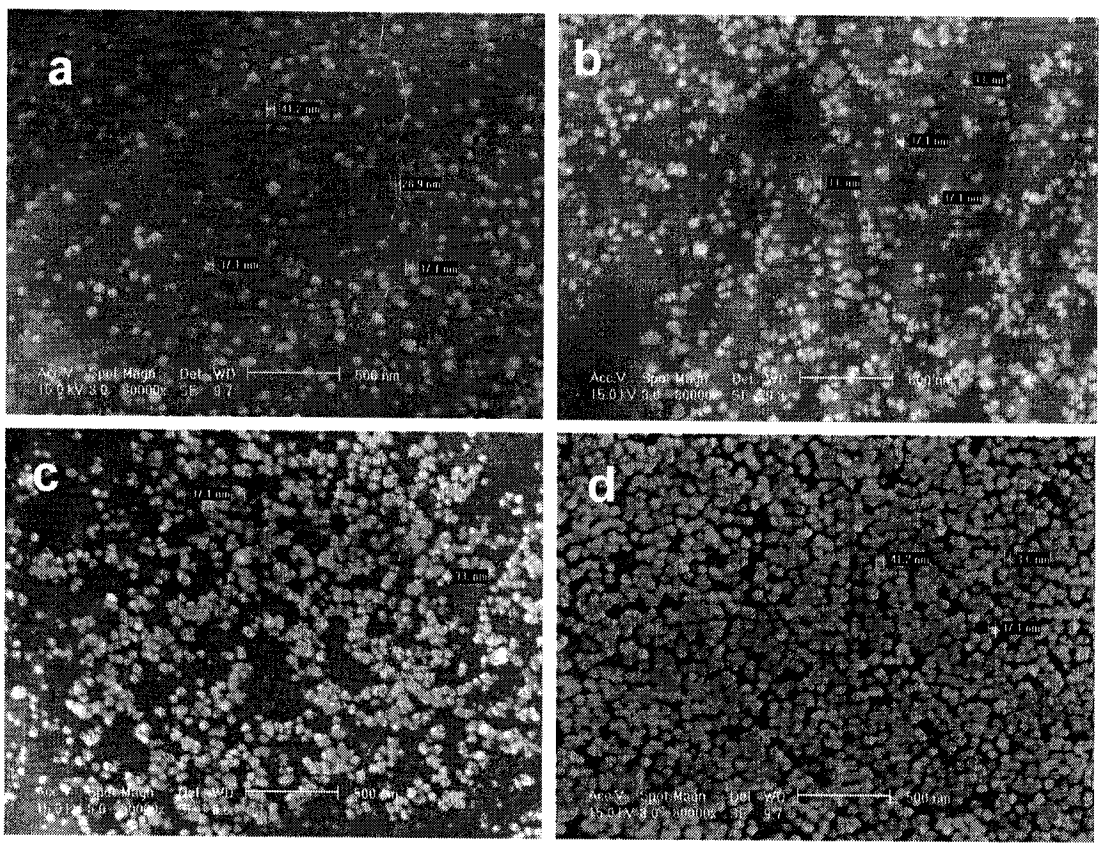

Figure 3-4 SEM micrographs showing palladium nanoparticles deposited on the surface of the stainless steel substrate at $PdCl_2$ concentration of 4.2 g/l in the plating bath (The deposition time: (a) 30 s, (b) 60 s, (c) 75 s and (d) 150 s)

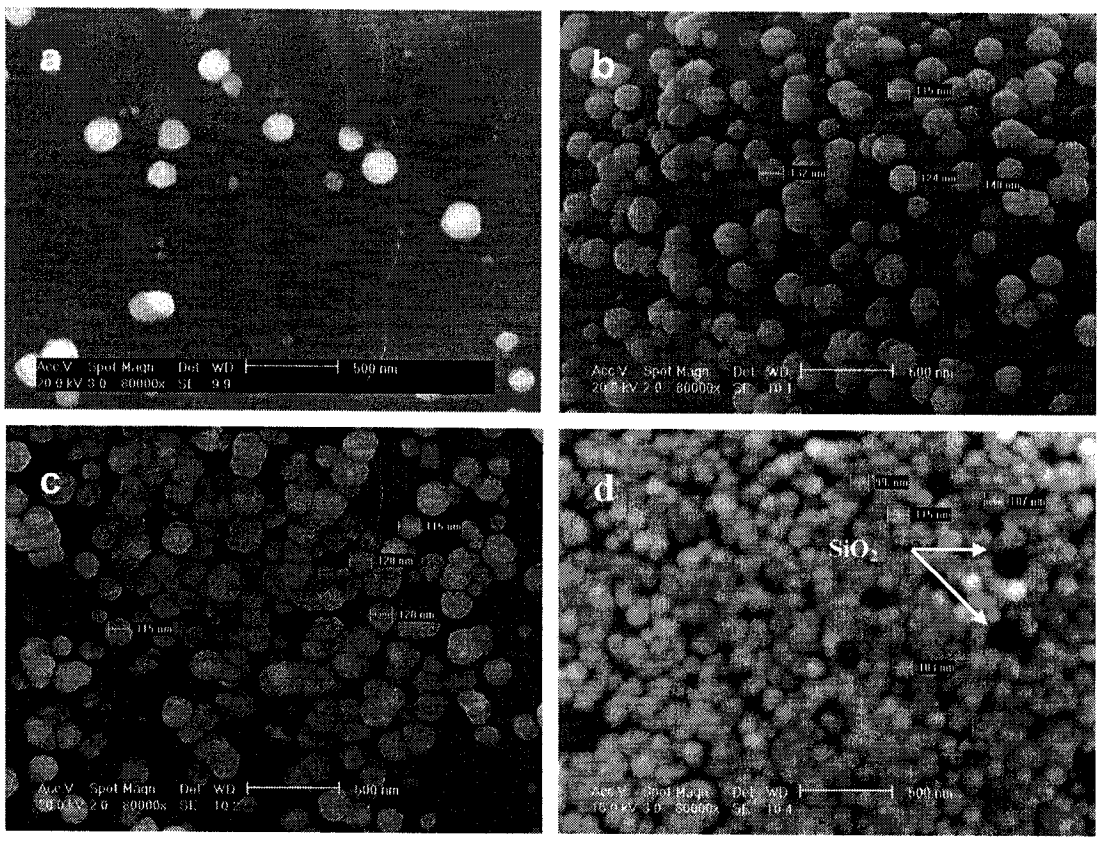

Figure 3-5 SEM micrographs showing palladium nanoparticles deposited on the surface of a stainless steel substrate at $PdCl_2$ concentration of 1.8~2 g/l in the plating bath (The deposition time: (a) 30 s, (b) 90 s, (c) 120 s and (d) 300 s)

SEM micrographs in Figures 3-3 ~ 3-5 illustrate palladium nanoparticles deposited on the stainless steel substrate at the time from 30 s to 300 s and at different concentration of $PdCl_2$ in the plating bath. One can see that deposited palladium nanoparticles are distributed at the substrate randomly and the particle size is varying with the concentrations of $PdCl_2$ in the plating bath. The higher the concentration of $PdCl_2$ in the plating bath is, the smaller the deposited palladium nanoparticles are, as illustrated in Figure 3-3. Comparing the size of palladium nanoparticles deposited on the steel substrate in different concentration of $PdCl_2$ but at the same deposition time of 150 s, we can see that the size of deposited palladium nanoparticles changes from 30~50 nm to 50~70 nm when the concentration of $PdCl_2$ in the plating bath is reduced from 4.2 g/l to 3 g/l, as shown in Figure 3-3 (a) and (b). When the concentration of $PdCl_2$ in the

plating solution changes from 2.4 g/l to 1.8~2.0 g/l, the size of deposited palladium nanoparticles increases from 70~100 nm to 100~130 nm, as shown in Figure 3-3 (c) and (d). However, the size of palladium nanoparticles does not change much with the extension of deposition time at the same concentration of $PdCl_2$ but they only vary with the concentration of $PdCl_2$ in the plating solution, as shown in Figures 3-4 and 3-5. The size of most palladium nanoparticles in Figures 3-3 (a) and 3-4 is in the range of 30~50 nm at the deposition time from 30 s to 150 s. When the concentration of $PdCl_2$ in the plating bath is reduced to 1.8~2 g/l, the size of most deposited palladium nanoparticles is in the range of 100~130 nm, as shown in Figure 3-5. However, the number of deposited palladium nanoparticles increases with deposition time, as shown in Figures 3-4 and 3-5. This experimental result is different from published reports that claim that the size of deposited nanoparticles is increasing with the deposition time.[15-17] In order to verify this experimental phenomenon, we also observed the palladium deposited on the stainless steel substrate within 30 s and found that the number of palladium nanoparticles is directly related to the deposition time and their size keeps constant at the same concentration of $PdCl_2$ in the plating solution. The deposition of palladium takes place according to the equation of autocatalytic reaction (3-1):

$$2Pd\,[NH_4]^{2+} + N_2H_4 + 4OH^{-1} \rightarrow 2Pd + N_2 + 4H_2O + 8NH_3 \qquad (3\text{-}1)$$

When the size of palladium clusters becomes critical in a homogeneous plating solution, these clusters are generated from the plating solution and deposited on the heterogeneous steel substrate forming nanoparticles. The critical size of clusters is determined by the concentration of $PdCl_2$ in the plating bath. Therefore, we can conclude that the deposition of palladium on the stainless steel substrate is controlled by the nucleation in the solution and their growth on the substrate surface is limited. As elucidated in the literature [18], in order to obtain nanosize metallic particles, a high supersaturation concentration is often required, which are best achieved when starting with non-complexed, highly reactive metallic species and very strong reducing agents. If the fraction of atoms consumed in the nucleation step is high, the increase in particle size due to the diffusional growth that immediately follows the nucleation burst is drastically limited and the particles are only slightly larger than the nuclei. Based on our experiments, when the concentration of $PdCl_2$ in the plating solution increases, the deposition and nucleation of palladium on the substrate is fast and all nuclei form instantaneously and the subsequent growth of palladium deposits is limited. The size of deposited particles is obviously reduced with increasing the concentration of $PdCl_2$ in the plating bath. Therefore, the size of palladium nanoparticles deposited on the steel substrate in the initial stages can be controlled by the concentration of $PdCl_2$ in the plating bath. The formation mechanism of palladium nanoparticles generated from the autocatalytic reaction and their size control are being further investigated.

Figure 3-5 (d) shows that most of the substrate is covered by palladium nanoparticles except some small areas occupied by SiO_2 inclusions. Based on the observation of palladium deposits after 300 s, we can conclude that an ultra-thin palladium membrane is built at the substrate surface. This membrane has the thickness of a few nanoparticle layers and some small areas containing SiO_2 inclusions are not fully covered by palladium nanoparticles. Palladium nanoparticles are not deposited at the surface of SiO_2 inclusions because these inclusions are not conductive and there is no

electronic exchange at their surfaces during the autocatalytic reaction. As illustrated in Figure 3-2 (b, c), the thickness of the palladium membrane can be estimated based on the size of SiO_2 inclusions.

SEM micrographs in Figure 3-6 (a-d) show a nanoparticle-monolayer palladium membrane made of nanoparticles deposited on the wall of a pore area. The thickness of the palladium membrane in this case, as shown in Figure 3-6 (a, b), is around 100 ~ 130 nm which is the same as the size of palladium nanoparticles in Figures 3-3 (d) and 3-5. When the concentration of $PdCl_2$ in the plating solution increases to 2.4 g/l, the thickness of palladium layer will decrease to 70~100 nm, as shown in Figure 3-6 (c, d). The palladium nanoparticle monolayer membrane is dense and palladium nanoparticles are close-packed and well-organized. These nanoparticles are amalgamated in one plane and may then fuse together to lower surface free energy. Such a monolayer membrane made of nanoparticles may not be dense enough for hydrogen purification. However, the membrane assembled by a few monolayers should be suitable for the extraction of hydrogen from a gas mixture.

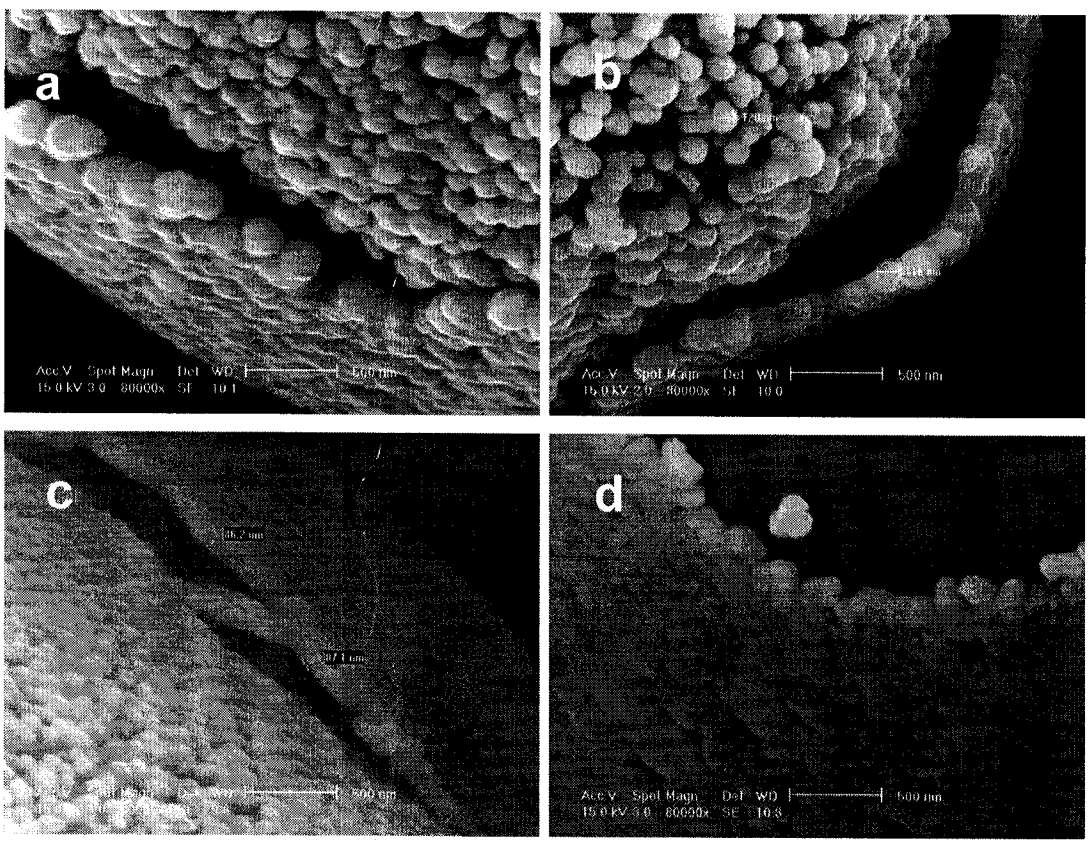

Figure 3-6 SEM micrographs showing nanoparticle-monolayer membranes deposited on the substrate surface
(The size: 100 ~ 130 nm, time: 120 s; concentration of $PdCl_2$: 1.8~2 g/l (a, b),
The size: 70 ~ 100 nm, time: 120 s, concentration of $PdCl_2$: 2.4 g/l(c, d))

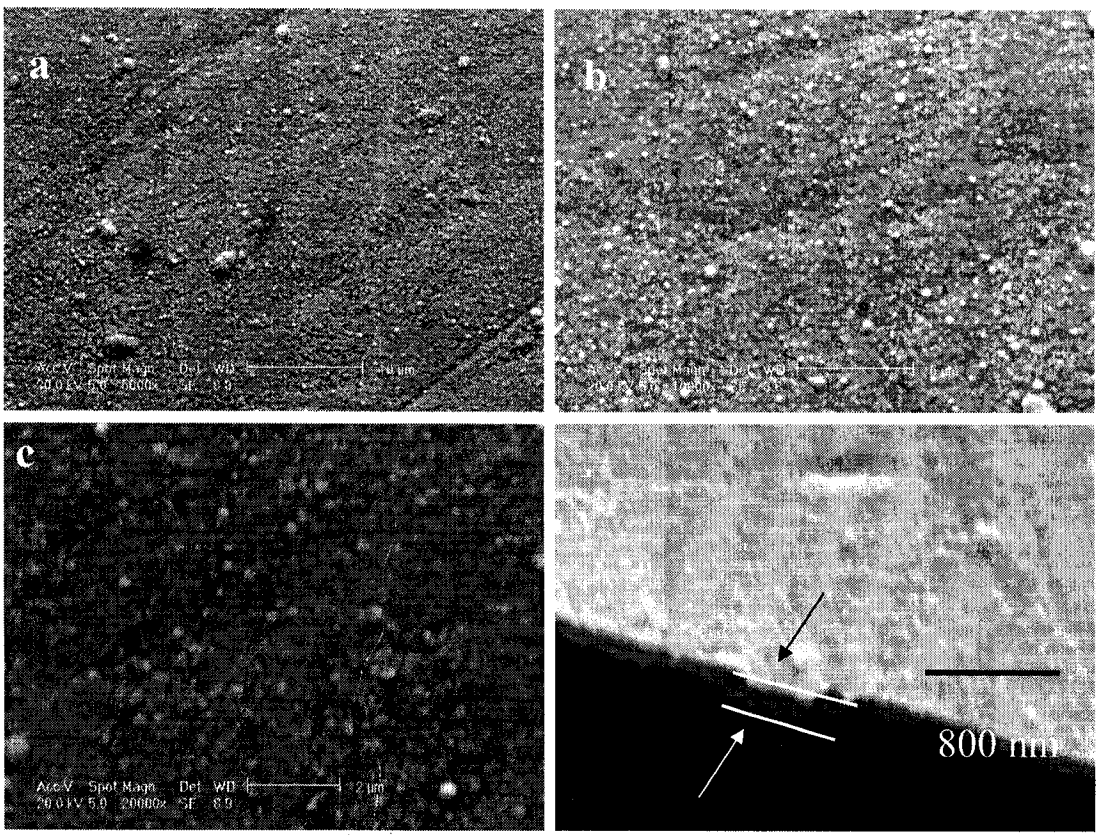

Figure 3-7 Microstructure of a palladium membrane deposited on a modified porous stainless steel substrate by electroless deposition
(The deposition time: 30 min; concentration of $PdCl_2$ in plating bath: 1.8~2 g/l)

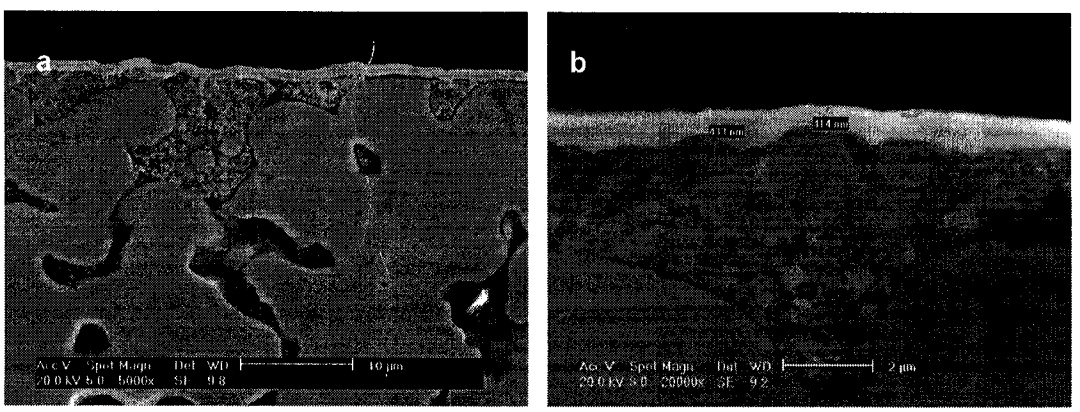

Figure 3-8 Cross section of palladium membrane deposited on modified porous stainless steel substrate by electroless deposition

Figures 3-7 and 3-8 illustrate the microstructures of the surface and cross-section of an ultra-thin palladium membrane deposited on a modified porous stainless steel substrate at the time of 30 min and $PdCl_2$ concentration of 1.8~2 g/l in the plating bath. One can identify nanoparticles from its surface microstructure in Figure 3-7 (a-c) and nickel powders soaked in the pore area in Figure 3-8 (a, b). This membrane having the diameter of ϕ 45 mm was used for hydrogen permeation tests. The tested area for hydrogen permeation at this membrane was 42 mm in diameter. It was solid and dense because there was no leakage detected when the gas tightness of the membrane was examined using nitrogen gas at gas pressure difference of 50 psi (3.4 atm.) from room temperature to 550°C. Its thickness was about 300 ~ 400 nm as shown in Figures 3-7 (d) and 3-8. The flux of hydrogen through this membrane is a function of hydrogen pressure and test temperature, as shown in Figure 3-9 (a, b). One can see that the flux of hydrogen through the membrane linearly rises with increasing the temperature and hydrogen pressure.

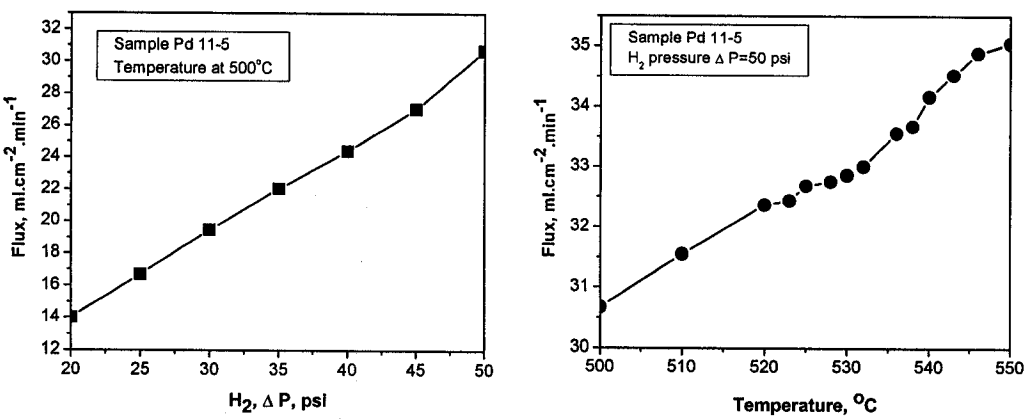

(a) (b)

Figure 3-9 Hydrogen flux vs. hydrogen pressure difference (a) and temperature (b)

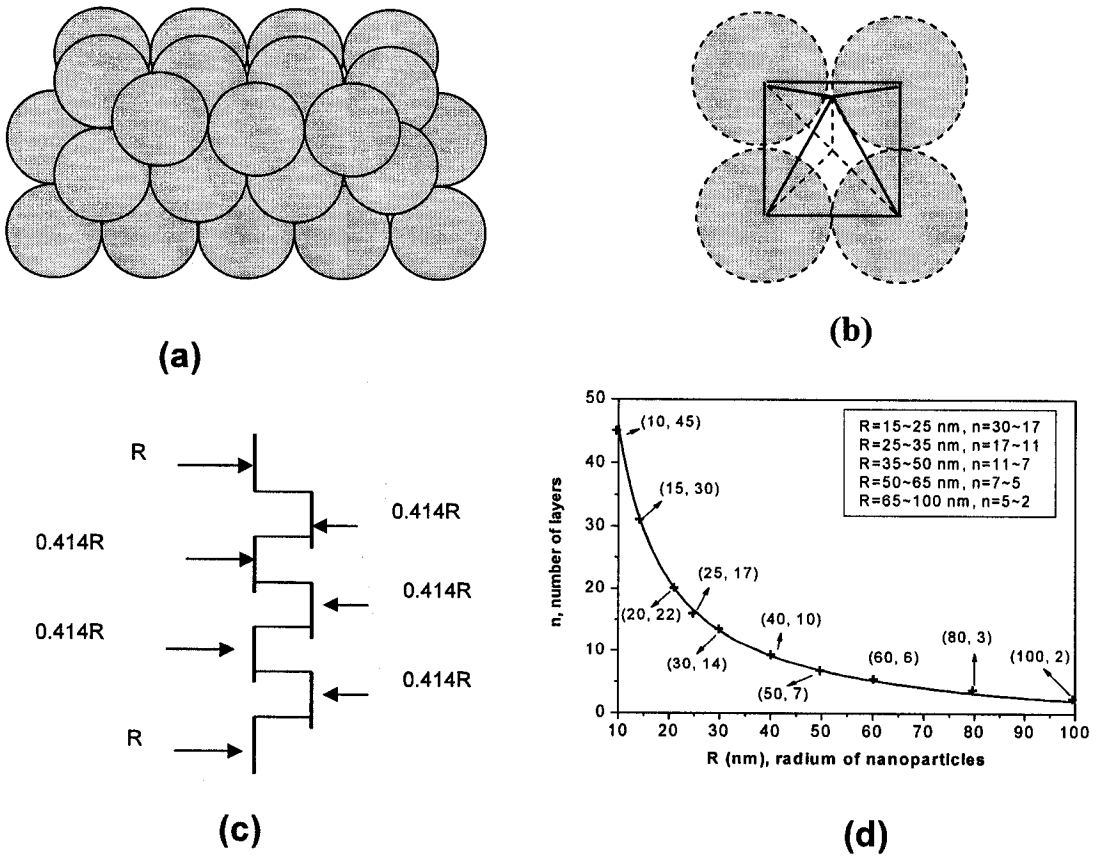

Figure 3-10 Schematics of particles packing (a-c) and the relationship between the radius of nanoparticles and the number of nanoparticle layers if the membrane thickness is 200 nm (d)

Since the palladium membrane is essentially made of nanoparticles, one can assure that palladium nanoparticles having the same size are packed in a simple geometrical array, as shown in Figure 3-10 (a) and the thickness of the membrane is T (nm), where n is the number of nanoparticle monolayer, and R is the radius of palladium nanoparticles. The relationship between T, n and R can be expressed in the equations (3-2) and (3-3) according to Figure 3-10 (b, c).

$$T=2R+ (n-2) \times 0.414R \qquad (3\text{-}2)$$

$$n = (T/R-1.172)/0.414 \qquad (3\text{-}3)$$

If the thickness of an ultra-thin palladium membrane is 200 nm, the number of layers is a function of the radius of nanoparticles, illustrated in Figure 3-10 (d). For example, when the radius of nanoparticle is 10 nm, the membrane having the thickness of 200 nm is

approximately assembled by 45 nanoparticle monolayers. As the size of palladium nanoparticles in Figures 3-3 (d) and 3-5 is about 100~130 nm, the membrane was built on the same experimental conditions and its thickness ranges from 300 nm to 400 nm. Thus, according to the equation (3-3), this membrane should be built about 12 nanoparticle monolayers. The experimental results obtained from hydrogen permeation tests demonstrate that this membrane is solid and dense, and it can be used for hydrogen extraction up to the temperature of 550°C and hydrogen pressure difference of 50 psi. Therefore, based on these experimental results, the required thickness of an ultra-thin palladium membrane can be designed and realized through the control of the concentration of $PdCl_2$ in the plating bath.

3.5 Conclusions

The observation of palladium deposited on a porous stainless steel substrate by an electroless process shows that the membrane is built from nanoparticles. The size of the palladium nanoparticles can be effectively controlled by changing the concentration of $PdCl_2$ in the plating solution. The thickness of an ultra-thin palladium membrane is directly determined by the diameter of palladium nanoparticles. The smaller the size of palladium nanoparticles is deposited, the thinner the dense palladium membrane will be built. The experimental data obtained from the ultra-thin palladium membrane having the thickness of 300 ~ 400 nm shows that this membrane is dense and it can be used at the temperatures of 550 °C and hydrogen pressure difference of 50 psi. This result allows to optimize the design of an ultra-thin palladium membrane and to control effectively its fabricated process in micro-devices application.

3.6 References

1. C.J.M. van Rijn, Nano and Micro engineered membrane technology, Membrane Science and Technology Series, 10, ELSEVIER, 2003
2. T. Mitsui, M. K. Rose, E. Fomin, D. F. Ogletree, M. Salmeron, Dissociative hydrogen adsorption on palladium requires aggregates of three or more vacancie, Nature 422, 705-707 (2003).
3. F. Favier, E.C. Walter, M.P. Zach, T. Benter, R.M. Penner, Hydrogen sensors and switches from electrodeposited palladium mesowire arrays, Science 293, 2227-2231 (2001).
4. B. L. French, Luke M. Davis, E. S. Munzinger, J. W. J. Slavin, P. C. Christy, D. W. Thompson, and R. E. Southward, Palladium-Polyimide Nanocomposite Membranes: Synthesis and Characterization of Reflective and Electrically Conductive Surface-Metallized Films, Chem. Mater. 17, 2091-2100 (2005).
5. S. Yoda, A. Hasegawa, H. Suda, Y. Uchimaru, K. Haraya, T. Tsuji, and K. Otake, Preparation of a Platinum and Palladium/Polyimide Nanocomposite Film as a Precursor of Metal-Doped Carbon Molecular Sieve Membrane via Supercritical Impregnation, Chem. Mater. 16, 2363-2368 (2004).
6. Z. Shi, S. Wu, J.A. Szpunar, and M. Roshd, An observation of palladium membrane formation on a porous stainless steel substrate by electroless deposition, Journal of Membrane Science, 280, 705-711 (2006).
7. C. Sachs, A. Pundt, R. Kirchheim, M. Winter, M. T. Reetz, and D. Fritsch, Solubility of hydrogen in single-sized palladium clusters, Phys. Rev. B 64, 075408 (2001).
8. Sz Csonka, A. Halbritter, G. Mihly, O. I. Shklyarevskii, S. Speller, and H. van Kempen, Conductance of Pd-H Nanojunctions, Phys. Rev. Lett. 93, 016802 (2004).
9. K.S. Rothenberger, A.V. Cugini, B.H. Howard, R.P. Killmeyer, M.V. Ciocco, B.D. Morreale, R.M. Enick, F. Bustamante, I.P. Mardilovich and Y.H. Ma, High pressure hydrogen permeance of porous stainless steel coated with a thin palladium film via electroless plating, J. Membr. Sci. 244, 55-68 (2004).
10. A. Johansson, J. Lu, J.-O.Carlsson and M. Boman, Deposition of palladium nanoparticles on the pore walls of anodic alumina using sequential electroless deposition, Journal of Applied Physics, Vol. 96, 5189-5194 (2004).
11. D.-W Lee, Y.-G. Lee, S.-E Nam, S.-K Ihm, K.-H. Lee. Study on the variation of morphology and separation behavior of the stainless steel supported membranes at high temperature, Journal of Membrane Science, 220, 137-153 (2003).
12. F.C. Gielens, H.D. Tong, C.J.M. van Rijn, M.A.G. Vorstman and J.T.F. Keurentjes, Microsystem technology for high-flux hydrogen separation membranes, Journal of Membrane Science, 243, 203-213 (2004).
13. S.V. Karnik, M.K. Hatalis, M.V. Kothare, Palladium based micro-membrane for water gas shift reaction and hydrogen gas separation, Processing of the 5th International Conference on Microreaction Technology (IMRET 5), Strasbourg, France, May 27-30, 2001.

14. S.-E. Nam, S.-H. Lee and K.-H. Lee, Preparation of a palladium alloy composite membrane supported in a porous stainless steel by vacuum electrodeposition, Journal of Membrane Science, 153, 163-173 (1999).
15. J. L. Fransaer and R. M. Penner, Brownian dynamics simulation of the growth of metal nanocrystal ensembles on electrode surfaces from solution. I. instantaneous nucleation and diffusion controlled growth, J. Phys. Chem. B 103, 7643-7653 (1999).
16. T. Hirsch, M. Zharnikov, A. Shaporenko, J. Stahl, D. Weiss, O. S. Wolfbeis, and V. M. Mirsky, Size-controlled electrochemical synthesis of metal nanoparticles on monomolecular templates, Angew. Chem. Int. Ed. 44, 6775-6778 (2005).
17. Y. Fu, L. Zhang, and J. Zheng, In-situ deposition of Pd nanoparticles on tubular halloysite template for initiation of metallization, Journal of Nanoscience and Nanotechnology, 5, 558-564 (2005).
18. D.V. Goia, Preparation and formation mechanism of uniform metallic particles in homogeneous solutions, J. Mater. Chem. 14, 451-458 (2004).

CHAPTER 4 [1]

MICROSTRUCTURE TRANSFORMATION OF PALLADIUM MEMBRANE IN HYDROGEN PERMEATION AT ELEVATED TEMPERATURE

4.1 Abstract

Palladium membrane used for hydrogen extraction from a gas mixture at elevated temperature is often deposited on a porous metal or ceramic substrate. This chapter demonstrates the effect of porous Inconel substrate on changes of the microstructure of palladium membrane during hydrogen permeation. It is found that the chemical reaction between palladium and phosphorus/phosphates takes place and forms the intermediate compound Pd_6P that gradually causes the surface layer damage of the membrane when palladium membrane deposited on this porous Inconel substrate is used for hydrogen extraction at the temperature of 550°C. Phosphorus is generated from the inorganic binders that are used in the fabrication of porous Inconel substrate. This chemical reaction should be noticed, as it will be detrimental to the performance of palladium membrane at high temperature. The obtained result also indicates that the deposition of palladium as hydrogenation catalysts should be avoided using on the work environment of phosphorus or phosphates.

4.2 Introduction

Palladium membrane can be used for hydrogenation catalysts and hydrogen extraction [1-5]. In order to reduce its thickness and expense as well as to improve its hydrogen permeability, the membrane is usually deposited on a relatively low selective porous substrate. This substrate should have a good mechanical strength at elevated temperature. Micro-porous metals and ceramics are often employed as the substrates because they can support palladium membranes used for hydrogen permeation at the temperatures of 300-850°C. [5-12] However, the selection of porous metals as the substrate is preferable. One reason is that they are easily integrated with other parts of hydrogen extraction system and have good mechanical strength at high temperature. On the contrary, microporous ceramic substrates are difficult to be integrated with other parts because they are brittle. The other reason is that the coefficient of thermal expansion of ceramic substrate does not match that of palladium membrane. This will cause cracking of the membrane when used at high temperature. Porous metal or ceramic substrates are usually fabricated using powder metallurgical process. Inorganic binders containing soluble phosphates or silicates must be employed in order to obtain good mechanical

---

[1] This chapter has been published as an article in journal of Membrane Science, 284, 424-430 (2006)

strength at elevated temperature. There are numerous reports of hydrogen separation and permeation with palladium membranes deposited on porous metal substrates. [5, 6, 9, 12, 13] However, so far the effect of porous metal substrate on the microstructure of palladium membrane during hydrogen permeation at high temperatures is not investigated. Most users buy their required porous metal substrates from the manufacturers and follow the introductions to employ them below their heat tolerance temperatures. The effects of the substrate on the microstructure transformation of palladium membrane are neglected. In this chapter, the surface microstructures of palladium membranes and their transformations are characterized and analyzed after they are used for hydrogen permeation at the temperature of 550°C holding different time.

4.3 Experimental section

In this research, a 2 μm grade porous Inconel plate, purchased from Mott Metallurgical Corporation is used as the substrate for the deposition of palladium membrane. The substrate is defined as 2 μm grade that means over 95% of particles having the size of 2 μm cannot pass through this substrate. The porosity of this substrate is about 40~60% and the pore size at the substrate surface ranges from 2 to 30 μm, as shown in Figure 4-1. This porous Inconel 600 substrate can be used at the maximum temperature of 1500°F (~820°C) in reducing atmosphere, according to the specification of this product offered by the company. The normal composition of Inconel 600 is (wt%): 72%Ni, 15.50%Cr, 8%Fe, 0.50%Si, 1.00%Mn, 0.15%C, 0.50%Cu, 0.015%S, <<0.015%P. It is fabricated using powder metallurgical process with micron size Inconel alloy particles. Inorganic binders containing soluble phosphates are often added in order to obtain good mechanical strength of the substrate at high temperature. Electroless deposition usually comprises a three-step process: (1) pretreatment of the substrate; (2) activation of the substrate surface, and (3) electroless deposition. Ten substrate specimens having a diameter of ϕ45 mm were cut from porous Inconel plate. They were cleaned in an ultrasonic bath with acetone for 15 minutes and one-side surface of these samples was activated with an acid and rinsed with deionised water. The other side surface of these samples was pasted with a plastic stick-paper. Then, these substrate samples were transferred immediately into electroless plating bath that kept a constant temperature of 60°C. They were suspended into the plating solution. The concentration of $PdCl_2$ in the plating solution was 4.2 g/l. The deposition time was 15 hrs. After deposition, the samples were cleaned with deionized water and dried in an oven at the temperature of 80°C for 5 minutes. Then the microstructure of the samples was analyzed using PHILIPS XL30 FE SEM (Filed Emission Scanning Electron Microscopy), equipped with an EDS (Energy Dispersive Spectroscopy, GENESIS 2000 X-ray Microanalysis System). The phase composition of these palladium membranes before and after hydrogen permeation was also investigated by X-ray diffraction (Rigaku Rotating Anode Diffractometer using monochromated Cu Kα radiation). The composition of electrolyte and other plating parameters are listed in Table 4-1 or referred to elsewhere. [6, 13-15] According to the weight increment of the samples before and after palladium deposition, the average thickness of each palladium membrane is calculated around 18 μm, which is almost the same as the measurement from their cross-section micrographs. The gas-tightness of each membrane was examined using nitrogen gas at the pressure of 50 psi starting from the

room temperature to 550°C and no nitrogen through the membranes was detected on the permeated side by gas chromatograph. Hydrogen selectivity of these solid palladium membranes is infinite because only hydrogen can pass through them and nitrogen is wholly blocked. The measurement of hydrogen permeability was carried out in a permeation cell at the temperatures from 300°C to 550°C and hydrogen pressure difference of 50 psi. The experimental apparatus used for hydrogen permeation was similar to the one described elsewhere. [16] Microstructure transformations of three same palladium membranes were observed using SEM after tested for hydrogen permeation at 550°C for 1 hr, 2 hrs, 4 hrs and 20 hrs, respectively. The remaining seven membrane samples were also tested to confirm the obtained results and phenomena.

Table 4-1 Composition of electroless plating solution and some experimental parameters

Component or parameters	Concentration and temperature
$PdCl_2$	4.2 g/l
$Na_2EDTA.2H_2O$	40.1 g/l
$NH_3.H_2O$ (28%)	198 ml/l
N_2H_4 (1M)	5.6 ml/l
pH	10 ~ 10.4
Temperature (°C)	60 °C

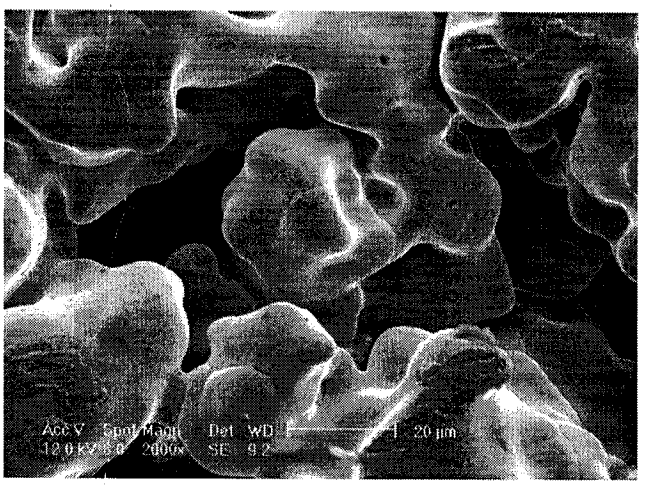

Figure 4-1 SEM micrograph showing surface microstructure of porous Inconel substrate

4.4 Results and Discussion

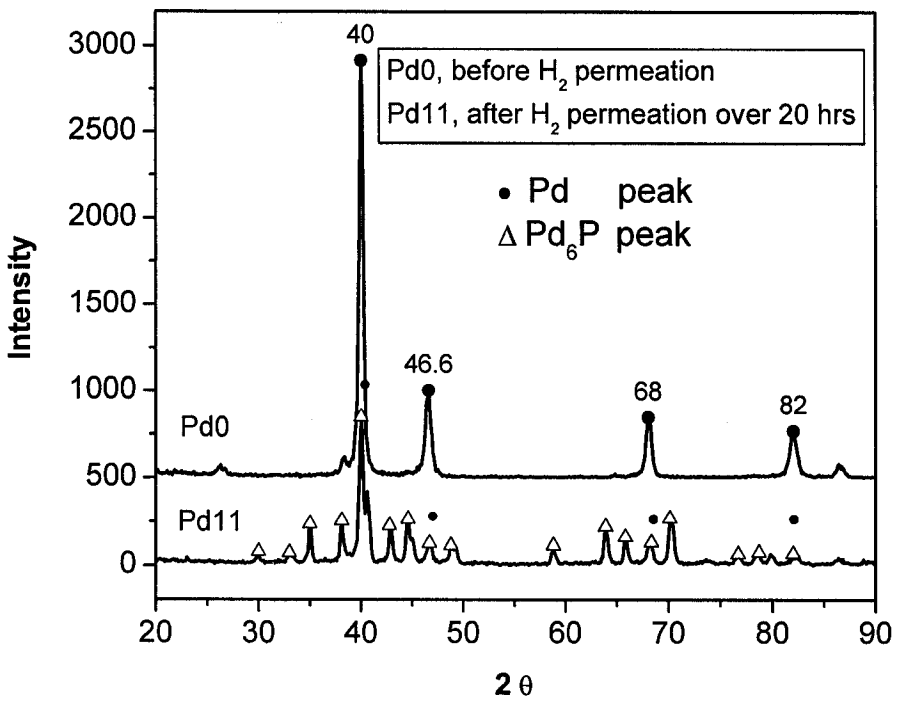

Figure 4-2 X-ray diffraction spectra from palladium membrane deposited on porous Inconel substrate, the spectrum of Pd0 measured from the original palladium membrane, and the spectrum of Pd11 measured from the membrane after hydrogen permeation test at the temperature of 550°C for 20 hrs

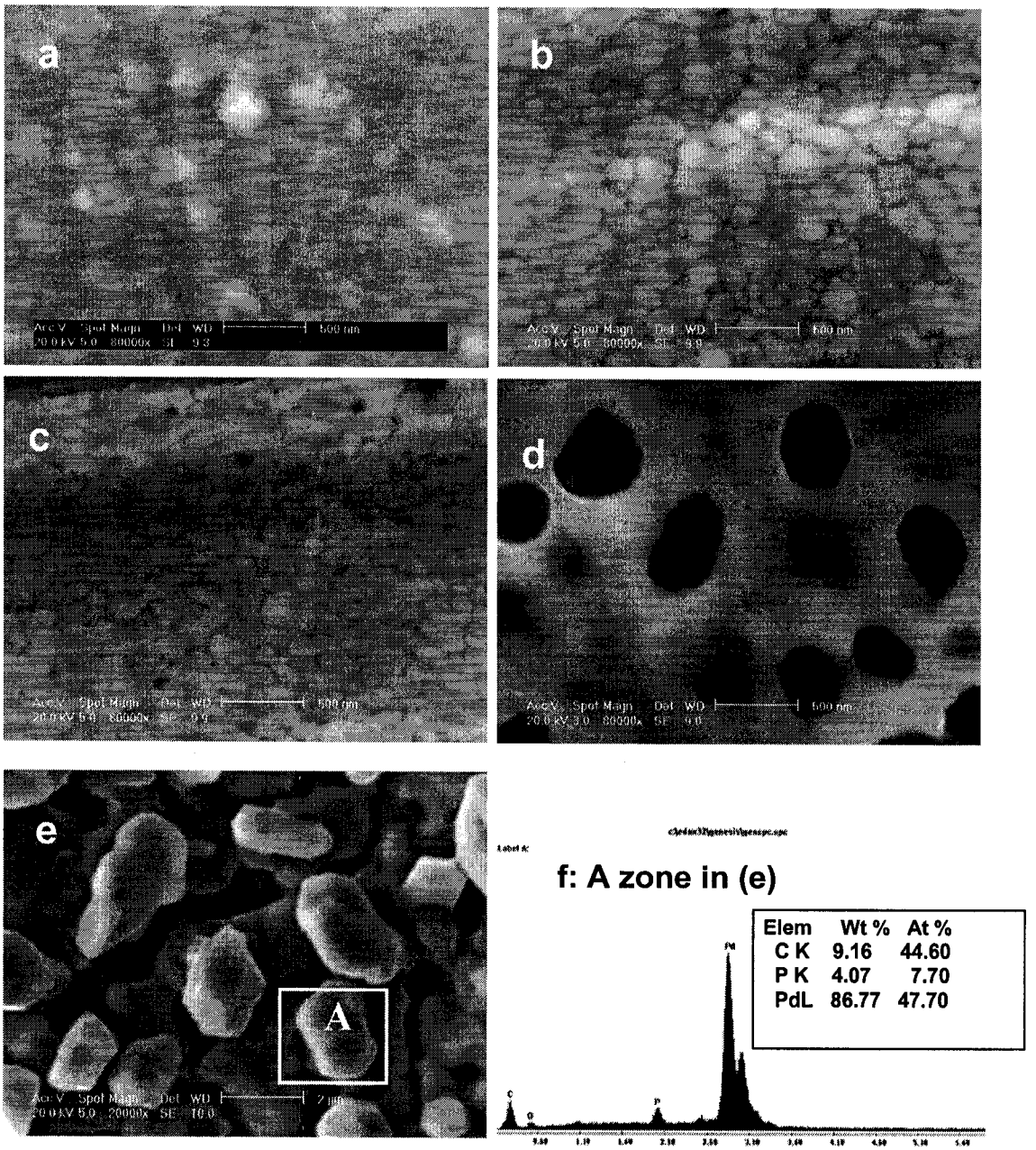

Figure 4-3 SEM micrographs showing the surface structures of the original palladium membrane after electroless deposition (a), and the membrane after hydrogen permeation tests at the temperature of 550°C for (b) 1hr, (c) 2 hrs, (d) 4 hrs, (e) 20 hrs; and (f) the energy-dispersive spectrum from the marked area A in the image (e)

Two x-ray diffraction spectra (XRD) were measured from the same palladium membrane before and after hydrogen permeation. The XRD spectra of Pd0 were obtained from the membrane that was deposited on porous Inconel substrate by electroless process without any other treatment. The other XRD spectra were measured from the membrane after it was used for hydrogen permeation test at the temperature of 550°C for 20 hrs. The analysis of XRD spectra reveals that the original membrane is made of palladium and that the surface microstructure of this membrane is composed of palladium and an intermediate compound Pd_6P after it was used for hydrogen permeation at 550°C for 20 hrs. Microstructure transformations of this palladium membrane used for hydrogen extraction at 550°C are illustrated in Figure 4-3(b-e) after hydrogen permeation time of 1 hr, 2 hrs, 4 hrs and 20 hrs. Palladium grains and grain-boundaries can be quite clearly seen in Figure 4-3(b). However, they are invisible at surface of the original palladium membrane, as shown in Figure 4-3(a). When hydrogen permeation time at 550°C extends to 2 hrs, there are many nano-size pores forming at its surface. The size of these pores ranges from 30 to 80 nm, as shown in Figure 4-3(c). Comparing the surface morphologies between Figure 3(b) and (c), one can see that many pores appear at grain boundaries with increasing hydrogen permeation time from 1 hr to 2 hrs. When it is reused for hydrogen permeation test at the temperature of 550°C in another 2 hrs (totally 4 hrs), the surface morphology of this membrane in Figure 4-3(d) is greatly different from that in Figure 4-3(c). One can see that the grains around the pore area cannot be identified easily and the size of pores enlarges to 300~500 nm. However, this palladium membrane was still solid and dense when the gas tightness of this membrane was examined with nitrogen gas at the temperature of 550°C and the absolute nitrogen gas pressure difference of 50 psi.

The qualitative analysis of the composition from the surface microstructure in Figure 4-3(d) illustrates that the content of phosphorus at surface of the membrane ranges from 0.5 to 0.9wt%. The question has to be asked where phosphorus arises from. There is no phosphorus or phosphate in the composition of the electroless-plating solution. Most parts in the permeation cell made of stainless steel contain a very low content of phosphorus (<0.045wt%P). There is no phosphorus in the graphite gasket, analyzed by EDS. The gases used for permeability measurement (H_2) and gas-tightness detection (N_2) are high purity (99.99%) and they do not contain phosphorus. Only the porous Inconel substrate is suspected. Phosphorus in the composition of normal Inconel alloy is less than 0.015wt%. However, this porous Inconel substrate is manufactured using powder metallurgical process. Soluble inorganic binders containing phosphates/dihydrogen phosphates are generally added in order to obtain good mechanical strength of the substrate at high temperature. The soluble dihydrogen phosphates are transformed into phosphates that remain in the substrate during the sintering process. They cannot be removed in the fabrication process. The deposition of palladium is carried out in the plating bath at the temperature of 60°C. This process does not affect the substrate. After palladium membrane is built, it will be used at elevated temperatures. The heat tolerance of this porous Inconel alloy is 820°C at reducing atmosphere, accoding to the specification from the company. So, the recommended temperature of this substrate is suitable for the temperature below 820°C. One may think that the applied temperature of this substrate after deposited palladium membrane can also be used below this heat tolerance temperature and the effect of porous Inconel substrate on the microstructure of palladium membrane can be neglected. However, in this research, we find that the chemical reaction between palladium membrane and phorphorus/phosphates can take

place at the temperature of 550° and the reaction products will damage the surface layer of the membrane when it is deposited on this porous Inconel substrate. One of the reaction products at surface of the membrane is identified as the compound Pd_6P by the qualitative analysis of EDS from the marked area A in Figure 4-3(e), as illustrated in Figure 4-3(f), because the atomic ratio between Pd and P is about 6:1. This measurement confirms the obtained result from x-ray diffraction spectra in Figure 4-2 after the membrane was used for hydrogen permeation over 20 hrs.

Based on the observation of surface microstructures of this palladium membrane with the extension of hydrogen permeation time presented in Figure 4-3(a-e). The microstructural transformations of the membrane can be described as three steps: (1) nanopores forming; (2) the pores broadening to be interconnected and (3) granulating. We find that the surface layer of this palladium membrane is gradually damaged by the chemical reaction between palladium membrane and phosphorus/phosphates with increasing hydrogen permeation time at 550°C. However, after used for hydrogen permeation at 550°C over 20 hrs, the palladium membrane was still dense when it was examined with nitrogen gas at the temperature of 550°C and the absolute nitrogen gas pressure difference of 50 psi, which can also be observed from the cross-section micrographs of the membrane, illustrated in Figures 4-4(a) and 4-5(a).

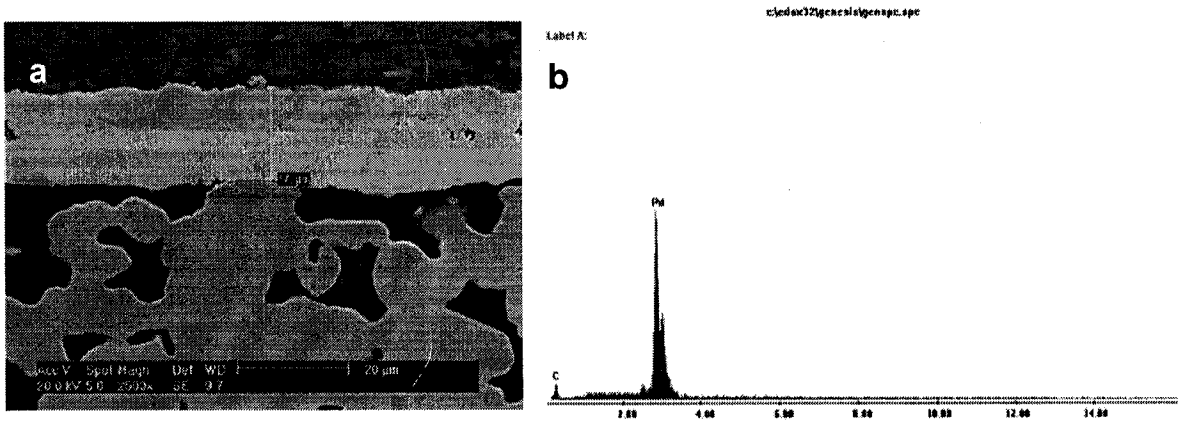

Figure 4-4 Cross-section of palladium membrane without exposure of hydrogen permeation area (a) and the energy-dispersive spectrum from the surface microstructure of this area (b)

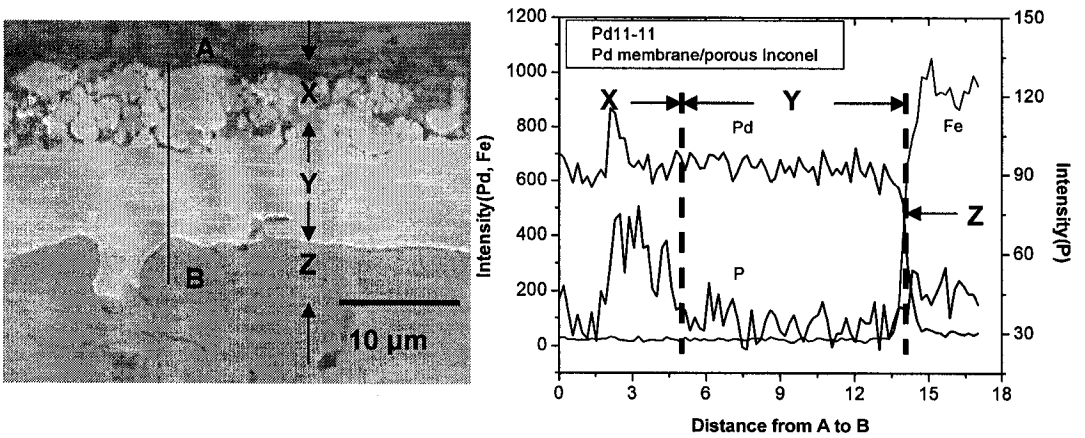

Figure 4-5 (a) SEM micrograph showing the cross-section microstructure of palladium membrane, and (b) the line scan of the elemental distributions of Pd, P and Fe from A to B, marked in the image (a)

Figure 4-4(a) shows the cross-section micrograph of this palladium membrane without hydrogen exposure area (or sealing area) after hydrogen permeation test at 550°C for 20 hrs. The observation of surface morphologies of the membrane at this sealing area illustrates the clear grains and grain boundaries due to annealing at high temperature and no damage appearing at the surface and cross-section morphologies. The analysis of EDS from the surface microstructure of this palladium membrane in the sealing area illustrates that there is no phosphorus, as shown in Figure 4-4(b). While it can be seen a serious damage happened at the surface morphology in Figure 4-3(e) and the cross-section in Figure 4-5(a) on the hydrogen permeation zone. The distribution of phosphorus is measured using line scan from A to B, as shown in Figure 4-5(b). One can see that the content of phosphorus at the reaction part (marked area X) is the highest. Phosphorus at the substrate (marked area Z) is less than that in the reaction part of this palladium membrane but it is higher than that in the non-reaction part (marked area Y) of the membrane. The observation of surface morphologies of palladium membrane after hydrogen permeation test also clearly illustrates that a serious damage occurs at the reaction area. Meanwhile, the composition analysis from the surface microstructure of this palladium membrane shows that the content of phosphorus in the granules formed at the hydrogen permeation area is up to 4~5 wt%. This result indicates that the surface layer of the membrane is damaged by the formation of Pd_6P from the chemical reaction between palladium and phosphorus/phosphates. It can be approximately measured that the damaged surface layer of the membrane extends over 1/3 of its thickness from the cross-section micrograph in Figure 4-5(a). This is also indirectly confirmed by the variation of hydrogen flux, as shown in Figure 4-6. The value of hydrogen flux through the membrane at the temperature of 550°C and absolute pressure difference of hydrogen at 50 psi is a linear function with hydrogen permeation time. One can see that the value of hydrogen flux increases about 50% after hydrogen permeation test for 20 hrs. The

increment of hydrogen flux is caused by the chemical reaction between palladium and phosphorus/phosphates. The damaged thickness (or called sacrificial thickness) of this membrane and the remained thickness (or called effective thickness) can be calculated from Figure 4-6.

As we know, the ability to transport hydrogen through a palladium membrane is quantified in terms of permeability, permeance or flux. [17] Hydrogen transport through a membrane is usually characterized by the measurement of hydrogen flux, which is defined as the rate of hydrogen passing through the membrane per unit area in the following equation (4-1) ($mol.m^{-2}.s^{-1}$). Theoretically, the flux of hydrogen through palladium membranes is directly proportional to the product of the hydrogen permeability (Q) and the difference between the hydrogen partial pressures across the membrane raised an exponent ($0.5 \leq n \leq 1$) but inversely proportional to the membrane thickness, as expressed in equation (4-1).

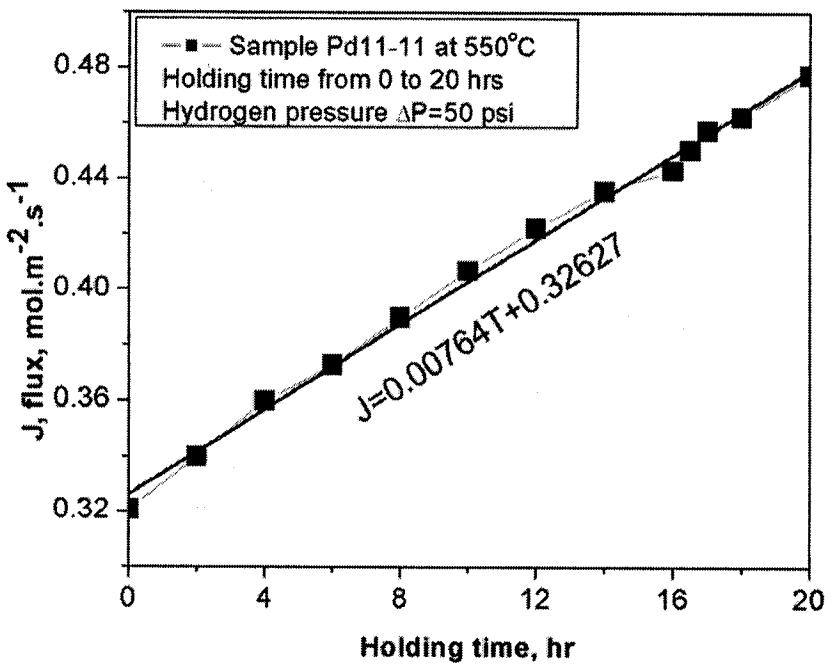

Figure 4-6 Variation of hydrogen flux with hydrogen permeation time at the temperature of 550°C (the average thickness of palladium membrane is 18 μm)

The exponent is determined by optimizing the linear fit via varying the value of n in a plot of flux versus $(P_{H_2 1}^n - P_{H_2 2}^n)$. Exponent values for thin membranes in the ranges of 0.5~1.0 have been reported for supported palladium, along with temperature-dependent exponents. [18] If these physical and process parameters are acquired, hydrogen flux as a function of temperature or pressure can be calculated and graphed. Based on the

measurement of hydrogen permeation through these palladium membranes that we prepared, the exponent value of n is 0.5.

$$J_{H_2} = -Q\frac{(P^n_{H_2,1} - P^n_{H_2,2})}{X} \qquad (4\text{-}1)$$

According to equation (4-1), the values of hydrogen flux through the same palladium membrane should be relatively stable with the extension of hydrogen permeation time when they are used at the same temperatures and hydrogen pressure difference $(P^n_{H_21} - P^n_{H_22})$. When palladium membranes are used for hydrogen permeation at the same conditions of temperature and pressure, hydrogen flux is only inversely proportional to their thicknesses. Based on the measured values of hydrogen flux through this palladium membrane with increasing hydrogen permeation time at 550°C, the sacrificial thickness in this palladium membrane can be calculated from equation (4-2). Here, we assume that the thickness of this palladium membrane is X_1 and its hydrogen flux is J_1, when it is used for hydrogen permeation at the beginning of the temperature of 550°C. When it is used for hydrogen permeation in 20 hrs, hydrogen flux J_2 will change with the variation of the membrane thickness X_2. The difference of the thickness between X_1 and X_2 is named as the damaged thickness or sacrificial thickness, ΔX, which is caused by the reaction attack. The value of ΔX can be calculated in the equation (4-2).

$$\Delta X = X_1 - X_2 = X_1\frac{J_2 - J_1}{J_2} \qquad (4\text{-}2)$$

Based on the measured values of hydrogen flux J_1, J_2 and the linear function of hydrogen flux with hydrogen permeation time in Figure 4-6, and the average thickness of the membrane, X_1=18 μm, the sacrificial thickness of the membrane ΔX is calculated about 6 μm, according to the equation (4-2). Thus, the effective thickness of this membrane remains about 12 μm, which can also be approximately measured from the cross-section micrograph in Figure 4-5(a). This membrane is still dense and no nitrogen leakage is detected in the gas tightness of this membrane with nitrogen gas at the permeated side under the absolute pressure difference of nitrogen at 50 psi and the temperature at 550°C.

In order to make sure the chemical reaction products between palladium and phosphorus, many intermediate phases may form, such as Pd_8P, Pd_6P, $Pd_{4.8}P$, Pd_3P, Pd_5P_2, Pd_7P_3 and PdP_2. in Pd-P binary diagram. [19] Based on our analyses of XRD in Figure 4-2 and EDS in Figure 4-3(f), the intermediate phase Pd_6P is identified as the reaction product. According to Pd-P binary diagram, if the content of phosphorus/phosphate in this membrane system is low, Pd_8P will be formed first. But this compound cannot be found in JCPDS-international center for Diffraction Data. The intermediate compounds listed in JCPDS cards are only $Pd_{15}P_2$, Pd_6P, Pd_9P_2, Pd_5P_2 and Pd_7P_3. Comparing these compounds in JCPDS cards with our measured results from XRD and EDS, The chemical reaction product at hydrogen permeation area of this membrane surface in Figure 4-3(e) is identified as Pd_6P.

Why does this reaction only occur at the surface of the membrane instead of the interface between the membrane and the substrate and how does phosphorus diffuse to the surface? We have already designed some experiments to confirm this phenomenon.

The first experiment was that we sintered a membrane for 4 hrs at the temperature of 550°C and the absolute nitrogen gas pressure difference of 50 psi. This membrane was built at the same porous Inconel substrate under the same deposition conditions as the previous one. After sintered, the surface microstructure of the membrane is observed and no damage is found except that the clear grains and grain-boundaries are identified due to annealing.

The second experiment was that we deposited palladium membrane on the same porous Inconel substrate, but it had already been coated a thinner Ni-P film (the content of phosphorus was about 0.5~0.6 wt%, analyzed by EDS) at its surface using electroless process. After that, this membrane was used for hydrogen permeation at the temperature of 550°C and hydrogen pressure difference of 50 psi. We find the same phenomena happened at the membrane surface of hydrogen permeation area, but there is no reaction in the interface between palladium membrane and Ni-P coated substrate surface.

The third experiment was that we deposited palladium membranes having different thickness on a 0.2 μm grade porous stainless steel substrate. This substrate was also purchased from the same manufacturer. After they were built, the membranes were used for hydrogen permeation tests under the same conditions. We find the same phenomena that the reaction product Pd_6P forms at the surface of hydrogen permeation area and surface layer of the membrane is gradually damaged.

In addition, the chemical reaction between palladium and phosphorus/phosphates under the hydrogen pressure at elevated temperature is probably followed the explanation of Pd_6PH_z structure. [19-21] Based on the structure of Pd_6PH_Z, together with our observation of the surface morphologies in Figure 4-3(a-e) and the cross-section in Figure 4-5(a), the chemical reaction between palladium and phosphorus/phosphates can only take place at the inlet side (higher hydrogen pressure side). It can be deduced as the following chemical equation (4-3):

$$6\,Pd + P + (Z/2)\,H_2 \rightarrow (Pd_6P)Hz \qquad (4\text{-}3)$$

It is possible that hydrogen acts as a catalyst to promote the reaction between palladium and phosphorus. However, the further reaction mechanisms, such as the diffusion behavior of phosphorus from the substrate to palladium membrane surface and the effect of hydrogen on this reaction, are being further investigated.

Based on the above results, when porous Inconel alloy is used as the substrate for the deposition of palladium membrane, the content of phosphorus/phosphate in the composition of the substrate should be as low as possible. It is recommended that the addition of inorganic binders during the fabrication of the porous metal substrates should be phosphate-free, when the substrates are used for the deposition of palladium membrane in application of hydrogen separation and purification. In the meantime, the result from the chemical reaction between palladium and phosphorus/phosphates also indicates that the deposition of palladium for hydrogenation catalysts should be avoided using under the work environment of phosphorus or phosphates

4.5 Conclusions

The chemical reaction between palladium and phosphorus/phosphates takes place and the reaction product, an intermediate compound Pd_6P forms during the process of hydrogen permeation at 550°C. This reaction will gradually damage surface microstructure of the membrane surface when palladium membrane is deposited on porous Inconel substrate. Phosphorus is originated from inorganic binders and from the trace in the substrate. This chemical reaction should be avoided, as it will be detrimental to the membrane during hydrogen permeation at high temperature. The experimental results also indicate that the deposition of palladium as hydrogenation catalysts is recommended not to use in the environment of phosphorus or phosphates.

4.6 References

1. V. Hollein, M. Thornton, P. Quicker and R. Dittmeyer, Preparation and characterization of palladium composite membranes for hydrogen removal in hydrocarbon dehydrogenation membrane reactors, Catal. Today, 67, 33-42 (2001).
2. A. Li, W. Liang and R.Hughes, Fabrication of dense palladium composite membranes for hydrogen separation, Catal. Today, 56, 45-51 (2000).
3. D. Astruc, F. Lu and J. R. Aranzaes, Nanoparticles as recyclable catalysts: the frontier between homogeneous and heterogeneous catalysis, Angew. Chem. Int. Ed. 44, 7852-7872 (2005).
4. B.L. French, L.M. Davis, E.S. Munzinger, J.W.J. Slavin, P.C. Christy, et al., Palladium-polyimide nanocomposite membranes: synthesis and characterization of reflective and electrically conductive surface-metallized films, Chem. Mater. 17, 2091-2100 (2005).
5. K.S. Rothenberger, A.V. Cugini, B.H. Howard, R.P. Killmeyer, M.V. Ciocco, et al., High pressure hydrogen permeance of porous stainless steel coated with a thin palladium film via electroless plating, Journal of Membrane Science, 244, 55-68 (2004).
6. Z. Shi, S. Wu, J. Szpunar, M. Roshd, An observation of palladium membrane formation on a porous stainless steel substrate by electroless deposition, Journal of Membrane Science, 280, 705-711 (2006).
7. K. Jarosch and H.I. de Lasa, Permeability, selectivity and testing of hydrogen diffusion membranes suitable for use in steam reforming, Ind. Eng. Chem. Res. 40, 5391-5397 (2001).
8. L. Paturzo and A. Basile, Methane Conversion to Syngas in a Composite palladium membrane reactor with increasing number of Pd layers, Ind. Eng. Chem. Res. 41, 1703-1710 (2002).
9. Y.H. Ma, I.P. Mardilovich and E.E. Engwall, Thin composite palladium and palladium/alloy membranes for hydrogen separations, Ann. N. Y. Acad. Sci. 984, 346-360 (2003).
10. J.N. Keuler, L. Lorenzen and S. Miachon, Preparing and testing Pd films of thickness 1–2 micrometer with high selectivity and high hydrogen permeance, Separation Science and Technology, 37, 379-401 (2002).
11. Varma, K.L. Yeung, R.S. Souleimanova and A.S. Mukasyan. Novel approach for thin dense nanoscale-grained metal films, Ind. Eng. Chem. Res. 41, 6323-6325 (2002).
12. C. Su, T. Jin, K. Kuraoka, Y. Matsumura and T. Yazawa, Thin palladium film supported on SiO_2-modified porous stainless steel for a high-hydrogen-flux membrane, Ind. Eng. Chem. Res. 44, 3053-3058 (2005).
13. J. Shu, B.P.A. Grandjean, S. Kaliaguine, Morphological study of hydrogen permeable Pd membranes, Thin Solid Film, 252, 26-34 (1994).
14. Z. Shi, S.Wu, J. Szpunar, "Bridge model" of nanoparticles deposited on pore area of the substrate during a membrane fabrication. Appl. Phys. Lett. 87, 12913 (2005).
15. Schlesinger, M.; Paunovic, M. Modern Electroplating, fourth edition, Toronto, Wiley, 2000.

16. S.-E. Nam, S.-H. Lee and K.-H. Lee, Preparation of a palladium alloy composite membrane supported in a porous stainless steel by vacuum electrodeposition, Journal of Membrane Science, 153, 163-173 (1999).
17. B.D. Morreale, M.V. Ciocco, R.M. Enick, B.I. Morsi, B.H. Howard, et al. The permeability of hydrogen in bulk palladium at elevated temperatures and pressures, Journal of Membrane Science, 212, 87-97 (2002).
18. H.B. Zhao, K. Pflanz, J.H. Gu, A.W. Li, N. Stroh, H. Brunner, G.X. Xiong. Preparation of palladium composite membranes by modified electroless plating procedure. Journal of Membrane Science, 142, 147-157 (1998).
19. L.-O. Gullman. X-ray diffraction and thermo-analytical investigation of the palladium-phosphorus system, J. Less-Common Met. 11, 157-167 (1966).
20. Y. Andersson, S. Rundqvist and R. Tellgren. Neutron powder diffraction investigations of hydrogenated $Pd_3P_{0.8}$ and Pd_6P, J. Solid State Chem. 52, 327-329 (1984).
21. Y. Andersson, S. Rundqvist, R. Tellgren and J. O. Thomas. Neutron powder diffraction investigations of pure and deuterated palladium phosphide Pd_6P, Acta Cryst. B37, 1965-1972 (1981).

CHAPTER 5 [1]

SYNTHESIS OF PALLADIUM NANOSTRUCTURES BY SPONTANEOUS ELECTROLESS DEPOSITION

5.1 Abstract

Palladium nanostructures are prospective in various applications of hydrogenation products. In this chapter, we demonstrate that three different types of palladium nanostructures can be synthesized simultaneously at the surface of porous stainless steel substrate by an electroless deposition process. The palladium nanowires and nanoparticle-monolayer membranes are deposited without any external field except an autocatalytic chemical reaction. A new method to fabricate palladium nanostructures for engineering applications is described.

5.2 Introduction

Metal nanostructures are important for nanotechnology applications as they are likely to play an important role as interconnects, sensors and active components in nanoscale devices. [1] The most common synthetic methods such as electrochemical and vapor depositions have been successfully used to develop high quality arrays of nanostructures in a large variety of materials. [2-10] For examples, the deposited palladium nanoparticles are widely used in hydrogenation catalysts; [11, 12] the thin palladium membranes can be used to extract high quality hydrogen from a gas mixture [13] and the palladium mesowires/nanowires used for hydrogen sensors and hydrogen-actuated switches that exhibit a fast response time for hydrogen detection. [8, 14] Most nanowires are created on templates or on lithograph patterns using electrochemical process. [15-18] The development of new techniques for the fabrication of palladium nanostructures in engineering application is continuously investigated. This chapter demonstrates that three types of palladium nanostructures can be created, when palladium is deposited on the porous stainless steel substrate by the electroless process. The palladium nanowires and nanoparticle-monolayer membranes are well-organized without any external field except an autocatalytic chemical reaction.

---

[1] This chapter has been published as an article in Chemical Physics Letters 422, 147-151 (2006)

5.3 Experimental section

In this research program, a 0.2 μm grade porous 316L stainless steel plate, purchased from Mott Metallurgical Corporation is used as the substrate for the deposition of palladium. The substrate is defined as 0.2 μm grade that means over 95% particles having the size of 0.2 μm are rejected by this substrate during filtering. It implies that the pore size in the substrate is, in general, less than 0.2 μm. The pores within the substrate are interconnected and their size at the substrate surface ranges from 0.2 to 10 μm, as shown in Figure 5-1 (a). There are a lot of irregular steps at free-pore area of the substrate surface, as shown in Figure 5-1 (b-d). Electroless deposition usually comprises a three-step process: (1) pretreatment of the substrate; (2) activation of the substrate surface; (3) electroless deposition. The samples having the size of 20 mm x 20 mm were cleaned in an ultrasonic bath with acetone for 15 minutes. After their surfaces were activated with an acid and rinsed with deionized water, the samples were transferred immediately into electroless plating bath that kept a constant temperature of 60°C. The concentrations of $PdCl_2$ in the plating bath were 1.8~2 g/l and 2.4 g/l. The deposition time was 120 s. After deposition, the samples were cleaned with deionized water and dried in an oven at temperature of 80°C for 5 minutes. Then they were observed and analyzed by a PHILIPS XL30 FEG SEM (Filed Emission Scanning Electron Microscopy), equipped with an EDS (Energy Dispersive Spectroscopy, GENESIS 2000 X-ray Microanalysis System). The composition of the electroless plating baths and plating conditions are listed in Table 6-1 or referred to elsewhere. [19, 20]

Table 5-1 Composition of electroless plating bath and other experimental parameters

Components	Concentrations or other parameters
$PdCl_2$	1.8~2 g/l, 2.4 g/l
$Na_2EDTA.2H_2O$	40.1 g/l
$NH_3.H_2O$ (28%)	198 ml/l
N_2H_4 (1M)	5.6 ml/l
PH	10~10.4
Temperature (°C)	60

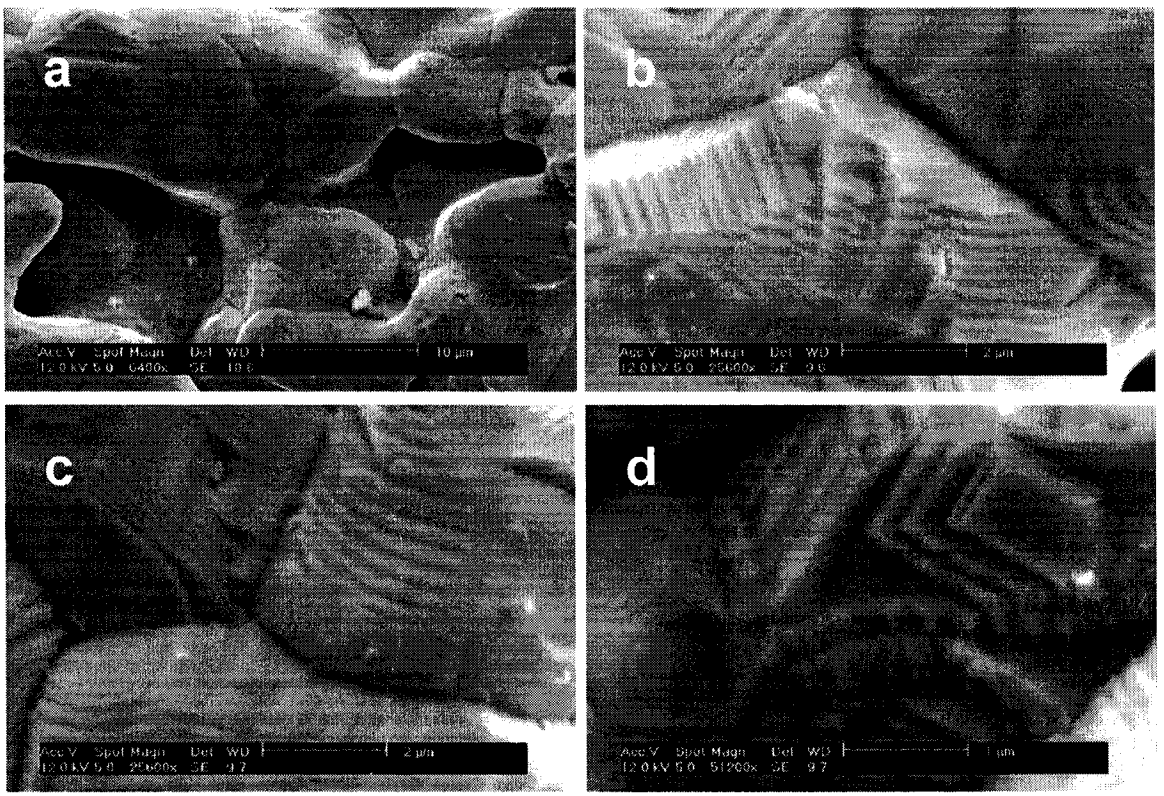

Figure 5-1 SEM micrographs of the porous stainless steel substrate
(a) The surface microstructure of the porous substrate;
(b-d) The irregular steps at free-pore area of the substrate

5.4 Results and Discussion

Electroless deposition occurs simply by immersion of samples in a plating bath and does not need rectifiers, batteries or anodes. The deposition of palladium is an autocatalytic process that takes place according to the chemical reaction (5-1):

$$2Pd(NH_3)_4^{2+} + N_2H_4 + 4OH^{-1} \rightarrow 2Pd^{0} + 8NH_3 + N_2 + 4H_2O \qquad (5\text{-}1)$$

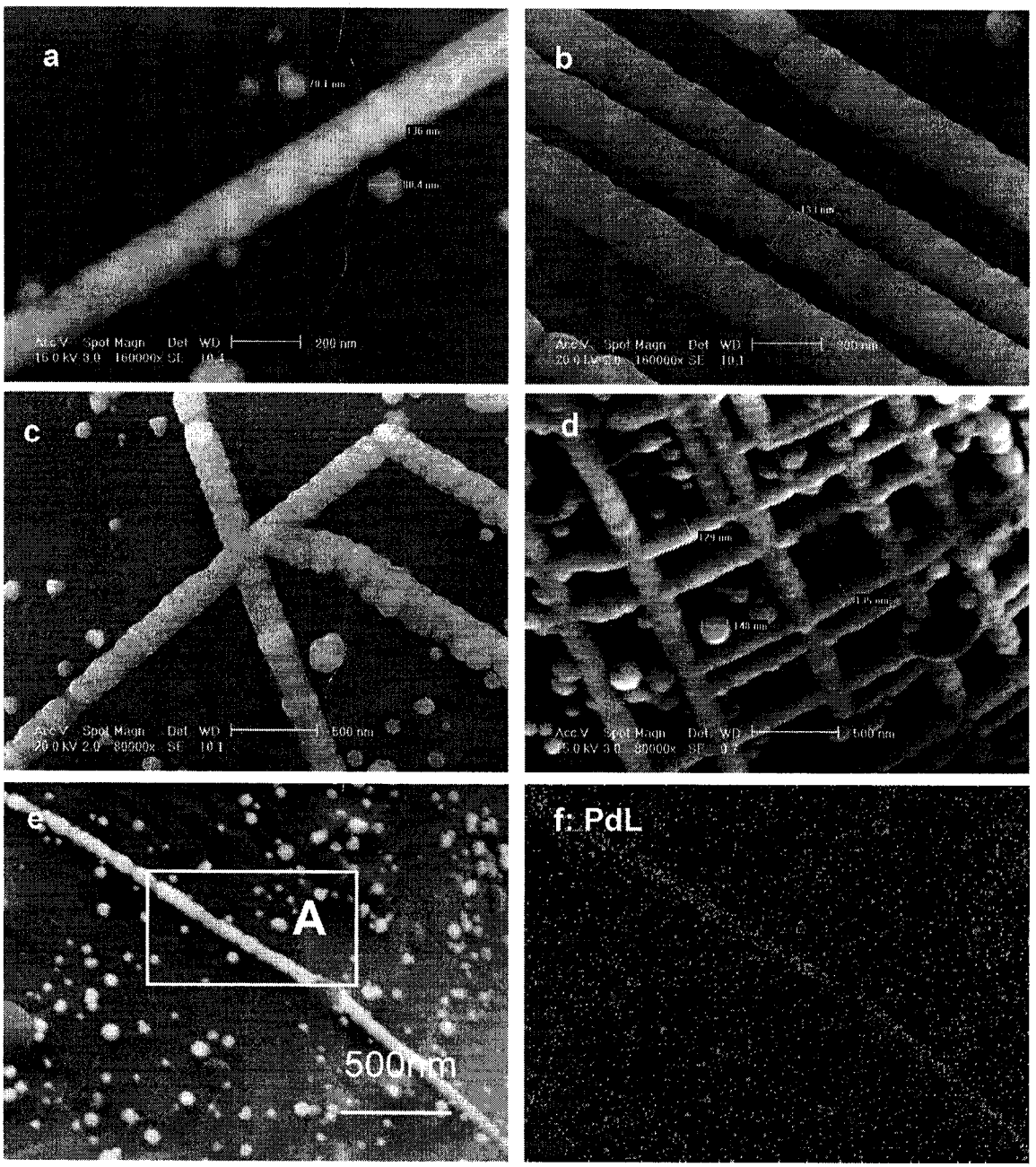

Figure 5-2 (a-e) continue to next page

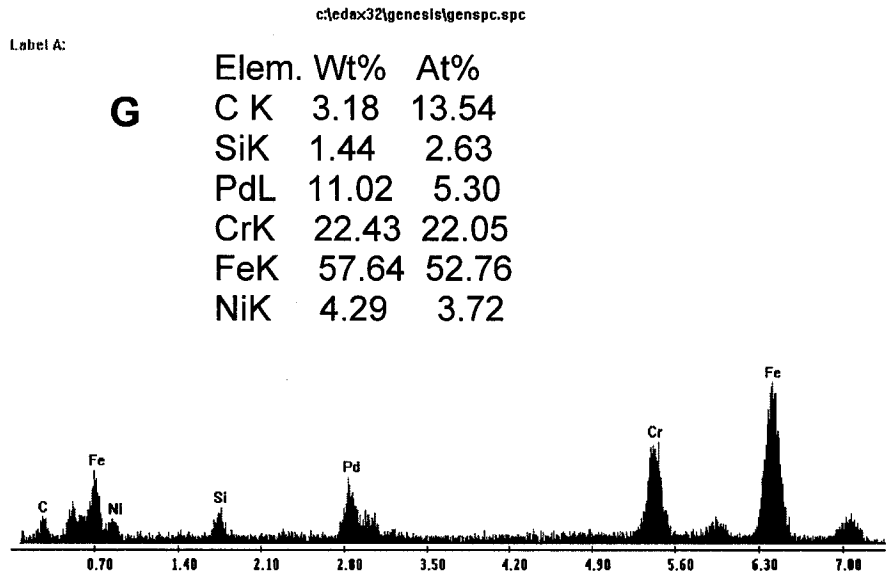

Figure 5-2 Micrographs showing a variety of palladium nanowire arrays, Pd elemental mapping, EDS and the analysis of composition
(a, b) Straight palladium nanowire or nanowires; (c) Crossing palladium nanowires; (d) Network structure of palladium nanowires; (e) Palladium nanowire; (f) Elemental mapping of palladium from the image (e); (g) The energy-dispersive spectrum and the analysis of the composition at the marked area in the image (e)
(Concentration of $PdCl_2$ in the solution is 1.8~2.0 g/l)

It is generally accepted that the deposition of palladium on conductive media is random and spontaneous, as this process has been often used to deposit a uniform dense palladium membrane on various substrates. [21-23] However, the deposition of palladium on the porous stainless steel substrate in the initial stage is not uniform and different palladium nanostructures are observed. Figure 5-2 (a-d) illustrates that the palladium nanowires in straight line, parallel lines, intersections and network structures are built on the rough surface of the porous stainless steel substrate. The palladium nanowires are continuous and the diameter of each nanowire is homogeneous along its length direction as shown in Figure 5-2 (a, b). One can see that in the initial stage the palladium nanowires are made of nanoparticles but the curvature characterizing the nanoparticle shape gradually disappears, as shown in Figure 5-2 (a, b). The palladium nanowire intersection and network arrays are illustrated in Figure 5-2 (c, d). All nanowires and nanowire network arrays display well-organized structures. The observation of nodes illustrated in Figure 5-2 (d) clearly indicates that the network structures are well linked. Figure 5-2 (f, g) shows the elemental mapping of palladium, the energy-dispersive spectrum and composition of the marked area in the SEM image Figure 5-2 (e). The line, for sure, is palladium nanowire that is deposited on the rough stainless steel surface. Moreover, the observation of the location where the nanowires are built from illustrates that they do not

really follow the irregular steps and boundaries between the steel particles but they are rather originated from there. After the nanowires start to assemble, they will follow a certain direction in order to minimize the interface energy instead of tracking these defects. This is the main reason that the structures of palladium nanowires in Figure 5-2 (a-e) are built in highly ordered manner by the spontaneous electroless deposition.

The SEM micrographs in Figure 5-3 (a-d) show that the nanoparticle-monolayer palladium membrane is deposited on the wall of a pore at the stainless steel substrate surface. The thicknesses of the palladium layers are about 100 ~ 130 nm in Figure 5-3(a-c) and about 70 ~100 nm in Figure 5-3(d), which are the same as the diameters of the palladium nanowires and nanoparticles in Figure 5-2 (a-e). The nanoparticle monolayer palladium membrane looks dense when it is packed with palladium nanoparticles. These nanoparticles link each other very well after the short deposition time of 120 s. The palladium nanoparticle monolayer membrane in Figure 5-3 (b, c) can form like that and does not collapse due to its gravity. This reveals that the inter-grain binding among the palladium nanoparticles is strong and the nanoparticle-monolayer membrane is not just piled up by the palladium nanoparticles in a mechanical manner. The nanoparticle-monolayer membrane is dense except that some small areas are not filled up with the palladium nanoparticles. Based on this phenomenon, if the size of palladium nanoparticles generated from the autocatalytic reaction can be effectively controlled, the thin membrane will be built.

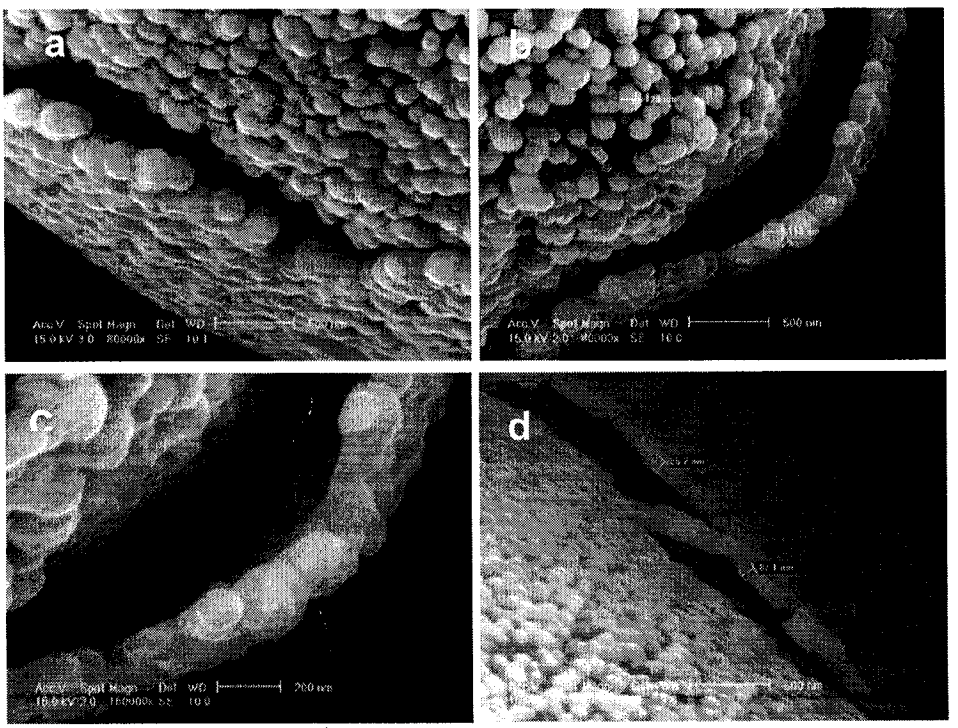

Figure 5-3 Nanoparticle-monolayer palladium membranes packed by palladium nanoparticles
(Concentrations of $PdCl_2$ in the solution: 1.8~2.0 g/l (a-c), 2.4 g/l (d))

Why is the palladium membrane formed as the nanoparticle-monolayer on the pore wall? The explanation is below. This stainless steel substrate is an interconnected porous structure. When it is suspended into the plating bath, the solution is stirred by an octagonal magnetic bar that will remove the gases generated from the chemical reaction (5-1) and result in the strong reaction dynamics. The autocatalytic reaction occurs on the solid-liquid interface between the sample surface and the solution. It involves reduction-oxidations with electron transfer across the surface. In addition, the pores are vertical and their sizes at the surface range from 0.2 to 10 μm, as shown in Figure 5-1 (a). But the size of pores inside the substrate is less than 0.2 μm. There is a capillary force driving the solution into the pores. As the size of the pores at the surface is much larger than that in the inside, both NH_3 and N_2 gases generating from the chemical reaction easily pass through the pores, which causes the solution not to permeate into the depth of the pores. Meanwhile, a surface tension exists between the wall of the pores and the solution that results in the quick nucleation of palladium on the wall of the pores because the reaction products N_2 and NH_3 can be easily removed from the pores after they nucleate and grow on the wall of the pores.

Figure 5-4 shows that palladium nanostructural arrays are built on the irregular steps at surface of the substrate. These irregular steps originated from the fabrication of the substrate in Figure 5-1 (b-d) are like the artificial patterns or V-groves. One can see that the palladium is also easily deposited on the irregular-steps of the substrate surface and forms nanowire arrays. This is similar to the processing of nanowires with V-groove patterns. [18] When comparing with the structure of palladium nanowires in Figure 5-2 (a-e) and in Figure 5-4 (a-d), the difference can be seen clearly. The palladium nanowires in Figure 5-2 are well-organized and continuous. The diameter of each nanowire is almost the same everywhere. While the palladium nanowire arrays in Figure 5-4 are formed as a result of the aggregation of palladium nanoparticles and the palladium nanostructure arrays are wholly followed the irregular steps at the surface of the substrate and the diameters are often different.

Comparing with the above three different palladium nanostructures, they are produced at the same substrate surface simultaneously at the short deposition time. Based on our observation and experiments, we find that palladium deposits can be managed in one dimension to form nanowires, as shown in Figure 5-2 (a-e), they can also be assembled in two-dimension to create one nanoparticle-monolayer membrane, as shown in Figure 5-3. Of course, they can also be primarily deposited on the irregular steps and form artificial patterns, as shown in Figure 5-4. Most of people usually think the palladium is deposited as a uniform membrane on the conductive substrate. In view of the above three arrays of palladium nanostructures formed on the same stainless steel surface at the deposition time of 120 s, this result clearly illustrates that the palladium deposited at the rough surface of the stainless steel substrate is not uniform. Meantime, the result also reveals that the different palladium nanostructures can be built on the rough stainless steel substrate surface in the initial stage. The obtained experimental result demonstrates a novel method to fabricate various palladium nanostructures by the simple electroless deposition process.

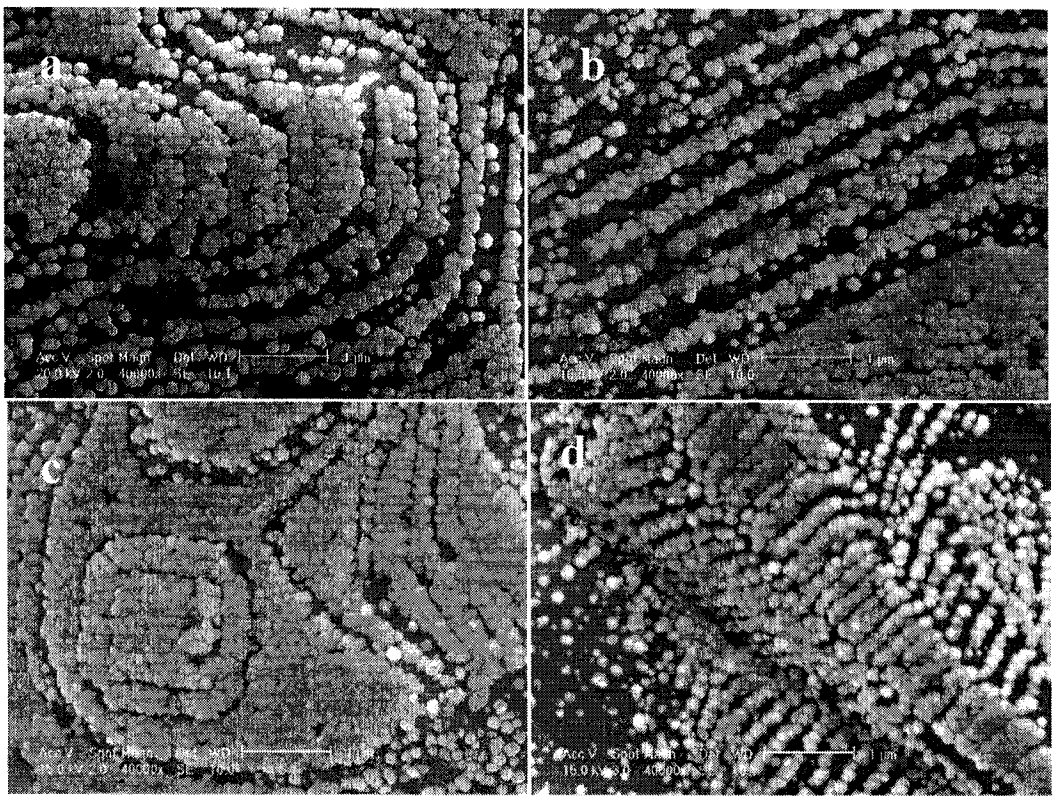

Figure 5-4 Palladium nanostructural arrays formed on the irregular steps at the surface of the porous stainless steel substrate
(Concentration of $PdCl_2$ in the solution: 1.8~2.0 g/l)

5.5 Conclusions

Based on the observation of palladium deposited on the porous stainless steel substrate by the electroless deposition process, it was found that palladium nanowires and nanoparticle-monolayer membranes can be created at the substrate surface. The obtained result demonstrates a simple and practical technique to fabricate palladium nanowires and thin palladium membrane for engineering applications.

5.6 References

1. C.N.R. Rao, A. Muller, A.K. Cheetham (Eds.), The chemistry of nanomaterials, synthesis, properties and applications, Vol. 1, Wiley-VCH, 2004.
2. Andrew N. Shipway, Eugenii Katz, Itamar Willner. Chemphyschem. Nanoparticle Arrays on Surfaces for Electronic, Optical, and Sensor Applications, 1, 18-52 (2000).
3. Robert A. W. Dryfe, Andrew O. Simm, and Brett Kralj. Electroless Deposition of palladium at bare and templated liquid/liquid interfaces, J. Am. Chem. Soc. 125, 13014-13015 (2003).
4. Srividhya Kidambi, Jinhua Dai, Jin Li, and Merlin L. Bruening. Selective hydrogenation by Pd nanoparticles embedded in polyelectrolyte multilayers, J. Am. Chem. Soc. 126, 2658-2659 (2004).
5. Taro Nishinaka, Atsushi Takano, Yuko Doi, Makiko Hashimoto, Akira Nakamura, Yushu Matsushita, Jiro Kumaki, and Eiji Yashima, Conductive metal nanowires templated by the nucleoprotein filaments, complex of DNA and RecA protein, J. Am. Chem. Soc.127, 8120 - 8125 (2005).
6. Y. Xia, P. Yang, Y. Sun, Y. Wu, B. Mayers, B. Gates, Y. Yin, F. Kim, H. Yan. One-dimensional nanostructures: synthesis, characterization, and applications, Adv. Mater. 15, 353-389 (2003).
7. Ghim W. Ho, Andrew S. W. Wong, Andrew T. S. Wee, and Mark E. Welland. Self-assembled Growth of Coaxial Crystalline Nanowires, Nano Letters, 4. 2023-2026 (2004).
8. F. Favier, E.C. Walter, M.P. Zach, T. Benter, and R.M. Penner. Hydrogen sensors and switches from electrodeposited palladium mesowire arrays, Science 293, 2227-2231 (2001).
9. Ali Javey and Hongjie Dai. Regular Arrays of 2 nm Metal Nanoparticles for Deterministic Synthesis of Nanomaterials, J. Am Chem. Soc. 127, 11942-11943 (2005).
10. Y. Gao, P. Jiang, D. F. Liu, H. J. Yuan, X. Q. Yan, Z. P. Zhou, J. X. Wang, L. Song, L. F. Liu, W. Y. Zhou et al. Synthesis, characterization and self-assembly of silver nanowires, Chemical Physics Letters, 380, 146-149 (2003).
11. Y. Nishihata, J. Mizuki, T. Akao, M. Uenishi, M. Kimura, T. Okamoto, N. Hamada, Self-regeneration of a Pd-perovskite catalyst for automotive emissions control, Nature, 418, 164 (2002).
12. Didier Astruc, Feng Lu, Jaime Ruiz Aranzaes, Nanoparticles as Recyclable Catalysts: The Frontier between Homogeneous and Heterogeneous Catalysis, Angew. Chem. Int. Ed. 44, 7852-7872 (2005).
13. S.V. Karnik, M.K. Hatalis, M.V. Kothare. A microreactor for hydrogen production in micro fuel cell applications, Journal of Microelectromechanical Systems, 13, 7-18 (2004).
14. Minhee Yun, Nosang V. Myung, Richard P. Vasquez, Choonsup Lee, Erik Menke, and Reginald M. Penner, Electrochemically grown wires for individually addressable sensor arrays, Nano Letters **4**, 419-422 (2004).

15. M.S. Sander, H. Gao. Aligned arrays of nanotubes and segmented nanotubes on substrates fabricated by electrodeposition onto nanorods, J. Am Chem. Soc. 127, 12158 (2005).
16. Z. Zhang, S. Dai, D.A. Blom, J. Shen. Synthesis of ordered metallic nanowires inside ordered mesoporous materials through electroless deposition, Chem. Mater. 14, 965-968 (2002).
17. C. Cheng, R.K. Goneia, Q. Gu, D.T. Haynie. Self-assembly of metallic nanowires from aqueous solution, Nano Letters, 5 175-178 (2005).
18. M.Z. Atashbar, D. Banerji, S. Singamaneri, V. Blizynyuk. Deposition of parallel arrays of palladium nanowires and electrical characterization using microelectrode contacts, Nanotechnology 15, 374-378 (2004).
19. J. Shu, B.P.A. Grandjean, S. Kaliaguine, Morphological study of hydrogen permeable Pd membranes, Thin Solid Film, 252, 26-34 (1994).
20. M. Schlesinger, M. Paunovic, Modern Electroplating, fourth edition, Wiley, Toronto, 2000.
21. I W Hanley. Nanostructure fabrication using block copolymers, Nanotechnology, 14, R39 (2003).
22. W.M. Tolles, B.B. Rath. Nanotechnology, a stimulus for innovation, current science, 85, 1746-1759 (2003).
23. M. Datta, S. A. Merritt, Mario Dagenais. Electroless remetallization of aluminum bond pads on CMOS driverchip for flip-chip attachment to vertical cavity surface emitting lasers (VCSEL's), IEEE Trans. Comp. Pack. Tech. 22 (1999) 299-306.

CHAPTER 6 [1]

SELF-ASSEMBLED PALLADIUM NANOWIRES BY ELECTROLESS DEPOSITION

6.1 Abstract

A simple approach to the self-assembly production of palladium nanowires by electroless deposition on a porous stainless steel template is reported. Various arrays of the self-assembled palladium nanowires in the form of single wire, parallel and curved wires, intersections and network structures are illustrated. This experimental result demonstrates that metal nanowires can be built in a self-assembled manner by assembly of nano-particles generated in the initial stages of the deposition without any external field except the chemical reaction. Such self-assembled nanowires may attract engineering applications because the electroless deposition process and the preparation of the substrate are simple and inexpensive.

6.2 Introduction

Nanowires have unique structure and properties that can be potentially used for a generation of new nanoelectronic devices and sensors for medical, environmental, or security-checking purposes. [1-4] Such wires with a diameter in nanometer scale are usually built on templates and sometimes can grow in a self-assembled manner, which means they are organized and grow into patterned structures without human intervention. [5, 6] Self-assembly of nanostructures is an interesting phenomenon that is usually observed in biological systems such as molecules, viruses, as well as plant and animal cells. [7, 8] The control of intermolecular forces can lead to the creation of new molecular structures. This is why molecular self-assembly is a highly promising field of research in nanotechnology. [9-13]. Metal nanowires can, in principle, also be for various applications. So far, electrochemical and vapour depositions are often used for the fabrication of nanowires. [14]

[1] This chapter has been published as an article in Nanotechnology, 17, 2161-2166 (2006)

Electrochemical deposition is a versatile technique that can be used to synthesize desired nanostructures for numerous applications in micro and nanodevices. [15] There are some reports on the fabrication of palladium nanowires. For examples, E.C. Walter, et al [16] created arrays of mesoscopic palladium wires for hydrogen sensors and hydrogen-actuated switches that exhibit a fast response time for hydrogen detection. G. Kaltenpoth, et al [17] prepared palladium-covered channel on Si (100) substrate for detection of hydrogen gas. M. Yun, et al [18] developed electrochemically grown palladium wires for individually addressable hydrogen sensor arrays. M. A. Bangar, et al [19] demonstrated a novel electrochemical method for dimensionally controlled growth of a single palladium nanowire between premicrofabricated electrodes. M. Z. Atashbar [20] et al synthesized palladium nanowires on the "V" shaped grooves of a highly oriented pyrolytic graphite (HOPG) and C. Cheng et al [21] built up self-assembly palladium nanowires along the direction of the electric field between the electrodes at aqueous solution. The vapor deposition method for the fabrication of nanowires includes physical vapour deposition (PVD), chemical vapour deposition (CVD), metallorganic chemical vapour deposition (MOCVD) and vapour-liquid-solid (VLS). For examples, semiconductor nanowires are successfully synthesized by VLS method, based on the mechanism of anisotropic crystal growth [14] and palladium nanowires can be grown in carbon nanotubes using microwave plasma-enhanced chemical vapour deposition [22].

Electroless deposition process is a simple and inexpensive method that has been often used for depositing a uniform dense palladium membrane on any arbitrary geometry substrate. [23, 24] This process can also be used to develop palladium nanoparticles, nanorods (or nanowires) and nanotubes on an anodic alumina template. [25, 26] However, so far, no palladium nanowire preparation on the rough stainless steel surface using electroless deposition technique was reported. In this chapter, we explore a simple method to fabricate Pd nanowires on the rough surface of porous stainless steel substrate and to investigate their formation and microstructural characteristics.

6.3 Experimental details

In this program, a 0.2 μm grade porous 316L stainless steel plate, purchased from Mott Metallurgical Corporation was used as a substrate. The substrate is defined as 0.2 μm grade that means over 95% of particles having the size of 0.2 μm are rejected by this substrate during filtering. The pore size at the substrate surface actually ranges from 0.2 to 10 μm. The samples were cut into the size of 20 mm x 20 mm and cleaned in an ultrasonic bath with acetone for 15 minutes. Electroless deposition usually comprises a three-step process: (1) pretreatment of the substrate; (2) activation of the substrate surface; (3) electroless deposition. After cleaning, the surfaces of the samples are activated with 10% hydrochloric acid, then, rinsed with deionized water. After this procedure, the samples were transferred immediately into the electroless plating bath for the deposition of palladium. The deposition time was 120 s and the plating bath was at a constant temperature of 60°C. The detailed palladium plating bath preparation using hydrazine as a reducing agent is presented in Table 6-1 and also elsewhere [27]. Microstructural characteristics of palladium deposited samples were observed and analyzed by a PHILIPS XL30 FE SEM (Field Emission Scanning Electron Microscopy)

equipped with an EDS (Energy Dispersive Spectroscopy, GENESIS 2000 X-ray Microanalysis System).

Table 6-1 Composition of electroless plating bath [27]

Component	Concentration
$PdCl_2$	1.8 ~ 2 g/l
$Na_2EDTA.2H_2O$	40.1 g/l
$NH_3.H_2O$ (28%)	198 ml/l
N_2H_4 (1M)	5.6 ml/l
pH	10 ~ 10.4
Temperature (°C)	60°C

6.4 Results and discussion

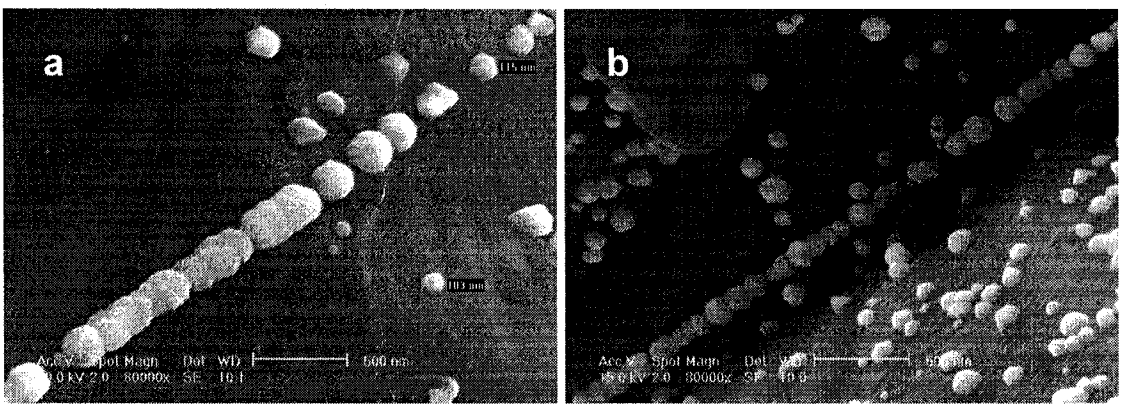

Figure 6-1 SEM micrographs showing the discontinuous palladium nanowire in the self-assembled manner

Electroless deposition occurs simply by immersion of samples in a plating bath and does not need rectifiers, batteries or anodes. The palladium deposition is an autocatalytic process according to the chemical reaction (6-1):

$$2Pd(NH_3)_4^{2+} + N_2H_4 + 4OH^{-1} \rightarrow 2Pd^0 + 8NH_3 + N_2 + 4H_2O \qquad (6\text{-}1)$$

It is generally accepted that electroless deposition of palladium on conductive media is random, spontaneous and uniform, as this process has been often used for depositing the dense palladium membranes on various substrates. However, if nucleation and growth of metal nano-grains are controlled by diffusion, the nano-grains may connect to each other in order to minimize their surface energy. So far, there is no report on metal nanowires assembled without any external field because it is difficult to control the transient time of nucleation and growth in one direction. Various self-assembled structures of palladium nanowires produced at our laboratory are described and illustrated below.

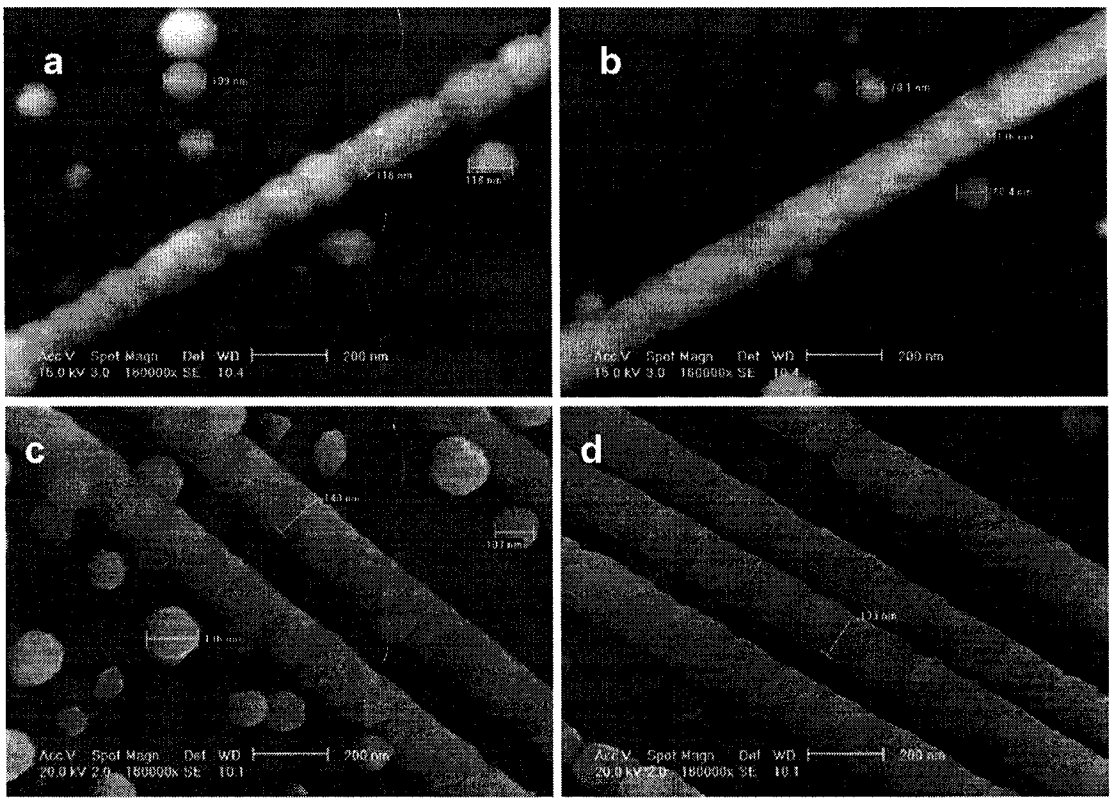

Figure 6-2 SEM micrographs showing the straight nanowire or parallel nanowires in the self-assembled manner (a, b) a straight nanowire; (b, c) the straight parallel nanowires

Figure 6-1 (a, b) shows the first stage of the formation of a palladium nanowire in a bead-by-bead manner. One part of it is already continuous and the amalgamation of the palladium nanoparticles is noticeable. Some areas are discontinuous but the tendency of nanowire formation is clear. The continuous palladium nanowires can be seen in Figure 6-2 (a, b). Figure 6-2(a) illustrates the stage when the nanowire is still composed of single palladium nanoparticles. But, as shown in Figure 6-2(b), the distinction between the single palladium nanoparticles and the nanowire gradually disappears. Similar morphologies of the parallel palladium nanowires are observed in Figure 6-2(c, d). All palladium nanowires form straight lines in the self-assembled manner.

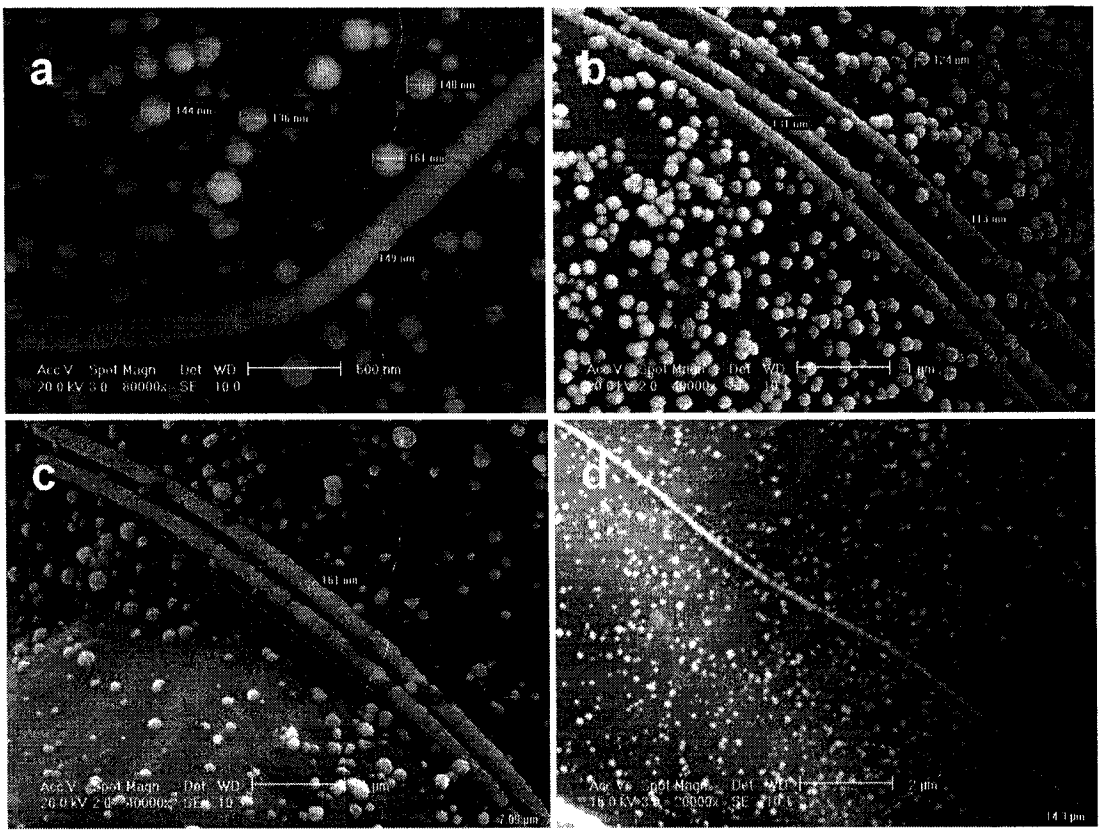

Figure 6-3 SEM micrographs showing the curved nanowire or nanowires in the self-assembled manner (a) a curved nanowire; (b, c) the parallel curved nanowires; (d) the length of a curved nanowire, over 14 μm

Figure 6-3 (a-d) shows the curved, yet continuous palladium nanowires that are similar to the straight nanowires in Figure 6-2 (a, b). The length of palladium nanowire in Figure 6-3(d) is over 14 μm. Scanning Electron microscope (SEM) images presented in Figure 6-4 (a-d) illustrate the intersection and network structures of palladium nanowires. Such network structures were fabricated in a self-assembled manner. A detailed observation of the nodes clearly indicates that the network structures are well linked. Moreover, the observation of the location where the network of nanowires is built indicates that they are probably originated at the defects of the substrate surface such as irregular steps or boundaries between the particles. After the nanowires start to assemble, they will follow certain directions of growth and do not track the defects. This is the reason why the above-mentioned structures of palladium nanowires in Figures 6-1~6-3 are called the self-assembled ones.

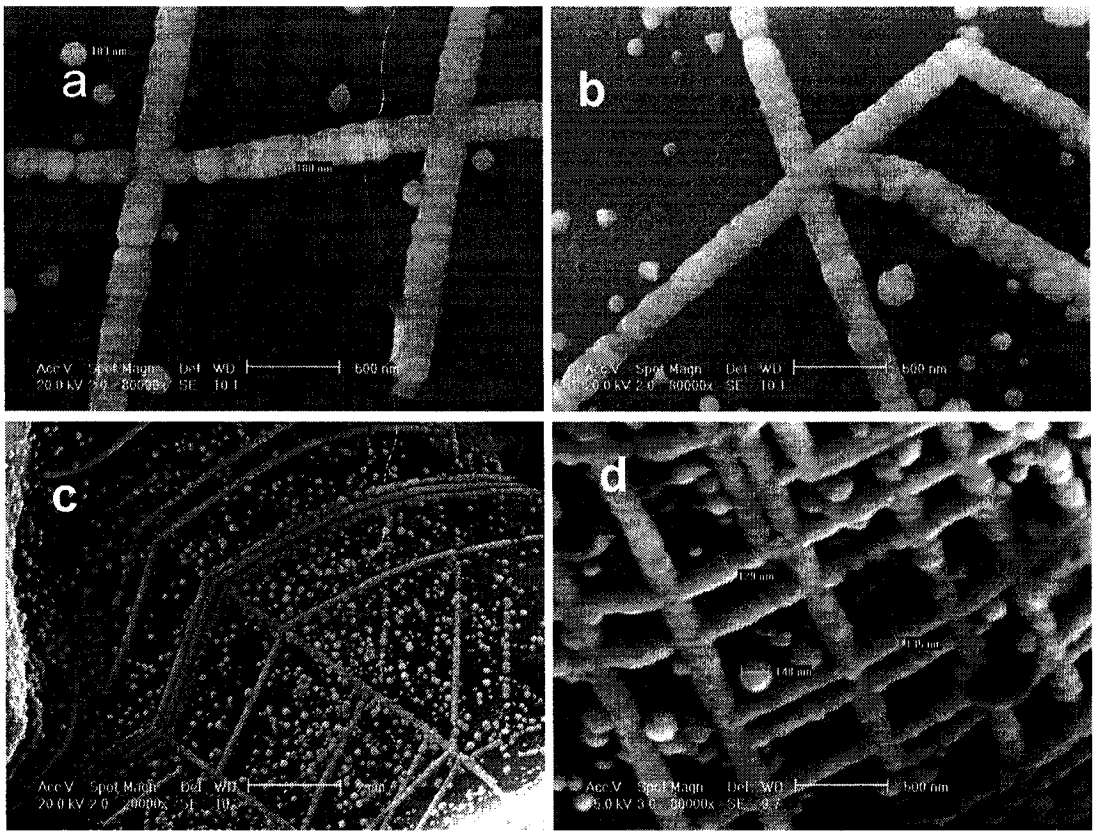

Figure 6-4 SEM micrographs showing the intersection (a, b) and network structures (c, d) of the self-assembled palladium nanowires

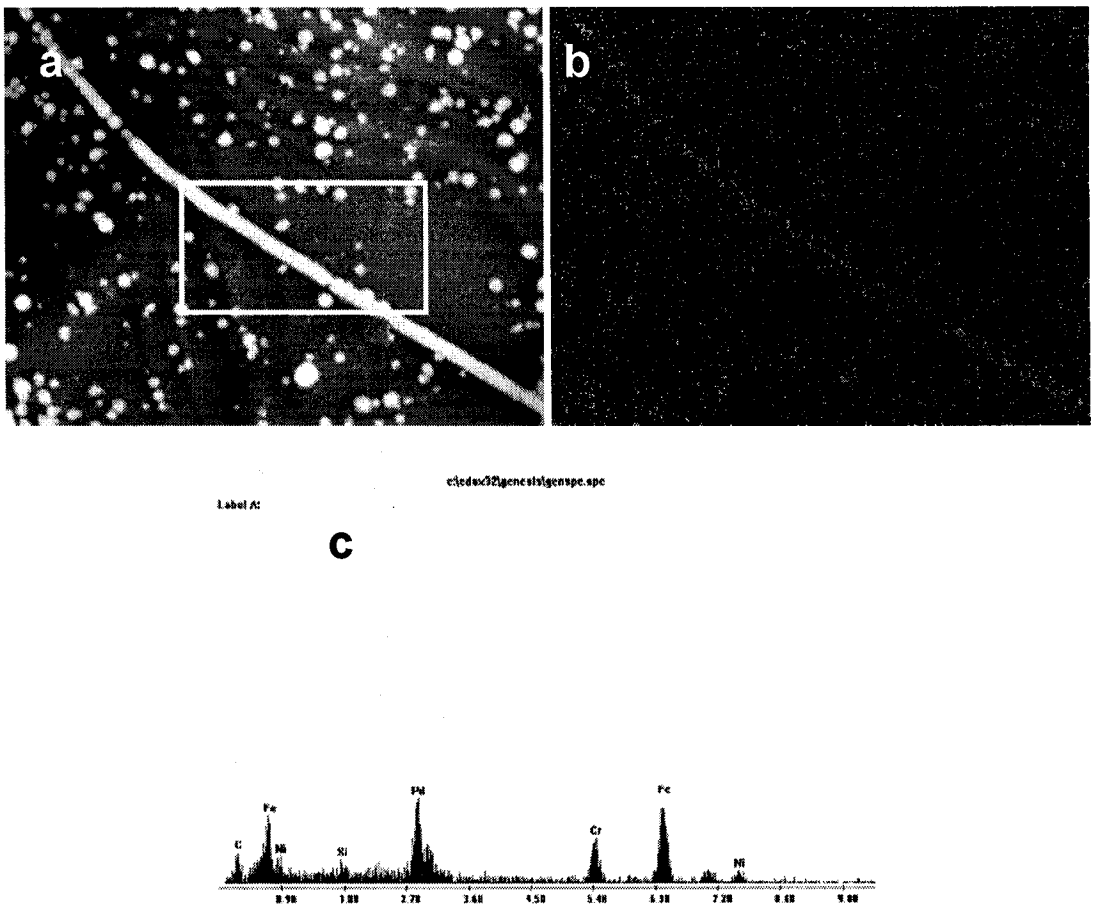

Figure 6-5 SEM micrograph of self-assembled palladium nanowire (a), palladium mapping (b) and energy-dispersive x-ray spectrum from the area A of the SEM image (c)

Figure 6-5 illustrates the micrograph of palladium nanowire formation on the stainless steel substrate, the palladium elemental mapping and the energy-dispersive X-ray spectra in the area A, marked in Figure 6-5 (a). One can see the palladium nanowire does not follow the irregular steps at the surface, as shown in Figure 6-5 (a). The line is identified as palladium nanowire that is created on the rough stainless steel surface, as shown in Figure 6-5 (b, c).

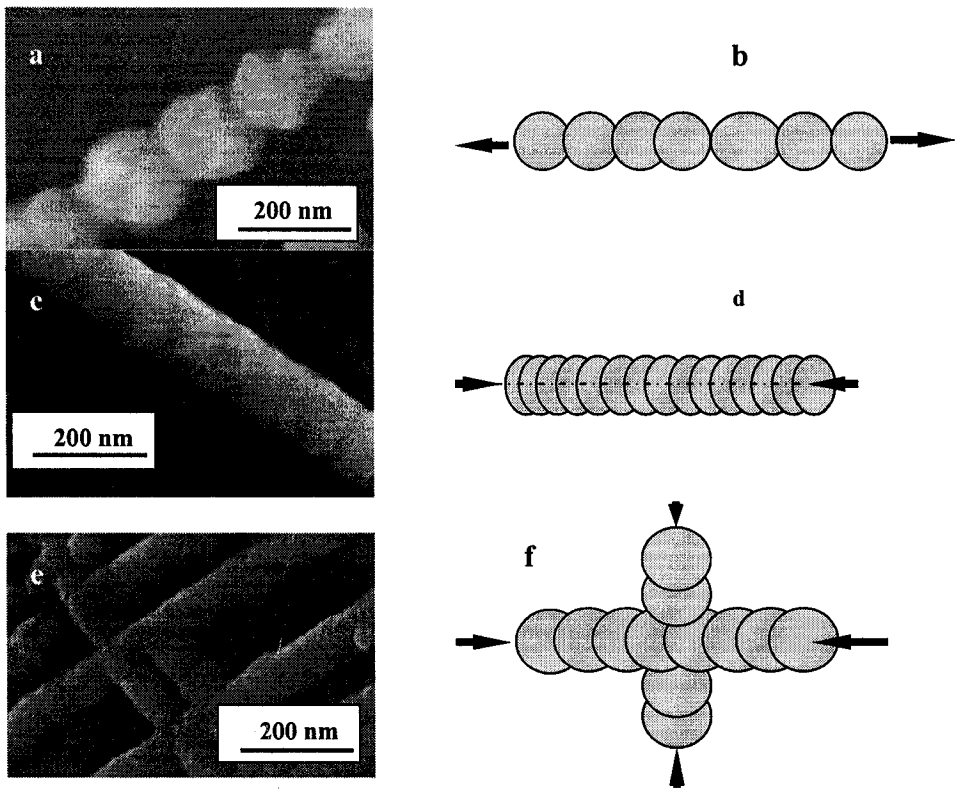

Figure 6-6 Schematics of the formation of the palladium nanowires and their linked nodes (a, c) the SEM images of the palladium nanowire; (b, d) schematics of the nanowire in self-assembly particle-by-particle; (e) the network structure of the palladium nanowires; (f) schematic of the node of the network in self-assembly particle-by-particle

Many theoretical studies of metal nanowires have been reported, such as the first-principle electronic-state calculations for Al nanowires [28] and the molecular-dynamics-based genetic algorithm simulations for the nanowires of Au [29], Cu [30] and Pd [31]. The direct observation from various stages of the self-assembly of palladium nanowires presented in Figures 6-1~6-3 may be used to support these theoretical calculations. Figure 6-6 (b, d, f) illustrates that the structures of palladium nanowires are assembled from its nanoparticles bead-by-bead. The observation of SEM micrograph in Figure 6-6 (c) shows that the nanoparticles link each other in certain order and then the neck between the particles disappears. This assembly results only from the autocatalytic reaction in a very short deposition time without any external field. Another interesting structure is the palladium nanowires network. A simple node in Figure 6-6 (e) links two palladium nanowires well, as illustrated at the schematic presentation in Figure 6-6 (f). Based on the formation of various structures of palladium nanowires in Figures 6-1~6-4, the palladium nanowires are well self-organized and it seems that the reduction of surface free energy is

the main driving force for aligning the nanoparticles to highly ordered wire and reducing the interface between them.

Since the self-assembled palladium nanowires were produced in our laboratory by the electroless process, these special structures from single wire to network for engineering application are being developed. Methods are being explored to extract the nanowires from the substrate and to manufacture the nanowires on the other substrates that can easily be integrated directly with some micro-devices.

6.5 Conclusions

The palladium nanowires can be self-assembled from its nanoparticles on a rough stainless steel substrate using the electroless deposition process. This discovery is promising because it will allow to the nanowires for various engineering applications and the deposition process and the preparation of the substrate are simple and inexpensive. The possibility of processing other metal nanowires, made of Cu, Ni, Au and Co in a self-assembled manner using the same approach is also being investigated.

6.6 References

1. Nicholas A. Melosh, Akram Boukai, Frederic Diana, Brian Gerardot, Antonio Badolato, Pierre M. Petroff, and James R. Heath. Ultrahigh-density nanowire lattices and circuits, Science 300, 112-115 (2003).
2. Yu Huang, Xiangfeng Duan, Qingqiao Wei, and Charles M. Lieber. Directed assembly of one-dimensional nanostructures into functional networks, Science 291, 630-633 (2001).
3. F. Favier, E.C. Walter, M.P. Zach, T. Benter, and R.M. Penner, Hydrogen sensors and switches from electrodeposited palladium mesowire arrays, Science 293, 2227-2231 (2001).
4. Hao Yan, Sung Ha Park, Gleb Finkelstein, John H. Reif, and Thomas H. LaBean. DNA-templated self-assembly of protein arrays and highly conductive nanowires, Science 301, 1882-1884 (2003)
5. G. M. Whitesides and B. Crzybowski. Self-assembly at all scales, Science 295, 2418–2421 (2002).
6. Kristen Fichthorn and Matthias Scheffler. Nanophysics: A step up to self-assembly, Nature 429, 617-618 (2004)
7. Niroshan Ramachandran, Eugenie Hainsworth, Bhupinder Bhullar, Samuel Eisenstein, Benjamin Rosen, Albert Y. Lau, Johannes C. Walter, and Joshua LaBaer. Self-assembling protein microarrays, Science 305, 86-90 (2004).
8. J. S. Martinez, G. P. Zhang, P. D. Holt, H.-T. Jung, C. J. Carrano, M. G. Haygood, and Alison Butler. Self-assembling amphiphilic siderophores from marine bacteria, Science 287, 1245-1247 (2000).
9. Dennis E. Discher and Randall D. Kamien, Self-assembly: Towards precision micelles, Nature 430, 519 – 520 (2004).
10. Dage Liu, Sung Ha Park, John H. Reif, and Thomas H. LaBean. DNA nanotubes self-assembled from triple-crossover tiles as templates for conductive nanowires, Proc Natl Acad Sci 101(3), 717–722 (2004).
11. Shuguang Zhang. Fabrication of novel biomaterials through molecular self-assembly, Nature Biotechnology 21, 1171 – 1178 (2003).
12. Patrick S. Doyle, Jerome Bibette, Aurelien Bancaud, Jean-Louis Viovy. Self-assembled magnetic matrices for DNA separation chips, Science 295, 2237-2238 (2002).
13. Bernard Kippelen. Optical materials: self-assembly reaches new heights, Nature Materials 3, 841-843 (2004).
14. Edited by C.N.R. Rao, A. Muller, A.K. Cheetham, The chemistry of nanomaterials, synthesis, properties and applications, Vol. 1, Wiley-VCH, p255.
15. Bharat Bhushan, Editor, Handbook of Nano-technology,Springer-Verlag Berlin Heidelberg 2004, p100.
16. E.C. Walter, F. Favier, R.M. Penner. Palladium mesowire arrays for fast hydrogen sensors and hydrogen-actuated switches, Analytical Chemistry 74, 1546-1553 (2002).

17. G. Kaltenpoth, P. Schnabel, E. Menke, E.C Walter, and M. Grunze, R.M. Penner. Multi-mode detection of hydrogen gas using palladium nanoparticle networks on silicon, Analytical Chemistry 75, 4756-4765 (2003).
18. M. Yun, N.V. Myung, R.P. Vasquez, E. Menke, and R.M. Penner. Electrochemically-grown wires for individually addressable sensor arrays, Nano Letters 4, 419-422 (2004).
19. Mangesh A. Bangar, Kumaran Ramanathan, Minhee Yun, Choonsup Lee, Carlos Hangarter, and Nosang V. Myung, Controlled growth of a single palladium nanowire between microfabricated electrodes, Chem. Mater. 16, 4955-4959 (2004).
20. Massood Z Atashbar, Deep Banerji, Srikanth Singamaneni and Valery Bliznyuk. Deposition of parallel arrays of palladium nanowires and electrical characterization using microelectrode contacts, Nanotechnology 15, 374–378 (2004).
21. Chuanding Cheng, Ravi Kanth Gonela, Qun Gu, and Donald T. Haynie. Self-assembly of metallic nanowires from aqueous solution, Nano Letters, 5, 175-178 (2005).
22. L.H. Chan, K.H. Hong, S.H. Lai, X.W. Liu and H.C. Shih. The formation and characterization of palladium nanowires in growing carbon nanotubes using microwave plasma-enhanced chemical vapor deposition, Thin Solid Films, 423, 27-32 (2003).
23. Lon A. Porter, Jr., Hee Cheul Choi, J. M. Schmeltzer, Alexander E. Ribbe, Lindsay C. C. Elliott, and Jillian M. Buriak. Electroless nanoparticle film deposition compatible with photolithography, microcontact printing, and dip-pen nanolithography patterning technologies, Nano Letters 2, 1369-1372 (2002).
24. K.S. Rothenberger, A. V. Cugini, B.H. Howard, R.P. Killmeyer, M.V. Ciocco, et al., High pressure hydrogen permeance of porous stainless steel coated with a thin palladium film via electroless plating, Journal of Membrane Science, 244, 55-68 (2004).
25. A. Johansson, J. Lu, J.-O. Carlsson and M. Boman. Deposition of palladium nanoparticles on the pore walls of anodic alumina using sequential electroless deposition, J. Appl. Phys. 96, 5189-5194 (2004).
26. Shufang Yu, Ulrich Welp, Leonard Z. Hua, Andreas Rydh, Wai K. Kwok, and H. Hau Wang. Fabrication of palladium nanotubes and their application in hydrogen sensing, Chem. Mater. 17, 3445-3450 (2005).
27. Schlesinger, M. and Paunovic, M. Modern Electroplating, fourth edition, (Wiley, Toronto, 2000)
28. Makita, T., Doi, K., Nakamura, K. and Tachibana, A. Toshiki Makita, Kentaro Doi, Koichi Nakamura, and Akitomo Tachibana. Structures and electronic properties of aluminum nanowires, J. Chem. Phys. 119, 538-546 (2003)
29. Baolin Wang, Shuangye Yin, Guanghou Wang, Alper Buldum, and Jijun Zhao. Novel Structures and Properties of Gold Nanowires, Phys. Rev. Lett. 86, 2046-2049 (2001).
30. Jeong Won Kang, Jae Jeong Seo, Ki Ryang Byun, and Ho Jung Hwang. Atomistic Defects in ultrathin copper nanowires: simulations, Phys. Rev. B. 66, 125405 (2002).

31. Li Hui, B. L. Wang, J. L. Wang, and G. H. Wang. Local atomic structures of palladium nanowire, J. Chem. Phys. 121, 8990-8996 (2004).

CHAPTER 7[1]

CONTROLLING DIAMETER OF PALLADIUM NANOWIRE BY ELECTROLESS DEPOSITION PROCESS

7.1 Abstract

Hydrogen sensor built using palladium nanowires has a huge market and attracts great interest for fuel cell application. However, the fabrication of palladium nanowires in a controllable manner is still being explored. This chapter demonstrates that the diameter of palladium nanowires can be controlled by concentration of $PdCl_2$ in the plating solution and deposition time. Based on our observation of palladium nanowire formation on porous stainless steel substrate, we find palladium nanowires are gradually assembled by nanoparticles with the extension of deposition time. The size of palladium nanoparticles generated from the autocatalytic reaction is directly dependent on concentration of $PdCl_2$ in the plating solution. The higher concentration of $PdCl_2$ in the plating solution, the smaller deposited palladium nanoparticles. The experimental results provide a simple and controllable method for the deposition of desired palladium nanowire arrays in potential engineering applications.

7.2 Introduction

Being a clean fuel, hydrogen promises a future of renewable, efficient, pollution-free energy. However, hydrogen has the potential for burning and explosion. Sensors are needed to detect hydrogen leaks and hydrogen quality. Palladium is an ideal material for hydrogen sensing because it selectively absorbs hydrogen gas. The first practical nanoscale hydrogen sensor made of palladium nanowires at Penner's group is high sensitivity for the small amount hydrogen detection in a rapid response and requires low power. [1] With the widespread use of hydrogen as a fuel, together with rapidly developing fuel cell technology, hydrogen sensor built using palladium nanowires has a huge market and attracts great interest. Some investigations of fabricating palladium nanowires have already been carried out. For example, Penner's group [1, 2] deposited palladium meso- or nanowires on highly oriented pyrolytic graphite (HOPG) surfaces, then transferring them with a polymer for building a nanoscale hydrogen sensor. Atashbar et al [3] used the same method to obtain step-edges decorated or "V-typed groove" palladium nanowires by electrodeposition. Cheng et al [4] observed self-assembled palladium nanowires around the electrodes from aqueous solution. Yun et al [5-7] electrochemically deposited palladium nanowires on electron-beam lithographic pattern for individually addressable sensor array. In addition, palladium nanowires deposited on different templates such as DNA [8], anodized alumina [9-11], mesoporous silica, [12] microcontact printing lithographic pattern on wafer [13, 14] and carbon tube [15-17] have

[1] This chapter as an article is to be submitted to Nanotechnology (Journal)

also been investigated. However, building palladium nanowires in a controllable manner is still being explored. We have already found that various palladium nanowire arrays can be easily built on porous stainless steel substrate. [18, 19] After that, many experiments have been carried out in order to control the diameter of palladium nanowires by electroless deposition process. This chapter demonstrates that the diameter of palladium nanowires can be controlled by concentration of $PdCl_2$ in the plating solution and deposition time. Based on our observation of palladium nanowire formation on porous stainless steel substrate, we find palladium nanowires are gradually assembled by nanoparticles. The size of palladium nanoparticles generated from the autocatalytic reaction is directly dependent on concentration of $PdCl_2$ in the plating solution. The higher concentration of $PdCl_2$ in the plating solution can generate the smaller palladium nanoparticles. The experimental results will provide a simple and controllable method for developing desired palladium nanowire arrays in potential engineering applications.

7.3 Experimental section

A 0.2 μm grade porous 316L stainless steel plate (30 cm x 38 cm) purchased from Mott Metallurgical Corp oration was used as a substrate in this program. Such metallic medium made by metal powders has been widely used as the substrates to provide mechanical strength for palladium membranes preparation. The surface of the 0.2 μm grade stainless steel substrate is coarse and there are many pores in size of ranging from 0.2 to 10 μm. The pores are interconnected and do not allow particles in size of 0.2 μm to pass through from one side to the other over 5%. Samples were cut into size 20 mm x 20 mm and cleaned in an ultrasonic bath with acetone for 15 min. After cleaned, the samples were activated using 10% hydrochloric acid and rinsed with deionized water. Then, they were transferred immediately into an electroless plating bath for the deposition of 30~300 s (the samples: 20 mm x 20 mm) at a constant temperature of 60°C. The concentrations of $PdCl_2$ in the plating baths are 4.2 g/l, 3.0 g/l and 1.8~2.0 g/l, respectively. The detailed palladium plating baths preparation using hydrazine as a reducing agent and experimental parameters are listed in Table 7-1. Microstructural characteristics and composition of the palladium deposits are observed and analyzed by a PHILIPS XL30 FE-SEM (Field Emission Scanning Electron Microscopy) equipped with an EDS (Energy Dispersive Spectroscopy, GENESIS 2000 X-ray Microanalysis System).

Table 7-1 Composition of electroless plating bath and experimental parameters

Component	Concentration and parameters
$PdCl_2$	4.2 g/l, 3.0 g/l and 1.8~2.0 g/l
$Na_2EDTA.2H_2O$	40.1 g/l
$NH_3.H_2O$ (28%)	198 ml/l
N_2H_4 (1M)	5.6 ml/l
PH	10 ~ 10.4
Temperature (°C)	60

7.4 Results and Discussion

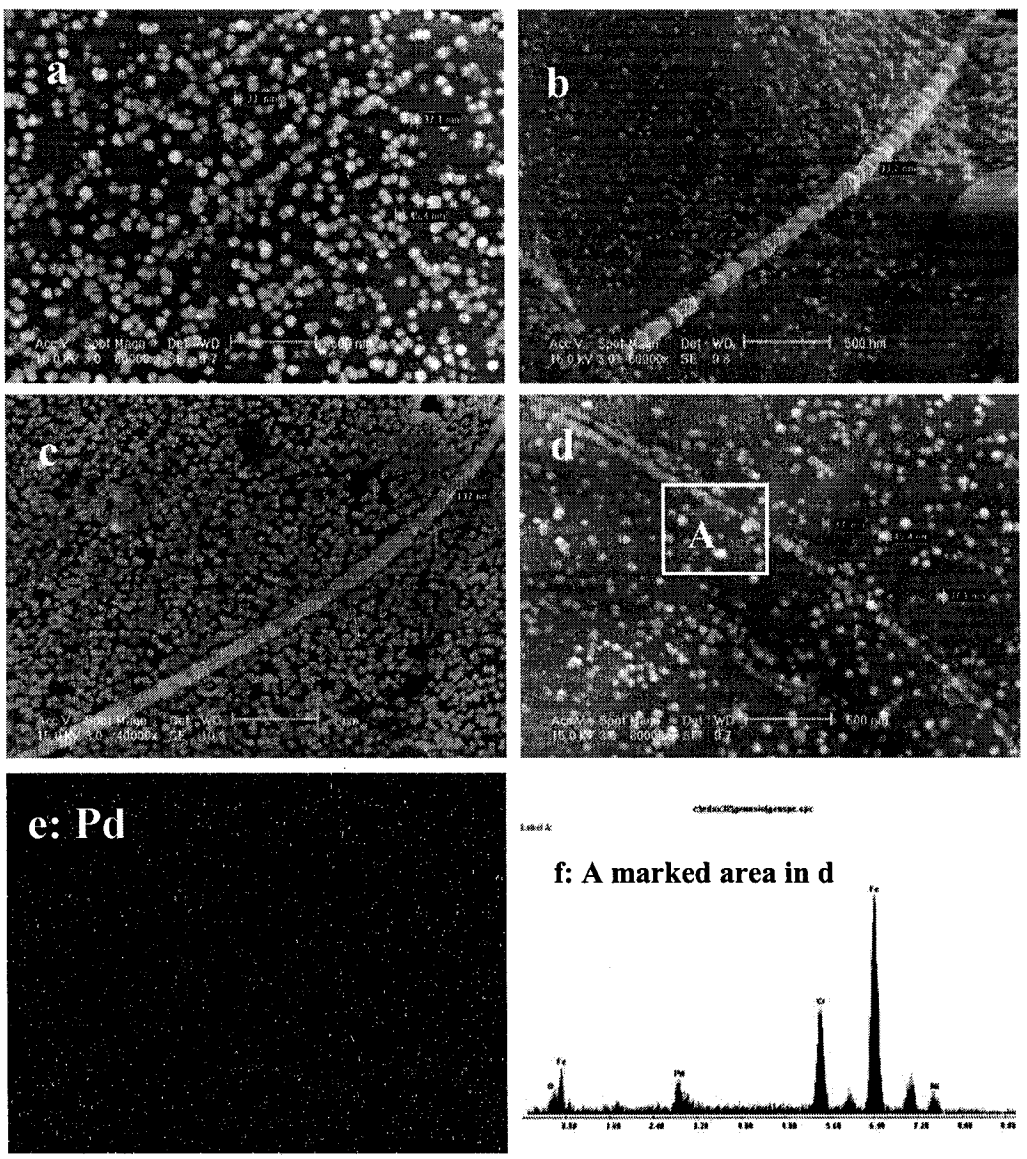

Figure 7-1 (a-d) SEM micrographs showing Pd nanowires deposited on porous stainless steel substrate at the deposition time from 75 s to 120 s ((a, d) time: 75 s, (b) time: 90 s, (c) time: 120 s, concentration of $PdCl_2$ is 4.2 g/l); (e) The elemental mapping of Pd from the SEM image (d); and (f) Energy dispersive spectrum measured from marked area A in the image (d)

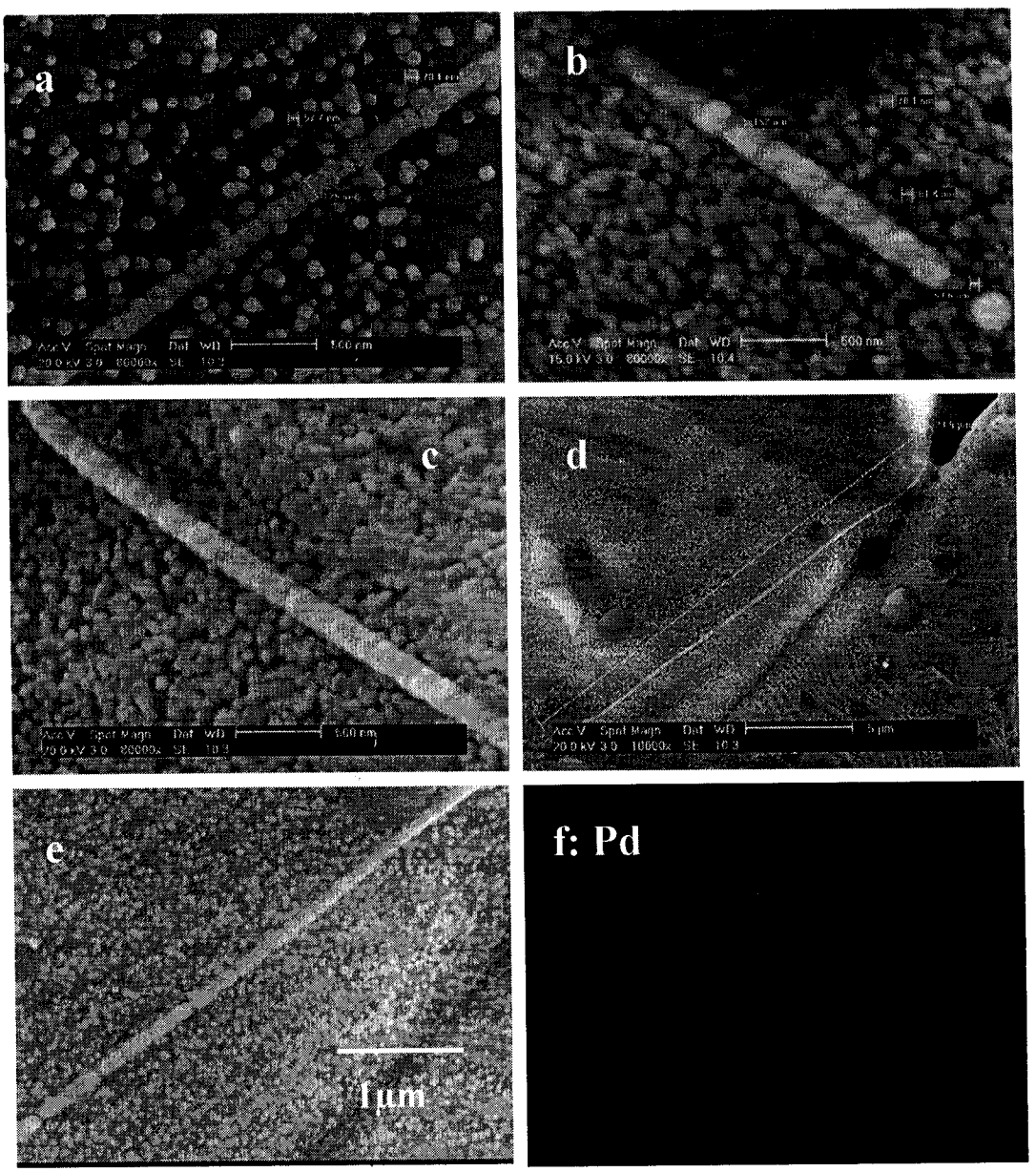

Figure 7-2 (a-e) SEM micrographs showing palladium nanowires deposited on porous stainless steel substrate within the deposition time from 90 s to 150 s ((a) time: 90 s; (b) time: 120 s; (c-e) time: 150 s, the length of palladium nanowire in (d): 23.5 µm; concentration of $PdCl_2$ in the plating solution: 3.0 g/l), and (f) The elemental mapping of palladium from the SEM image (e)

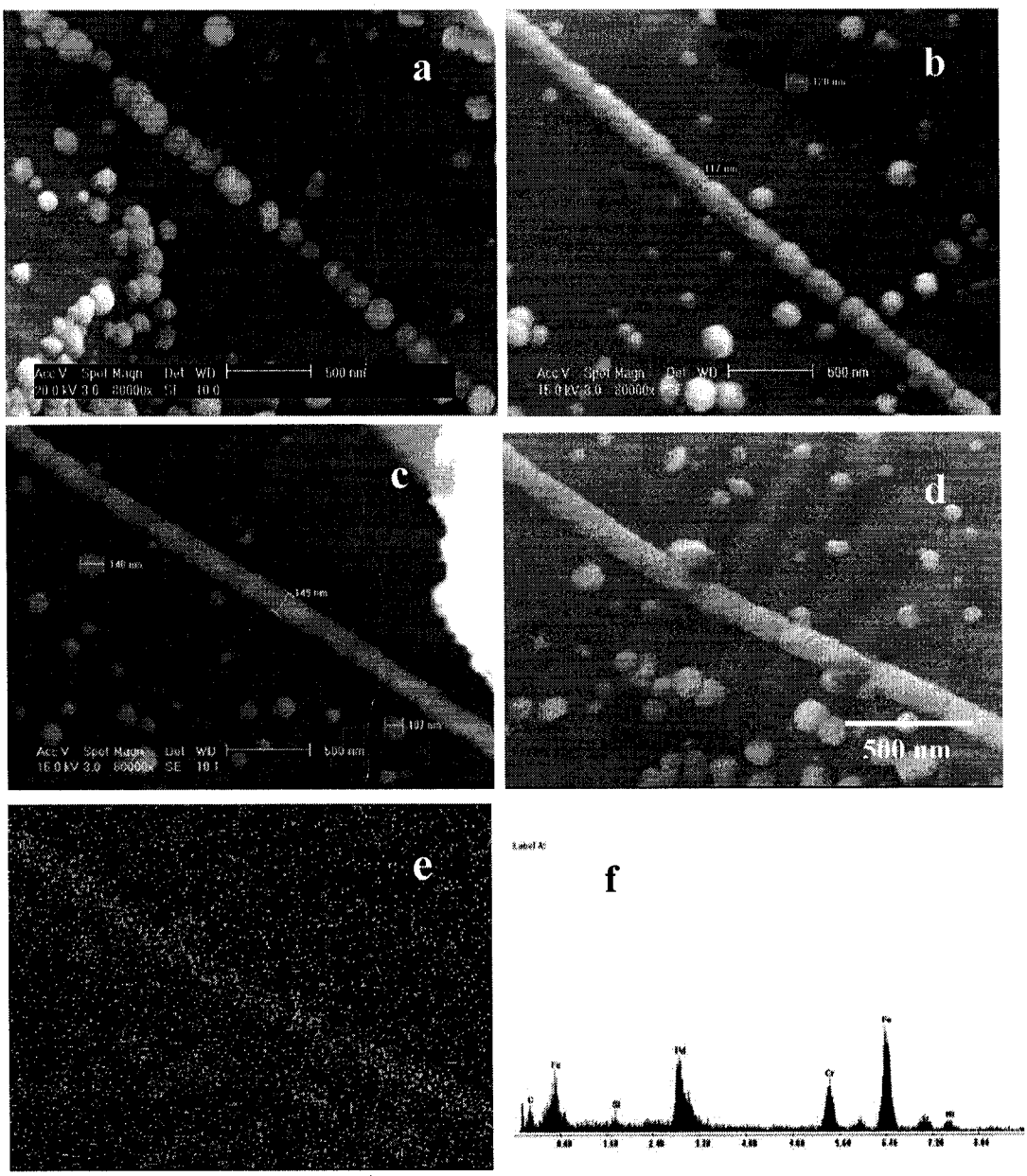

Figure 7-3 (a-d) SEM micrographs showing palladium nanowires deposited on porous stainless steel substrate at the deposition time from 75 s to 120 s (time: 75 s; (b) time: 90 s; (c, d) time: 120 s, the concentration of $PdCl_2$ is 1.8~2.0 g/l); (e) the elemental mapping of palladium from the SEM image (d), and (f) Energy dispersive spectrum, measured from the image (d)

Electroless deposition is a process that requires neither electrodes nor any external source of electricity to deposit a metal. [20] The deposition of palladium is an autocatalytic process that is controlled by the chemical reduction of palladium ions in an aqueous solution containing a reducer without any external electrical power. It can be described by the chemical reaction equation (7-1):

$$2Pd\,[NH_3]_4^{2+} + N_2H_4 + 4OH^{-1} \rightarrow 2Pd^{o} + N_2 + 4H_2O + 8\,NH_3 \qquad (7\text{-}1)$$

Based on the above equation, palladium generated from the plating solution is directly dependent on concentration of Pd^{2+}, the value of pH (the addition of $NH_3.H_2O$ or OH^{-1}), the addition of reducer (N_2H_4) and experimental temperature.

In order to make sure the effects of these process parameters on the formation of palladium nanowires at surface of porous stainless steel substrate, series of experiments are designed and carried out. This paper demonstrates the effect of concentration of $PdCl_2$ in the plating solution on the formation of palladium nanowires. The obtained results are described below.

Palladium deposited on the surface of porous stainless steel substrate by electroless process is spontaneous and uniform because this substrate is conductive. Based on our investigation of palladium deposits in the initial stages, we find that different palladium nanowire arrays are built on the steel substrate. [18, 19] The formation of palladium nanowire starts by alignment of particles then which form a continuous and homogeneous nanwire.

SEM micrographs in Figure 7-1(a-d) illustrate palladium deposited on porous stainless steel substrate within the deposition time from 75 s to 120 s when the concentration of $PdCl_2$ in the plating solution is 4.2 g/l. One can see that a discontinuous palladium nanowire is built in Figure 7-1 (a). The nanowire made of nanoparticles is easily identified and the diameter of this nanowire is measured about 30~ 50 nm, which is the same range as that of deposited nanoparticles. When the deposition time extends to 90 s, the nanowire is solid and its diameter is measured about 93 nm, as shown in Figure 7-1(b), it is difficult to identify nanoparticles in this nanowire. When small palladium nanoparticles gather together to form a nanowire, their interfaces are eliminated due to the interface tension and this process is driven by the reduction of surface free energy. They look like fusing together and well organized. With increasing deposition time to 120 s, one can see that the nanowire becomes homogeneous and measured diameter of this wire is 137 nm.

Figure 7-1 (e) and (f) illustrates the elemental mapping of palladium from the SEM image in Figure 7-1(d) and energy-dispersive spectrum from marked area A in the SEM micrograph of Figure 7-1 (d). We are sure that deposited nanoparticles and nanonanowires are composed of palladium.

Figure 7-2 illustrates the deposition of palladium on porous stainless steel substrate with deposition time from 90 s to 150 s when concentration of $PdCl_2$ in the plating solution is 3.0 g/l. One can see that a continuous palladium nanowire is built in Figure 7-2(a). The nanowire made of nanoparticles is easily recognized at the deposition time of 90 s and the diameter of this nanowire is measured about 125 nm, but the size of most nanoparticles distributed on the substrate surface ranges from 50 nm to 70 nm. After deposition time extends to 120 s, the diameter of palladium nanowire increases up to 152 nm, as shown in Figure 7-2(b). With increasing deposition time to 150 s, the nanowire is

built homogeneously and its diameter is about 200 nm, as illustrated in Figure 7-2(c). It is difficult to distinguish the interfaces of nanoparticles from the nanowires in Figure 7-2(b, c). However, the size of most nanoparticles distributed on the surface does not change and still remains in the same range from 50 to 70 nm with the extension of deposition time from 90 s to 150 s in Figure 7-2(a) to (c). Figure 7-2(d) displays that the length of a nanowire built on the substrate surface is over 23.5 μm and it is not located along grain-boundary.

The elemental mapping of palladium in Figure 7-2(f) is measured from the SEM image in Figure 7-2(e). This nanowire, for sure, is made of palladium.

Figure 7-3 illustrates palladium nanowires deposited on porous stainless steel substrate within the deposition time from 75 s to 120 s when concentration of $PdCl_2$ in the plating solution is about 1.8~2.0 g/l. One can see that some palladium nanoparticles are arranged and aligned to a discontinuous nanowire in Figure 7-3(a) at the deposition time of 75 s. They are lined up bead by bead. When the deposition time extends to 90 s, the nanowire is mostly continuous. Only one break in the structure is observed, as shown in Figure 7-3(b). One can observe that the diameter of this nanowire is the same as that of these scattered nanoparticles deposited at the substrate surface and it is also not located at grain-boundary of the substrate surface. When the deposition time extends to 120 s, the nanowire is built continuously and homogeneously everywhere and the diameter is measured about 149 nm, as illustrated in Figure 7-3(c). It is difficult to see the interfaces of nanoparticles from the nanowire when they are well organized to form the nanowire. However, we can indistinctly recognize that this nanowire is also made of nanoparticles but these nanoparticles are deformed due to the interface tension when they gather together, as shown in Figure 7-3(c, d). Figure 7-3(e) and (f) illustrates the elemental mapping of palladium and energy dispersive spectrum from the SEM image presented in Figure 7-3(d), we are sure that deposited nanoparticles and nanonanowire are composed of palladium.

Palladium nanowires are well organized by nanoparticles. The size of palladium nanoparticles deposited is determined by concentration of $PdCl_2$ in the plating solution. The higher the concentration of $PdCl_2$ in the plating solution is, the bigger the palladium nanoparticles are obtained. Therefore, the diameter of palladium nanowires can also be controlled by concentration of $PdCl_2$ and appropriate deposition time.

Figure 7-4 (a) illustrates the interfacial microstructure of deposited palladium nanoparticles on the steel substrate. One can see that the nanoparticles are not wetting with the steel substrate because the contact angle θ is greater than 90°. The contact angle θ can be expressed in equation (7-2).

$$\cos\theta = \frac{\sigma_{Pd-sub} - \sigma_{sub-L}}{\sigma_{Pd-L}} \tag{7-2}$$

Where θ is the contact angle of deposited palladium nanoparticle on the steel substrate surface, σ_{Pd-sub} is the interface tension between palladium nanoparticle and the steel substrate, σ_{sub-L} is the interface tension between the substrate and the plating solution, σ_{Pd-L} is the interface tension between palladium nanoparticle and the plating solution. Based on the observation in Figure 7-4 (a), together with the schematic in Figure 7-4 (c),

the contact angle of deposited palladium nanoparticles on the steel substrate is greater then 90°. It means that palladium nanoparticles are not wetting with the substrate. The interface tension σ_{Pd-sub} is less than the interface tension σ_{sub-L}. If deposited palladium nanoparticles were easily removed and rearranged during the deposition process, this possibility should be further investigated.

Palladium nanoparticles generated from the plating solution should have spherical structure, similar to these micrographs in the report [21]. The shape of nanoparticles changes a little bit due to the interfacial tension between the nanoparticles and the substrate when they are deposited on the steel substrate. SEM micrographs in Figure 7-3 show the formation of a continuous palladium nanowire at the same deposition time of 120 s. One can see the transitions from a continuous nanowire arranged from nanoparticles to a homogeneous one. The necks linking nanoparticles are gradually eliminated due to lower interface tension between nanoparticles. Combining the microstructure characteristics of the uniform nanowires in Figures 7-1~7-3 and 7-4 (b) with deposited palladium nanoparticles in Figure 7-4 (a), we can obtain the same phenomenon. The phenomenon also confirms that nanocrystalline metals are soft when they are at very small grain sizes. [22, 23] It has also been observed elsewhere [19] when palladium nanoparticles deposited on the wall of cavities or at the substrate surface stick together to form one nanoparticle monolayer. It is explained below when two nanoparticles combine together.

Figure 7-5 (a-f) displays the structure characterization of two nanoparticles when they join together due to the interface tension. The surface energy of the two particles system will change with the contact angle between two particles.

Here, we assume that palladium nanoparticles generated from the autocatalytic reaction are the same size and have a spherical structure. The center distance between two particles can be expressed in equation (7-3).

$$d=2R\sin\theta/2 \tag{7-3}$$

Where, d is the center distance between two particles, R is radius of the particle. θ is the contact angle between two particles. The center distance between two particles changes with the interface tension according to the formation of the palladium nanowire in Figures 7-3 (a-d) and 7-4 (b), so we can conclude that palladium nanoparticles generated from the autocatalytic reaction are not solid and easily deformed when they get together. The work of two adhesive nanoparticles (or surface energy) is expressed in equation (7-4) and the variation of adhesive work can be calculated in equation (7-5) when two particles combine together.

$$\begin{aligned} W &= (2*4\pi R^2 - 2*2\pi Rh)\sigma_{Pd-Pd} \\ &= (8\pi R^2 - 4\pi R^2 \cos\frac{\theta}{2} tg\frac{\pi-\theta}{4})\sigma_{Pd-Pd} \\ &= 4\pi R^2 \sigma_{Pd-Pd}(2-\cos\frac{\theta}{2} tg\frac{\pi-\theta}{4}) \end{aligned} \tag{7-4}$$

$$\Delta W = -4\pi R^2 \sigma_{Pd-Pd} \cos\frac{\theta}{2} tg\frac{\pi-\theta}{4} \tag{7-5}$$

Where, the height of spherical cap at the overlapping part of two palladium nanoparticles can be calculated according to the geometric structures in Figure 7-5(a-f), $h = R\cos\frac{\theta}{2}tg(\frac{\pi-\theta}{4})$, R is radius of the particle. θ is the contact angle between two particles. $\sigma_{Pd\text{-}Pd}$ is the interface tension between two palladium nanoparticles. The variation of adhesive work between the two particles system is function with the contact angle, as shown in Figure 7-5 (g). The systematic surface energy is gradually declined when the contact angle of two nanoparticles is gradually reduced and deposited palladium nanoparticles on the steel substrate surface link together to form a homogeneous nanowire. Seeking the original location of palladium nanowires deposited at the surface of porous steel substrate, we can find that palladium nanoparticles are easily deposited on the grain-boundaries or irregular steps at the initial stage. When nanoparticles connect together to gradually form a nanowire, they will follow the principle of interface and surface energy minimization and do not follow the orientation of defects, as shown in Figure 7-3(c). The microstructural characteristics of palladium nanowires in Figures 7-1 ~ 7-3 and 7-4 (b) are quite different from that of the nanowires deposited along the defect orientation [19] or microcontact printing pattern. [22-25] However, the mechanism of palladium nanowire formation is still being further investigated.

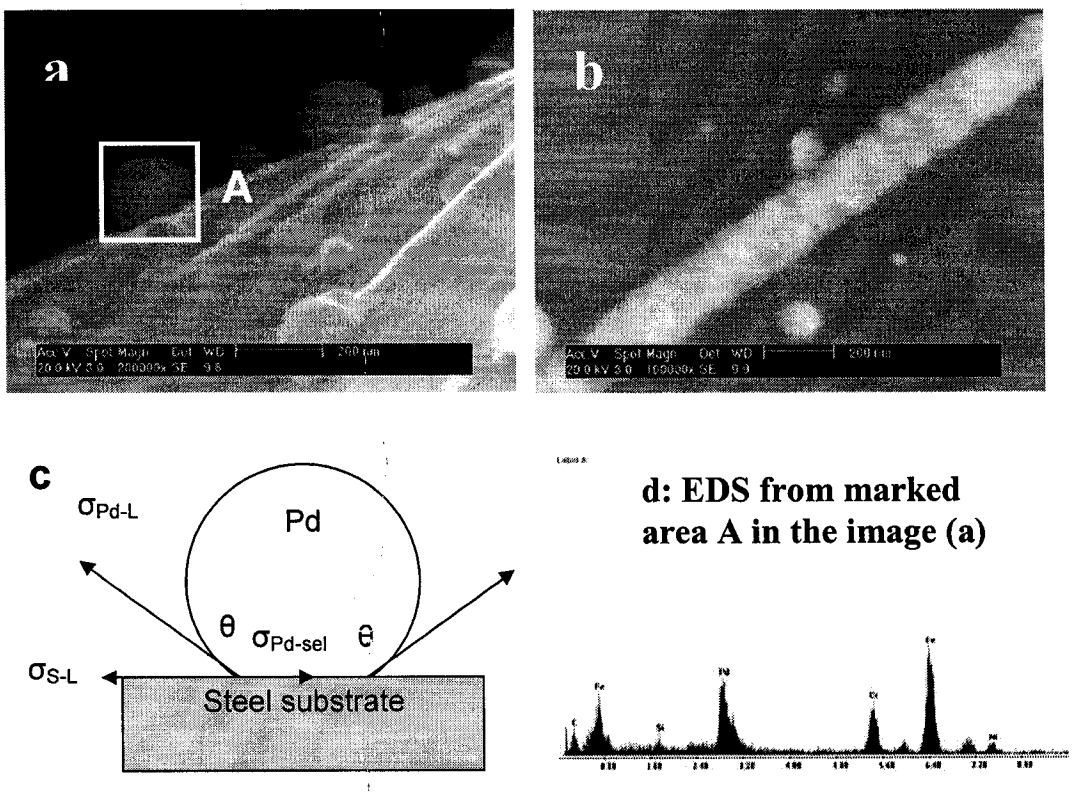

Figure 7-4 (a, b) SEM micrograph showing the palladium nanoparticles deposited at the surface of porous stainless steel substrate; (c) Schematic showing non-wettability behavior when palladium nanoparticles are deposited on the steel substrate surface; and (d) The energy-dispersive spectrum from the marked area A of the image (a)

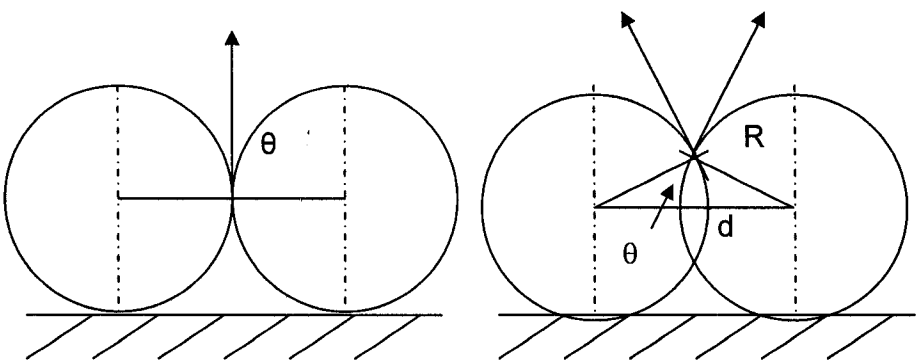

(a) θ=π (b) θ=(2/3)π

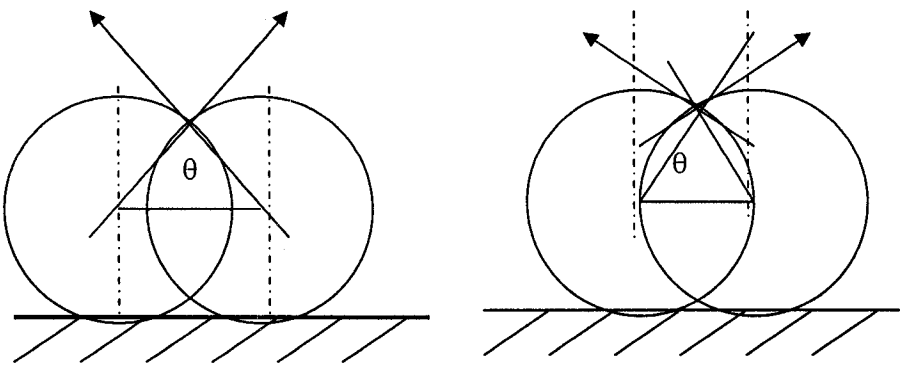

(c) θ=(1/2)π (d) θ=(1/3)π

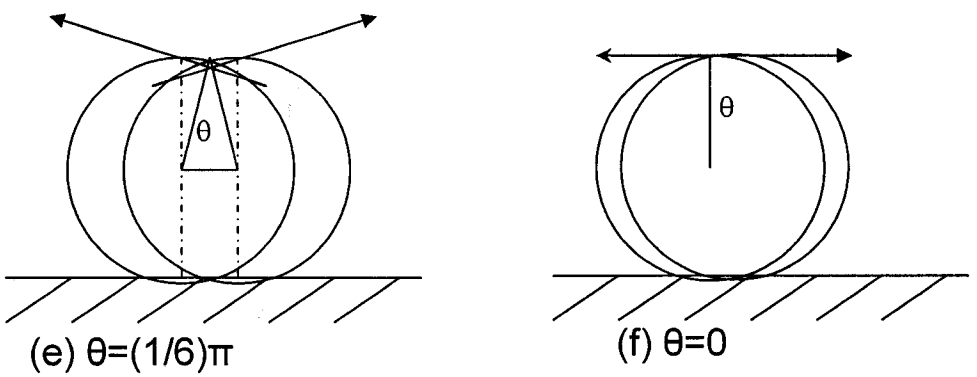

(e) θ=(1/6)π (f) θ=0

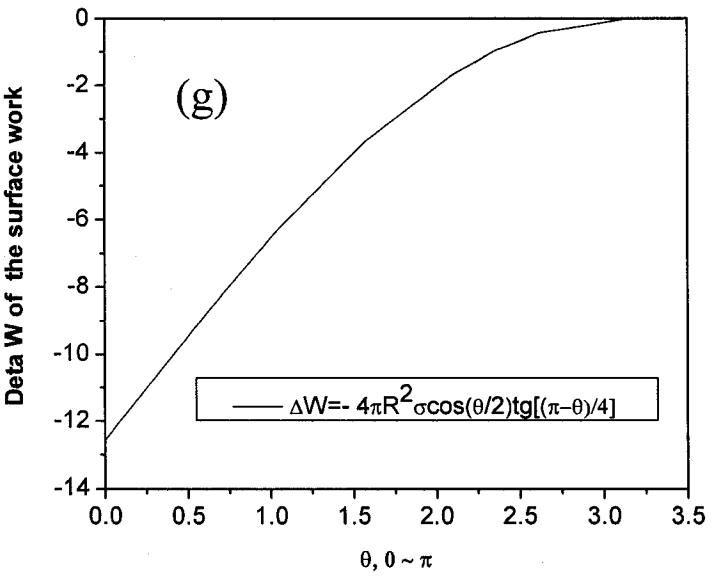

Figure 7-5 Schematics of variations of the contact angle θ between two palladium nanoparticles (a-f); and the reduction of surface energy (works) is function with the contact angle θ when the two particles connect together (g)

7.5 Conclusions

Palladium nanowires are well organized from nanoparticles at rough stainless steel surface. Palladium nanoparticles generated from autocatalytic reaction are not wetting with the steel substrate. They are not solid and they can be easily deformed due to the interfacial tension when they connect each other. With the extension of deposition time, palladium nanowires will be built homogeneously and the diameter of these nanowires is greater than that of single nanoparticle because palladium nanoparticles used for assembly of nanowires are easily deformed due to interface tension when they combine. Their diameters can be effectively controlled by concentrations of $PdCl_2$ in the plating solution with appropriate deposition time. The experimental results provide a simple technique for building palladium nanowire arrays in a controllable manner for potential engineering applications.

7.6 References

1. F. Favier, E.C. Walter, M.P. Zach, T. Benter, and R.M. Penner. Hydrogen sensors and switches from electrodeposited palladium mesowire arrays, Science 293, 2227-2231 (2001).
2. E.C. Walter, F. Favier, R.M. Penner. Palladium Mesowire Arrays for Fast Hydrogen Sensors And Hydrogen-Actuated Switches, Analytical Chemistry 74, 1546-1553 (2002).
3. Massood Z Atashbar, Deep Banerji, Srikanth Singamaneni and Valery Bliznyuk. Deposition of parallel arrays of palladium nanowires and electrical characterization using microelectrode contacts, Nanotechnology 15, 374-378 (2004).
4. Chuanding Cheng, Ravi Kanth Gonela, Qun Gu, and Donald T. Haynie. Self-assembly of metallic nanowires from aqueous solution, Nano Letters, 5, 175-178 (2005).
5. M. Yun, N.V. Myung, R.P. Vasquez, C. Lee, E. Menke, R.M. Penner, Electrochemically grown wires for individually addressable sensor arrays, Nano Letters 4, 419-422 (2004).
6. Mangesh A. Bangar, Kumaran Ramanathan, Minhee Yun, Choonsup Lee, Chrlos Hangarter and Nosang V, Myung. Controlled growth of a single palladium nanowire between microfabricated electrodes, Chem. Mater. 16.4955-4959 (2004).
7. Yeonho Im, Chiinsup Lee, Richard P. Vasquez, Mangesh A. Bangar, Nosang V. Myung, Eric J. Menke, Reginald M. Penner, and Minhee Yun. Investigation of a single Pd nanowire for use as a hydrogen sensor, Small, 2, 356-358 (2006).
8. Zhaoxiang Deng and Chengde Mao, DNA-templated fabrication of 1D parallel and 2D crossed metallic nanowire arrays, Nano Letters, 3, 1545-1548 (2003).
9. A. Johansson, J. Lu, J. –O. Carlsson and M. Boman. Deposition of palladium nanoparticles on the pore walls of anodic alumina using sequential electroless deposition, J. Appl. Phys. 96, 5189-5194 (2004).
10. Zongtao Zhang, Sheng Dai, Douglas A. Blom, and Jian Shen, Synthesis of ordered metallic nanowires inside ordered mesoporous materials through electroless deposition, Chem. Mater. 14, 965-968 (2002).
11. Kyungtae Kim, Moonjung Kim, Sung M. Chio, Pulsed electrodeposition of palladium nanowire arrays using AAO template, Materials Chemistry and Physics 96, 278-282 (2006).
12. K.-B. Lee, S.-M. Lee, J. Cheon, Size-Controlled Synthesis of Pd Nanowires Using a Mesoporous Silica Template via Chemical Vapor Infiltration, Advanced Materials, 13, 517-520 (2001).
13. Matthias Geissler, Heiko Wolf, Richard Stutz, Emmanuel Delamarche, Ulrich-Walter Grummt, Bruno Michel, and Alexander Bietsch. Fabrication of metal nanowires using microconnect printing, Langmuir, 19, 6301-6311 (2003).
14. Alain Carvalho, Matthias Geissier, Heinz Schmid, Bruno Michel, and Emmanuel Delamarche, Self-assembled monolayers of eicosanethiol on palladium and their use in microcontact printing, Langmuir, 18, 2406-2412 (2002).

15. L.H. Chan, K.H. Hong, S.H. Lai, X.W. Liu and H.C. Shih. The formation and characterization of palladium nanowires in growing carbon nanotubes using microwave plasma-enhanced chemical vapor deposition, Thin Solid Films, 423, 27-32 (2003).
16. Jennifer Sippel-Oakley, Hung-Ta Wang, Byoung S Kang, Zhuangchun Wu, Fan Ren, Andrew G. Rinzler and Stephen J Pearton, Carbon nanotube films for room temperature hydrogen sensing, Nanotechnology, 16, 2218-2221 (2005).
17. A. Govindaraj, B.C. Satishkumar, Manashi Nath, and C.N.R. Rao, Metal nanowires and intercalated metal layers in single-walled carbon nanotube bundles, Chem. Mater. 12, 202-205 (2000).
18. Zhongliang Shi, Shanqiang Wu, Jerzy A Szpunar. Self-assembled palladium nanowires by electroless deposition, Nanotechnology, 17, 2161-2166 (2006).
19. Zhongliang Shi, Shanqiang Wu, Jerzy A Szpunar. Synthesis of palladium nanostructures by spontaneous electroless deposition, Chemical Physics Letters, 422, 147-151 (2006).
20. Electroless plating - Fundamental and Applications. Edited by Glenn O. Mollory, June B. Hajdu, William Andrew Publishing/Noyes, 1990, p 511.
21. D.V. Goia, Preparation and formation mechanism of uniform metallic particles in homogeneous solutions, J. Mater. Chem. 14, 451-458 (2004).
22. Byron D. Gates, Qiaobing Xu, Michael Stewart, Declan Ryan, C. Grant Willson, and George M. Whitesides. New approaches to nanofabrication: molding, printing, and other techniques, Chem. Rev. 105, 1171-1196 (2005).
23. Sarah J. Hurst, Emma Kathryn Payne, Lidong Qin, Chad A. Mirkin Multisegmented one-dimensional nanorods prepared by hard-template synthetic methods, Angew. Chem, Int. Ed. 45, 2672-2693 (2006).
24. Matthias Geissler, Heiko Wolf, Richard Stutz, Emmanuel Delamarche, Ulrich-Walter Grummt, Bruno Michel, and Alexander Bietsch. Fabrication of metal nanowires using microconnect printing, Langmuir, 19, 6301-6311 (2003).
25. Alain Carvalho, Matthias Geissier, Heinz Schmid, Bruno Michel, and Emmanuel Delamarche, Self-assembled monolayers of eicosanethiol on palladium and their use in microcontact printing, Langmuir, 18, 2406-2412 (2002).

CHAPTER 8 [1]

EFFECT OF SILICA ON THE ARRAYS OF PALLADIUM NANOWIRES OR NANOPARTICLES

8.1 Abstract

The observation of palladium deposited on a porous stainless steel substrate by electroless plating process in the initial stages is carried out with FE-SEM in this chapter. It is found that palladium nanowires can be formed from nanoparticles and be well-organized by nanoparticles on the rough surface of the substrate, but somewhere of the nanowires are broken by SiO_2 inclusions or palladium nanoparticles make a detour around these SiO_2 inclusions to build the nanowires continuously, and that palladium nanoparticles cannot be deposited at the surface of SiO_2 inclusions in the initial stages but they can gradually cover the SiO_2 inclusions with the extension of deposition time because deposited palladium nanoparticles surround them. The understanding of these phenomena is linked to the fact that SiO_2 inclusion is nonconductive and cannot carry the electron transfer in the autocatalytic reaction. The obtained results can be used to design required patterns for the fabrication of palladium nanostructural arrays in engineering application.

8.2 Introduction

One of the most important applications of palladium is for hydrogenation catalysts and hydrogen extraction after it is deposited on a substrate as a membrane. [1-3] The interaction between palladium and hydrogen has been studied extensively and it is well known that palladium can adsorb or absorb hydrogen very well. [4, 5] When deposited palladium membrane is used for hydrogen extraction, it has high hydrogen permeability, chemical compatibility and infinite hydrogen selectivity. Palladium is usually deposited on a porous metal or ceramic substrate to build a durable ultra-thin membrane for improving hydrogen flux and reducing its cost, as it is a noble metal. [6-10] Porous metal substrate having highly permeability, relatively low selectivity and interconnected porous structure primarily provides mechanical integrity as well as appropriate coefficient of thermal expansion with deposited palladium membrane. Such substrate is often selected to provide for palladium membrane in the high temperature application.

On the other hand, studies of palladium in the form of nanowires have recently received extensive attention because of the applications of hydrogen sensing and other nano-devices. For example, the sensor made of palladium nanowires exposed to a gas mixture can detect hydrogen concentration over a range from 1 to 10% in a rapid response as fast as 20 ms. [11] There are already some reports of palladium nanowires fabrication using electrochemical deposition process. One is palladioum nanowires (or

---

[1]This chapter as an article, is submitted to Materials Science and Engineering A (Journal)

mesowires) electrodeposited on a highly oriented pyrolytic graphite (HOPG) surface for the fabrication of hydrogen sensors and hydrogen-activated switches. In this application, palladium nanowires (or mesowires) were deposited from aqueous solution of Pd^{2+} onto step edges or the "V" shaped grooves generated on the HOPG surface. [11-14] The other is the fabrication of highly ordered metallic nanowires directly from palladium acetate solution in self-assembly by an applied alternating current electric field of relatively high intensity and frequency. [15] In addition, palladium nanowires can also be created in different templates by electrochemical process. [16-21] However, new approach to creating palladium nanowires for engineering application is still being explored.

Electroless deposition of palladium is the mature method either in the electronics application or in the fabrication of palladium membrane for hydrogen extraction and hydrogenation catalysts as this method can be operated simply and is inexpensive. [22] However, the quality and microstructure of palladium deposition is directly dependent on the surface microstructure of the substrate. [23] The understanding of palladium deposition on the porous steel substrate in the initial stages is very important for ongoing membrane fabrication. Therefore, the purposes of this chapter are to observe the deposition of palladium on porous stainless steel substrate in the initial stages and to analyze the effect of one kind of impurity, SiO_2 inclusions at the substrate surface on the deposition of palladium. The results reveal the noteworthy concerns in applications of the palladium deposits for hydrogen extraction, electronics or somewhere in the similar approach.

8.3 Experimental section

In this program, a 0.2 μm grade porous 316L stainless steel plate, purchased from Mott Metallurgical Corporation was used as a substrate. This substrate having good mechanical strength and inter-connected porosity was fabricated by powder metallurgical process. These interconnected porosities are defined as pores that are connected to the surfaces of the component and allow fluid flow from one side to the other. The porosity of the substrate is defined as a 0.2 μm grade that means over 95% of 0.2 μm size particles and fluids are rejected by this support during filtering. Samples were cut into the size of 20x20 mm and cleaned in an ultrasonic bath with acetone for 15 minutes. After that, their surfaces were activated and rinsed with deionized water. Then, these samples were transferred immediately into an electroless plating bath for the deposition time from 30 to 300 s at a constant temperature of 60°C. The detailed palladium plating baths preparation using hydrazine as a reducing agent was described elsewhere. [23, 24] Microstructural characteristics of palladium deposited samples were observed and analyzed by a PHILIPS XL30 FE SEM (Filed Emission Scanning Electron Microscopy) equipped with an EDS (Energy Dispersive Spectroscopy, GENESIS 2000 X-ray Microanalysis System).

8.4 Results and discussion

The deposition of palladium is an autocatalytic process without any external electrical power. This process has been widely used for depositing a uniform and dense membrane on complex geometry substrates. Since the surface of the porous substrate is coarse, there are also many different defects such as contaminants, irregular steps and

grain boundaries. These defects may affect the deposition of palladium because this process is related to electronic transfer in the chemical reaction. So far, there is no report about the effect of these defects on the deposition of palladium at the surface of porous stainless steel substrate in the initial stages. This investigation is very important because the observation of palladium deposition in the initial stages will help us understand how the palladium deposits nucleate and grow and how palladium deposits fill with the porous area as well as how the surface microstructure of the substrate affects the deposition of palladium. How the palladium deposits fill into the porous area in the porous substrate has been already reported elsewhere. [24] In preparing palladium membrane, the goal is to make it as thin as possible yet defect-free, which performs the high flux during hydrogen extraction from a mixture of gases. When an ultra-thin membrane is to be built, the defects at the surface of the substrate are a big problem. Some defects are very difficult to be controlled or eliminated. When it is built on the defects area, the thin palladium membrane is weak and easily broken at high temperature and pressure. The effects of one kind of contaminant, SiO_2 inclusions at the substrate surface on the deposition of palladium in the initial deposition time are described below.

8.4.1 Source of SiO_2

The porous stainless steel substrate, which was fabricated by a powder metallurgical process, is often used to provide the mechanical strength for the support of palladium membrane. One kind of contaminants, SiO_2 inclusion cannot be avoided. SiO_2 inclusion may be originated from two main sources. One is from the original particles that are supplied for the powder metallurgical process. The other is from inorganic silicate binders because soluble silicates are often used as binders for improving mechanical strength of the substrate at high temperature during the fabrication by powder metallurgical process.

SEM micrographs in Figure 8-1 (a, b) illustrate the surface morphologies of the porous stainless steel substrate. Some spherical particles are found at the surface. The analysis of EDS illustrates that the inclusion particles are composed of SiO_2. When SiO_2 inclusion is originated at the surface of the porous steel substrate, it will cause the substrate microstructure to have conductive and non-conductive areas because SiO_2 is non-conductive. If the thickness of deposited palladium membrane is much larger than the size of these contaminants, the effect of these contaminants will be negligible. If an ultra-thin palladium membrane is built on a substrate, the contaminants at the substrate surface will not be neglected. The effects of SiO_2 inclusions on the deposition of palladium are illustrated below.

8.4.2 Effect of SiO_2 on the formation of palladium nanowires

Figure 8-1 (c-f) shows that palladium nanowires and palladium nanowire arrays are well organized from palladium nanoparticles. But the continuity of palladium nanowires is cut off by SiO_2 inclusions, as shown in Figure 8-1 (c, d) or palladium nanoparticles make a detour around SiO_2 inclusions as shown in Figure 8-1 (e). The same phenomenon is observed in the network of the palladium nanowires, as shown in Figure 8-1 (f). Some nodes in the network arrays of palladium nanowires are occupied by the

sphere SiO_2 inclusions that cause the palladium nanowire to be broken or palladium nanoparticles make a detour around them to build the nanowires continuously. The analysis of EDS from SiO_2 inclusion, the marked area A in the SEM image of Figure 8-2 (a) and the elemental mappings from the SEM image of Figure 8-2 (c) are illustrated in Figure 8-2 (b) and 8-2 (d-f), respectively. These spherical inclusions are identified as the composition of SiO_2 and it is found that palladium cannot be deposited at the surface of SiO_2 inclusions. This result has already been used for designing pattern to build metal nanowires in a position-assembled Micro-Electro-Mechanical Systems (MEMS). [25] In order to confirm this phenomenon, we also deposited palladium wires on E-beam silicon pattern using electroless process and measured the electrical resistance. The following section demonstrates the morphologies and measured results.

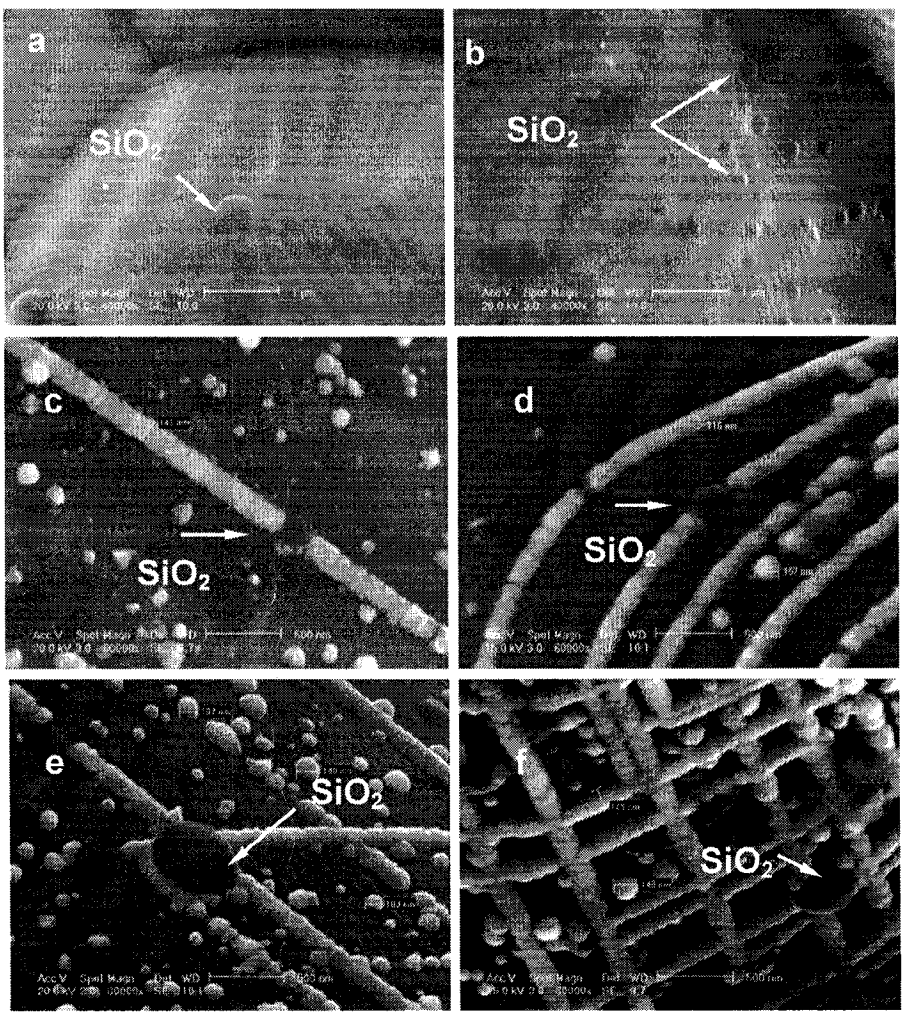

Figure 8-1 SEM micrographs showing the surface microstructure of the porous stainless steel substrate (a, b), and the effects of SiO_2 inclusions at the surface of the steel substrate on the arrays of palladium nanowires (c-f) (The deposition time: 120 s, the concentration of $PdCl_2$: 1.8~2 g/l)

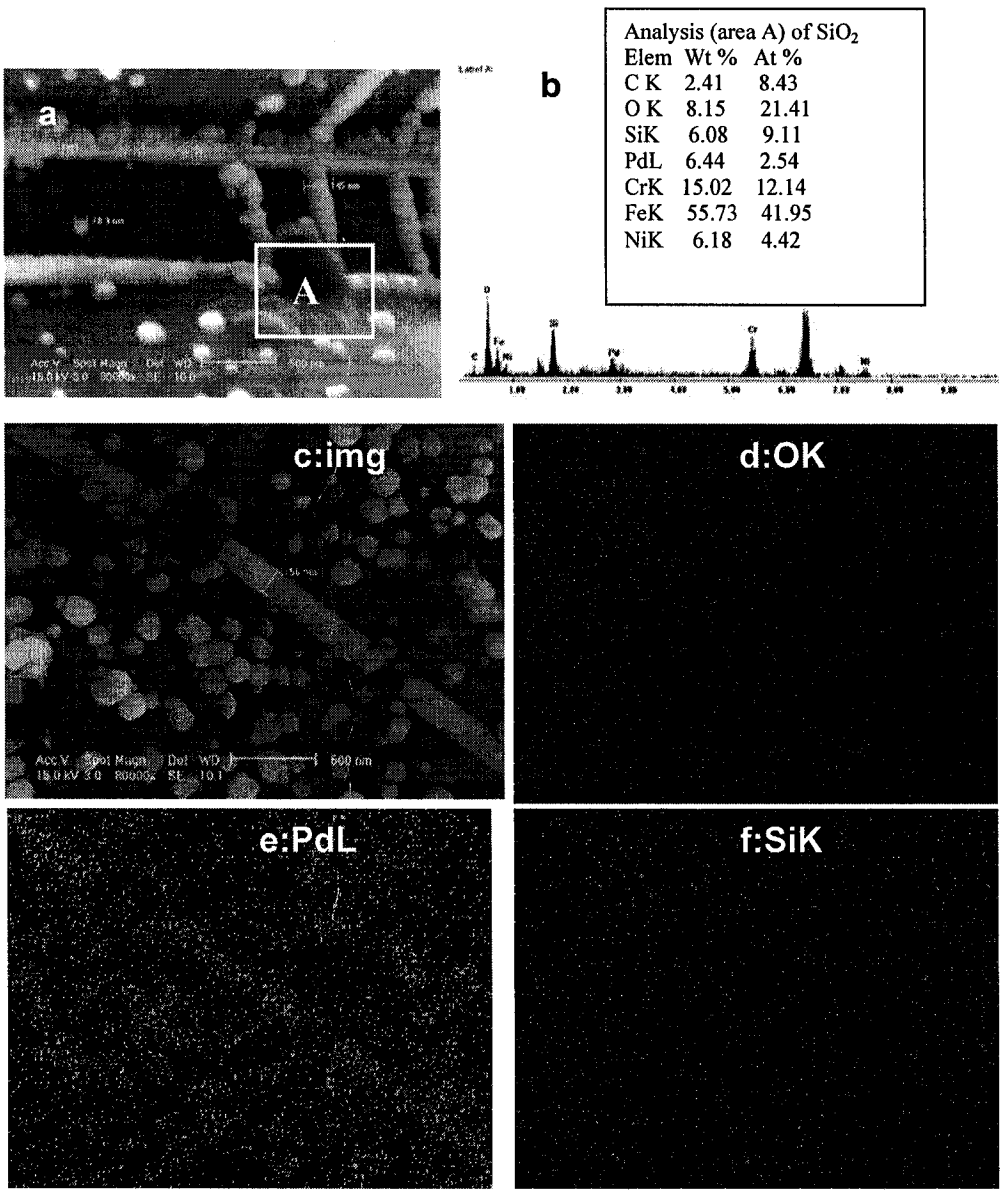

Figure 8-2 SEM micrograph showing palladium nanowire arrays are broken by SiO_2 inclusion (a, c), energy-dispersive x-ray spectrum and the analysis of composition (b) from the marked area A in the SEM image (a), and elemental mappings of O, Pd and Si (d-f) from the SEM image (c)

8.4.3 Palladium wires deposited on E-beam silicon pattern

Figure 8-3 shows that palladium wires were deposited on E-beam silicon pattern using electroless process. In order to measure the electrical resistance, gold and silver electrodes were set up, as illustrated in Figure 8-3 (c). After carefully observing palladium wires on silicon pattern by FE-SEM, we found there were 120 wires, but 40 wires were discontinuous. Figure 8-4 illustrates the linear function between voltage and current when measured in the two different voltage ranges. Based on Ogm's law, the electrical resistance of each continuous palladium wire can be calculated. The electrical properties of palladium wires under hydrogen atmosphere are being further investigated.

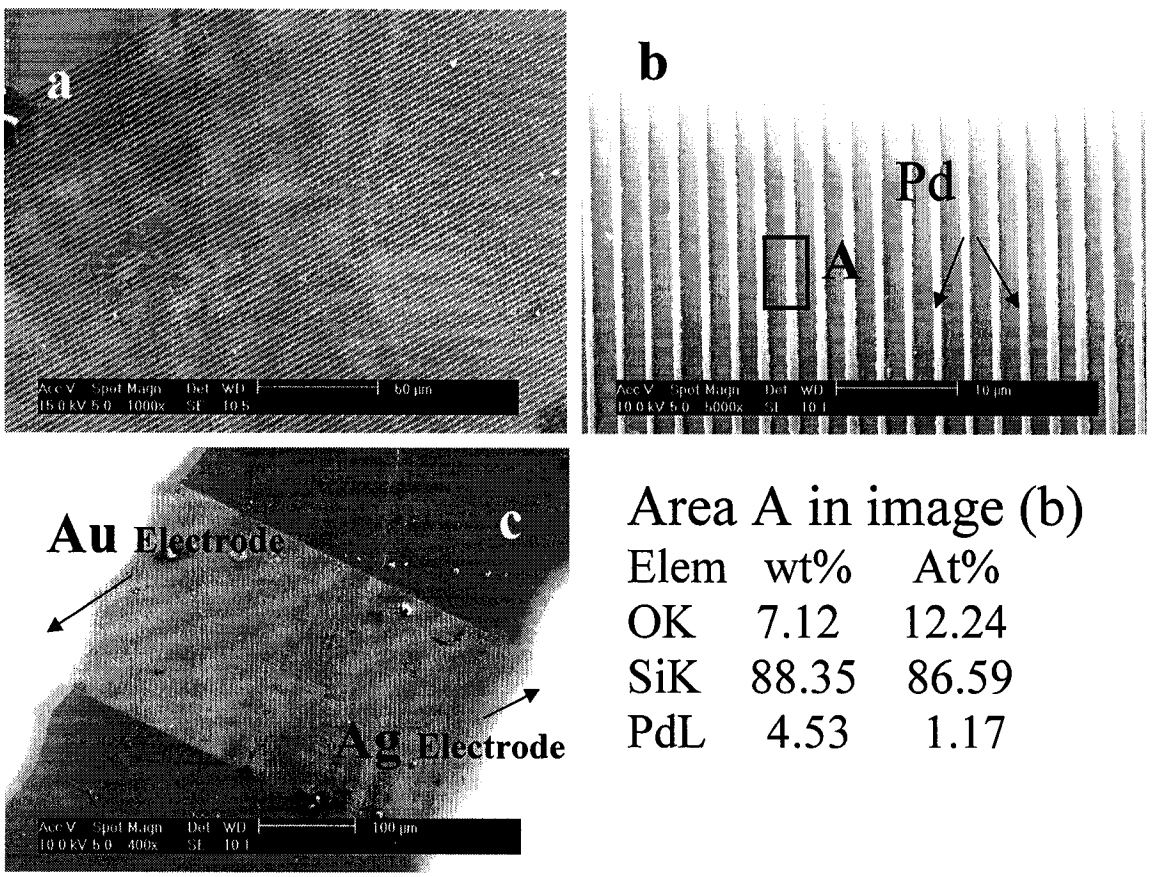

Figure 8-3 SEM micrographs showing the deposited palladium wires on E-beam silicon pattern. (a) E-beam silicon pattern (the interval between Si and SiO_2); (b) palladium wires deposited on silicon pattern and analysis of composition on the marked area A; (c) palladium wires linked by Au and Ag electrodes for electrical properties measurement

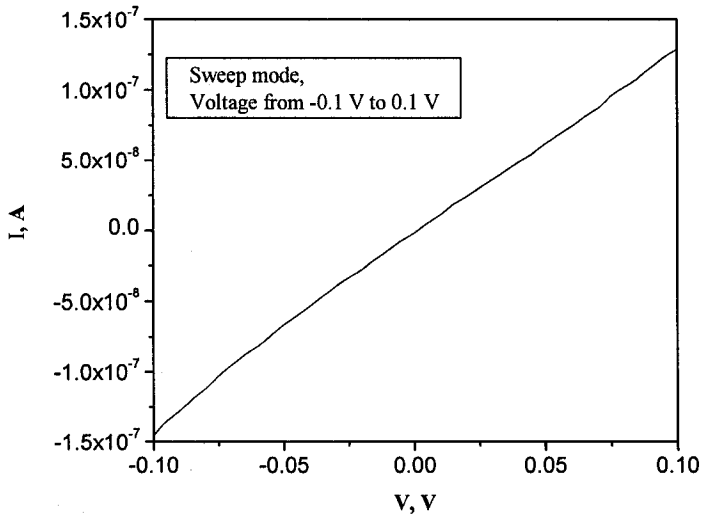

(a)

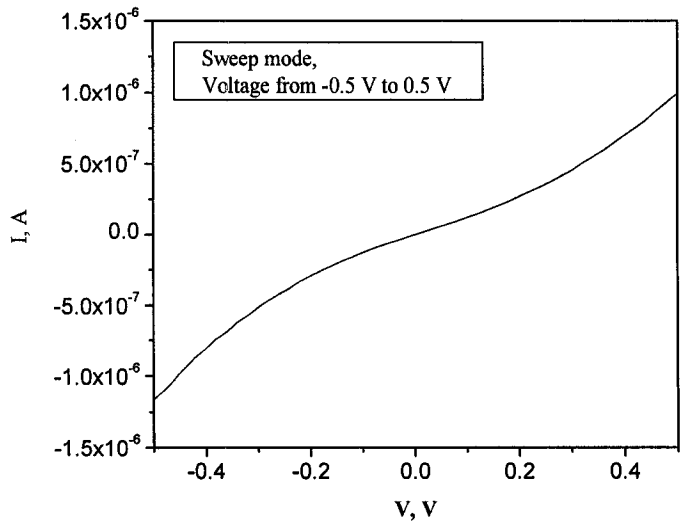

(b)

Figure 8-4 Relationship between voltage and current measured from parallel palladium wires on E-beam silicon pattern
((a) Voltage range from -0.1 V to 0.1 V; (b) Voltage range from -0.5 V to 0.5 V)

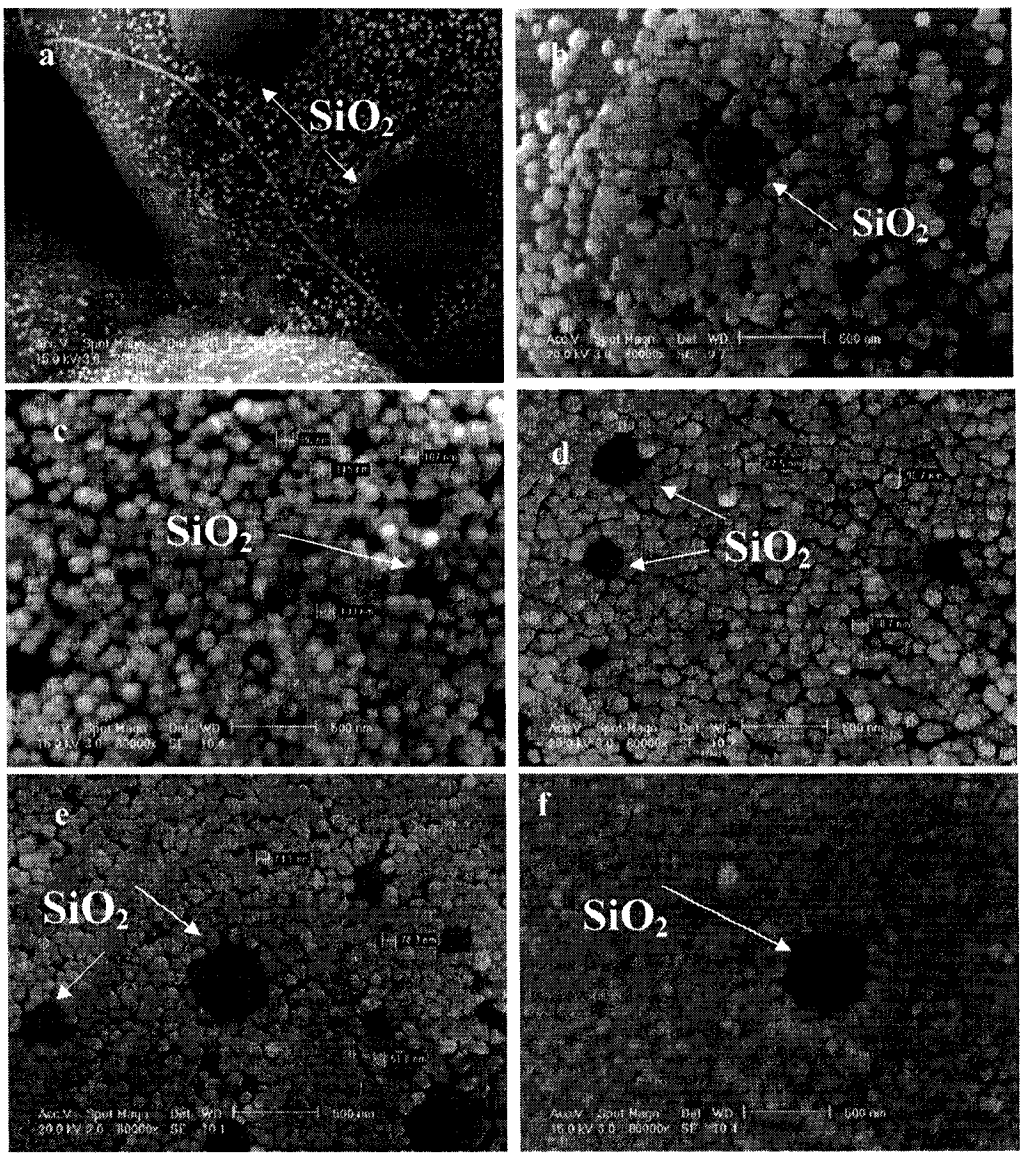

Figure 8-5 SEM micrographs showing the deposition of palladium around SiO_2 inclusions at the surface of the steel substrate with the extension of deposition time (The deposition time: (a) 75 s, (b) 120 s, (c, d) 150 s, (e) 180 s and (f) 300 s)

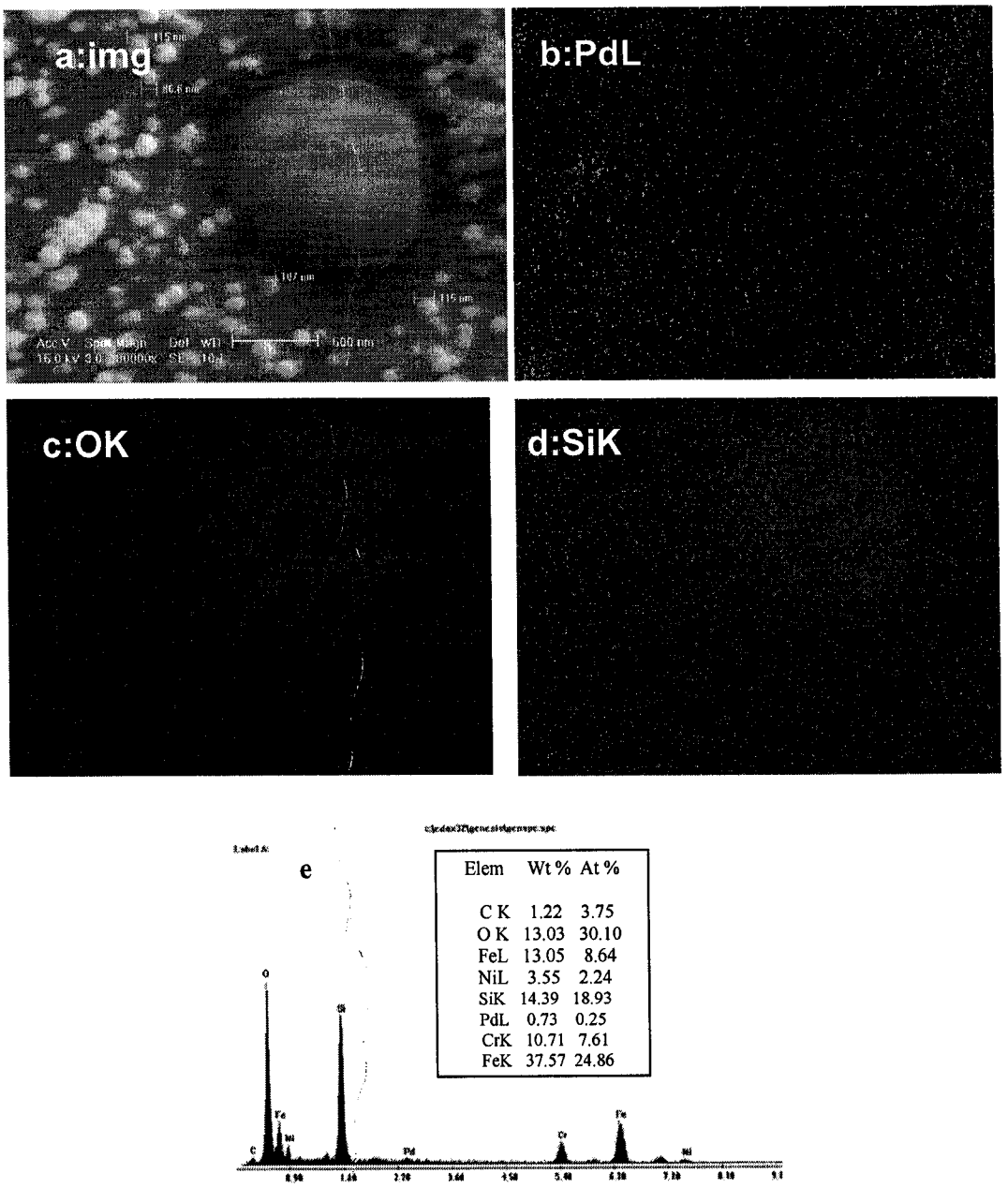

Figure 8-6 (a) SEM micrograph showing palladium deposited at the substrate surface except the occupied area by SiO_2 inclusion, (b-d) the elemental mappings of Pd, O and Si (b-d) from the SEM image (a), and (e) energy-dispersive x-ray spectrum and the composition analysis from the SEM image (a)

8.4.4 Effect of SiO_2 on the deposition of palladium nanoparticles

SEM micrographs in Figure 8-5 (a-f) illustrate that palladium nanoparticles are deposited on the surface of porous stainless steel substrate at different deposition time from 75 s to 300 s. One can see that there is no palladium nanoparticle deposited at the surface of SiO_2 inclusions, as shown in Figure 8-5 (a). This phenomenon is verified by the elemental mappings in Figure 8-6 (b-d) and EDS analysis in Figure 8-6 (e). With the extension of deposition time, palladium nanoparticles will gradually cover these SiO_2 inclusions layer by layer, as shown in Figure 8-5 (b-f). As above mentioned, palladium nanoparticles make a detour around SiO_2 inclusion in Figure 8-1 (e, f). Here, it is the same that palladium nanoparticles are deposited around SiO_2 inclusions exposed at the substrate surface. The deposited palladium nanoparticles can easily catch up oncoming ones and gradually cover the SiO_2 inclusion with increasing the deposition time. Accordingly, if the thickness of an ultra-thin palladium membrane built on the surface of the steel substrate is not greater than the size of SiO_2 inclusions, the contaminant SiO_2 inclusions will have great effect on the quality of the membrane, as the membrane in the bulge area is thinner and weaker.

The autocatalytic process is the most common of all chemical methods used to deposit palladium membranes from aqueous solutions. The chemical reaction for the deposition of palladium can be expressed in the following two equations (8-1) and (8-2) that clearly show the electronic transfer between the solution and the substrate in the deposition process. [26, 27]

$$2Pd(NH_3)_4^{2+} + 4e^{-1} \rightarrow 2Pd^0 + 8NH_3 \qquad E^0 = 0\ V \qquad (8\text{-}1)$$

$$N_2H_4 + 4OH^{-1} \rightarrow N_2 + 4H_2O + 4e^{-1} \qquad E^0 = 1.12V \qquad (8\text{-}2)$$

This autocatalytic reaction takes place fast, once the reaction is initiated. The metal deposited serves as the catalyst, thus ensuring continuous buildup of the metal. [28] According to the observation of palladium nanowires in Figure 8-1 (c-f) and the deposited palladium nanoparticles in Figure 8-5, one can see that the basic unit for the formation of nanowires and membrane is palladium nanoparticle. As the stainless steel substrate is conductive, electronic transfer can be carried out between the substrate surface and the solution. The other reaction products such as NH_3 and N_2 will also nucleate and grow, When they become bubbles and are removed from the substrate surface, it will make palladium deposit on the steel surface quickly. The number and the size of the palladium nuclei generated in the solution depend on the redox potential of the above reactions, concentration of the reactants and additives, temperature and pH in the solution. The final size of the palladium deposits on the substrate depends on the nucleation rate, the fraction of the atoms involved in the formation of the nuclei and the extent of the aggregation processes during the deposition process. If the fraction of palladium atoms consumed in the nucleation step is high, the increase in particle size due to the diffusional growth that immediately follows the nucleation burst is drastically limited. [29] When the concentration of $PdCl_2$ in the plating bath is 1.8~2 g/l, the size of palladium nanoparticles deposited on the substrate is around 100~130 nm and they are the same range as the diameter of palladium nanowires. The size of deposited palladium nanoparticles on this

steel substrate has been investigated and the result shows that the particle size has the same range with the extension of deposition time from 30 to 300 s, only the number of deposited nanoparticles increases. The formation mechanism of palladium nanoparticles generated from the solution is being further investigated.

As a result, palladium nanowires are well organized by nanoparticles without any external field except the autocatalytic reaction. However, they are broken by SiO_2 inclusions at the substrate surface or the deposited nanoparticles make a detour around them to keep the nanowires incessantly. For this reason, one can design the substrate pattern based on their dissimilar conductivities of the microstructures to build the required palladium nanowire arrays.

8.5 Conclusions

Based on the observation of palladium deposited on the porous stainless steel substrate in the initial stages, we can obtain the following conclusions:

(1) Palladium nanowires are well organized on the rough stainless steel substrate surface. But they are broken by SiO_2 inclusions or palladium nanoparticles make a detour around the SiO_2 to build the nanowires continuously.

(2) Palladium nanoparticles cannot be deposited on the surface of SiO_2 inclusion at the initial stages due to its non-conductivity. But palladium nanoparticles will gradually cover the SiO_2 inclusion due to advance palladium deposits surrounding them with the extension of deposition time.

(3) When an ultra-thin palladium membrane is required to be built on a porous metal substrate, the nonconductive SiO_2 inclusion should be avoided. This effect can be used to design the pattern structure for fabricating the required palladium nanostructure arrays by the electroless deposition.

8.6 References

1. A. Kolmakov, D.O. Klenov, Y. Lilach, S. Stemmer, M. Moskovits. Enhanced gas sensing by individual SnO_2 nanowires and nanobelts functionalized with Pd catalyst particles, Nano Letters 5, 667-673 (2005).
2. B.L. French, L.M. Davis, E.S. Munzinger, J.W.J. Slavin, P.C. Christy, D.W. Thompson, R.E. Southward. Palladium-polyimide nanocomposite membranes: synthesis and characterization of reflective and electrically conductive surface-metallized films, Chem. Mater. 17, 2091-2100 (2005).
3. R. Diaz-Ayala, L. Arroyo, R. Raptis, C.R. Cabrera. Thermal reduction of Pd molecular cluster precursors at highly ordered pyrolytic graphite surfaces, Langmuir 20, 8329-8335 (2004).
4. T. Mitsui, M.K. Rose, E. Fomin, D.F. Ogletree and M. Salmeron. Dissociative hydrogen adsorption on palladium requires aggregates of three or more vacancies, Nature 422, 705-707 (2003).
5. E.C.H. Sykes, L.C. Fernandez-Torres, S.U. Nanayakkara, B.A. Mantooth, R.M. Nevin, P.S. Weiss. Observation and manipulation of subsurface hydride in Pd{111} and its effect on surface chemical, physical, and electronic properties, Proc. Natl. Acad. Sci. 102 17907-17911 (2005).
6. C. Su, T. Jin, K. Kuraoka, Y. Matsumura, T. Yazawa. Thin Palladium Film Supported on SiO_2-Modified Porous Stainless Steel for a High-Hydrogen-Flux Membrane, Ind. Eng. Chem. Res. 44, 3053-3058 (2005).
7. J. Tong, Y. Kashima, R. Shirai, H. Suda, Y. Matsumura. Thin defect-free Pd membrane deposited on asymmetric porous stainless steel substrate, Ind. Eng. Chem. Res. 44, 8025-8032 (2005)
8. F.C. Gielens, H.D. Tong, C.J.M. van Rijn, M.A.G. Vorstman, J.T.F. Keurentjes. Microsystem technology for high-flux hydrogen separation membranes, Journal of Membrane Science 243, 203-213 (2004).
9. J. Shu, B.P.A. Grandjean, S. Kaliaguine. Morphological study of hydrogen permeable Pd membranes, Thin Solid Film 252, 26-31 (1994).
10. Yi Hua Ma, Ivan P. Mardilovich and Erik E. Engwall. Thin composite palladium and palladium/alloy membranes for hydrogen separation. Ann. N. Y. Acad. Sci., 984: 346-360 (2003)
11. F. Favier, E.C. Walter, M.P. Zach, T. Benter, R.M. Penner. Hydrogen sensors and switches from electrodeposited palladium mesowire arrays. Science 293, 2227-2231 (2001)
12. E.C. Walter, F. Favier, R.M. Penner, Palladium mesowire arrays for fast hydrogen sensors and hydrogen-actuated switches, Anal. Chem. 74, 1546-1553 (2002).
13. Mangesh A. Bangar, Kumaran Ramanathan, Minhee Yun, Choonsup Lee, Carlos Hangarter and Nosang V. Myung. Controlled growth of a single palladium nanowire between micorfabricated electrodes. Chem. Mater. 16, 4955-4959 (2004).
14. Massood Z Atashbar, Deep Banerji, Srikanth Singamaneni and Valery Bliznyuk. Deposition of parallel arrays of palladium nanowires and electrical characterization using microelectrode contacts, Nanotechnology 15, 374-378 (2004).

15. C. Cheng, R.K. Gonela, Q. Gu, D.T. Haynie. Self-assembly of metallic nanowires from aqueous solution. Nano Letters 5, 175-178 (2005).
16. Xu-Hui Sun, Ning-Bew Wong, Chi-Pui Li, Shuit-Tong Lee, Pil-Sook G. Kim, and Tsun-Kong Sham. Reductive self-assembling of Pd and Rh nanoparticles on silicon nanowire templates, Chem. Mater. 16, 1143-1152 (2004).
17. Shufang Yu, Ulrich Welp, Leonard Z. Hua, Andreas Rydh, Wai K. Kwok, and H. Hau Wang. Fabrication of palladium nanotubes and their application in hydrogen sensing, Chem. Mater. 17, 3445-3450 (2005).
18. Zongtao Zhang, Sheng Dai, Douglas A. Blom, and Jian Shen. Synthesis of ordered metallic nanowires inside ordered mesoporous materials through electroless deposition, Chem. Mater. 14, 965-968 (2002).
19. Stefan Degen, Conrad Becker and Klaus Wandelt. Thin alumina films on Ni_3Al (111): a template for nanostructured Pd cluster growth, Faraday Discuss 125, 343-356 (2004).
20. Z. Deng, C. Mao. DNA-templated fabrication of 1D parallel and 2D crossed metallic nanowire arrays, Nano Letters 3, 1545-1548 (2003).
21. A. Johansson, J. Lu, J.-O. Carlsson, M. Boman. Deposition of palladium nanoparticles on the pore walls of anodic alumina using sequential electroless deposition, Journal of Applied Physics 96, 5189-5194 (2004).
22. P.P.A.C. Pex, Y.C. van Delft, L.A. Correia, H.M. van Veen, D. Jansen, J.W. Dijkstra, Proc. of the 8th Inter. Conf. on Inorg. Membr. Cincinnati, 2004, July 18-22, 524.
23. Zhongliang Shi, Shanqiang Wu, Jerzy A Szpunar. Synthesis of palladium nanostructures by spontaneous electroless deposition, Chemical Physics Letters, 422, 147-151 (2006).
24. Zhongliang Shi, Shanqiang Wu, Jerzy A Szpunar. "Bridge Model" of nanoparticles deposited on pores area of the substrate during a membrane fabrication, Appl. Phys. Lett. 87, 121913 (2005).
25. Matthias Geissler, Heiko Wolf, Richard Stutz, Emmanuel Delamarche, Ulrich-Walter Grummt, Bruno Michel, and Alexander Bietsch. Fabrication of metal nanowires using microcontact printing, Langmuir 19, 6301-6311 (2003).
26. Lon A. Porter, Jr., Hee Cheul Choi, Alexander E. Ribbe, and Jilian M. Buriak. Controlled electroless deposition of noble metal nanoparticle films on germanium surfaces. Nano Letters, 2002, 2, No. 10, 1067-1071
27. Y.S. Cheng, K.L. Yeung. Effects of electroless plating chemistry on the synthesis of palladium membranes, Journal of Membrane Science 182, 195-203 (2001).
28. G.O. Mallory, J.B.Hajdu (Eds.), Electroless plating-Fundamentals and applications, William Andrew Publishing/Noyes, 1990.
29. Dan V. Goia. Preparation and formation mechanisms of uniform metallic particles in homogeneous solutions, J. Mater. Chem. 14, 451-458 (2004).

CONCLUSIONS, ORIGINAL CONTRIBUTIONS AND FUTURE WORK

Conclusions

- An observation of palladium membrane formation on porous stainless steel substrate reveals that the membrane is made of palladium nanoparticles. The particle size can be controlled by the concentration of $PdCl_2$ in the plating baths. The higher the concentration of $PdCl_2$ in the plating bath, the smaller the generated palladium nanoparticles.
- A bridge model is presented to describe the membrane formation on the pore area and this bridge structure is confirmed by the cross-section of the membranes deposited on the porous substrates. Understanding of the deposition progress of a membrane formation around the pore areas is significant for determining the deposition time in the fabrication of the dense palladium membrane.
- Palladium cannot be deposited on the surface of non-conductive contaminant like SiO_2 inclusions that appear at the substrate in the initial stages. However, with the extension of deposition time, palladium nanoparticles will gradually cover the SiO_2 inclusions layer by layer with the advance palladium nanoparticles depositing on the substrate and surrounding around them. The effect of the inclusion contaminants on the palladium deposits cannot be neglected when an ultra-thin membrane is to be built.
- According to our experimental results, the thickness of a palladium membrane deposited on 0.2 μm grade porous stainless steel substrate can be effectively controlled around 1.5~2 μm, and the thickness of a palladium membrane deposited on 2 μm grade porous Inconel substrate can be effectively controlled around 7.5~8 μm. Comparing with the thickness of palladium membranes built on the same substrates in literature, the membrane prepared in this program reduces extensively.
- The measurement of the flux of hydrogen through the membranes indicates that hydrogen flux rises with reducing the thickness of the membranes, increasing the permeation temperature, increasing hydrogen partial pressure in the mixture of gases and increasing the absolute pressure difference of hydrogen.
- The observation of palladium membranes deposited on the porous stainless steel and Inconel substrates used for hydrogen permeation at the temperature of 550°C for 20 hrs and the absolute pressure difference of hydrogen at 50 psi, demonstrates that the surface microstructure casues the surface damage due to the chemical reaction between palladium and phosphorus/phosphates with the extension of hydrogen permeation time. Phosphorous may be generated from the substrates that contain some inorganic binders (PO_4^{3-}, $H_2PO_4^-$) when they were made by the powder metallurgical process. The chemical reaction product is identified as the intermediate phase PdP_6 by X-ray diffraction and EDS analyses.

- Three different types of palladium nanostructures are synthesized simultaneously at the surface of porous stainless steel substrate by an electroless deposition process. Palladium nanowires and nanoparticle monolayer membranes are deposited without any external field except an autocatalytic chemical reaction.
- Various palladium nanowire arrays having the morphologies of single wire, parallel and curved wires, intersections and network structures are generated. The obtained results demonstrate that palladium nanowires can be built in a self-assembled manner by assembly of palladium nanoparticles generated in the initial stages of the deposition. Such self-assembled nanowires may attract engineering applications because the electroless deposition process and the preparation of the substrate are simple and inexpensive.
- The diameter of palladium nanowires can be effectively controlled by the concentrations of $PdCl_2$ in the plating solution and deposition time. Based on our observation of palladium nanowire formation on the porous stainless steel substrate, palladium nanowires are gradually assembled by nanoparticles. The size of palladium nanoparticles generated from the autocatalytic reaction is directly dependent on the concentration of $PdCl_2$ in the plating solution. The higher the concentration of $PdCl_2$ in the plating solution is, the smaller the generated palladium nanoparticles are. The experimental results provide a controllable method for the fabrication of desired palladium nanowire arrays in the potential engineering applications.

Contribution to original knowledge

- A method for the deposition of thin palladium membrane on porous stainless steel substrate was developed. A bridge model is presented to describe the formation of the membrane. This model is well illustrated by the examination of the cross-section of the membrane. The obtained result will contribute to design and build thin membrane structure in the electroless deposition process.
- The effect of the SiO_2 inclusions (from the fabrication process) on the palladium deposits is investigated and it is found that palladium cannot be deposited on its surface in the initial stages of deposition.
- A chemical reaction between phosphorus/phosphates and palladium at high temperature was proposed. This reaction will cause the surface damage of the membrane. It is recommended that porous ceramics and metals used as substrates for the deposition of palladium membranes should not contain phosphate or dihydrogen phosphate in the inorganic binders during their fabrication.
- It is the first time to use the electroless deposition process to manufacture palladium nanowires on the surface of porous stainless steel substrate.
- The process of the formation of palladium nanowires was described and identified as three stages with the extension of deposition time. It is found that palladium nanoparticles generated from the autocatalytic reaction are not solid and can be easily deformed due to the interfacial tension when they connect with to form nanowires.

- It was demonstrated that the diameter of palladium nanowires can be effectively controlled by the concentration of $PdCl_2$ in the plating solution. The higher the concentration of $PdCl_2$ in the plating solution is, the smaller the diameter of deposited palladium nanowires is.

Future Work

- To investigate the mechanism of palladium nucleation and growth in aqueous solution in order to understand and control the size of deposited palladium nanoparticles and nanowires.
- To investigate the chemical reaction between palladium and phosphorus or phosphate under hydrogen atmosphere at high temperature, in order to understand the reaction mechanism and avoid this reaction happened.
- To set up a method to measure the physical properties of palladium nanowires and to build desired nanowire arrays for engineering application.